ELECTROREMEDIATION OF OFFSHORE MUDS

CONTAMINATED WITH HEAVY METALS

by

Sanghee Shin

A Dissertation Presented to the
FACULTY OF THE USC GRADUATE SCHOOL
UNIVERSITY OF SOUTHERN CALIFORNIA
In Partial Fulfillment of the
Requirements for the Degree
DOCTOR OF PHILOSOPHY
(ENVIRONMENTAL ENGINEERING)

December 2011

ProQuest LLC.
789 East Eisenhower Parkway
P.O. Box 1346
Ann Arbor, MI 48106 - 1346

Dedication

to my parents –

Kwag-Ok and Min-Ja Shin

Acknowledgments

I would like to thank Professor Najmedin Meshkati, my advisor and chair of Ph.D. committee for his support and guidance. He has always guided me to organize my thoughts during my research. He deserves the highest of praise.

Dr. George V. Chilingar helped me to obtain a secure foundation of knowledge in the fields of Environmental and Petroleum Engineering. Out of classrooms, he showed me how a scholar should live his daily life. I was really honored to have a chance to work with him closely.

I also would like to thank to my other Ph.D. committee members, Professors Jiin-Jen Lee, Vincent W. Lee, Jean-Pierre Bardet, Muhammad Sahimi, and Solomn Golomb and outside committee members Sibel Pamukcu and Muhammad Haroun.

Dr. Sibel Pamukcu gave me a chance to work with her at Lehigh University and thoroughly trained me in her electrokinetics laboratory. She shared with me her unique knowledge of electrokinetics. Dr. Muhammad Haroun kindly invited me to his electrokinetics laboratory at the Petroleum Institute of Abu Dhabi, UAE, where I worked for six months. He was an excellent mentor, teacher and friend.

I would also like to extend special thanks to my family for their support and encouragement in completing this research. My parents, Kwang-Ok and Min-Ja Shin have provided their endless support throughout my study. Without their support, I would not have been able to study and do research. My brother, Sang-Kyun Shin, deserves my special thanks for his words of encouragement, while I was studying at USC.

Table of Contents

List of Tables

List of Figures

Abstract

The electroremediation process requires much needed research work to be optimized for up-scaling and improving economic efficiency. This is particularly true when applying the technology to highly heterogeneous and complex mineralogy materials such as offshore sediments and muds. Laboratory batch tests were performed on field retrieved specimens of contaminated offshore muds near Abu Dhabi Ports of United Arab Emirates. The influence of various process parameters that determine the optimum operating conditions and sustainable enhancement of electrokinetic remediation was investigated. Excellent results of decontamination of seven heavy metals were achieved.

The removal of heavy metals by management of the *in-situ* chlorine gas (Cl_2) production was also investigated. The tests showed a high removal efficiency of heavy metals at the cathode end of cores after 24 hours of EK application in the presence of chlorine gas. In the initial tests, high electrokinetic flow potential was achieved; however, high levels of chlorine gas were produced in high-salinity environments. This was improved by controlling and maintaining a certain fraction of the chlorine gas (Cl_2) in place.

The pH was controlled by the identified optimum fraction of chlorine gas maintained *in-situ* and transported from the anode to cathode. The transports of seven heavy metals were evaluated in this study. The chlorine gas can have two impacts on the

transport of metals in the system. One is to oxidize the metal ions to a higher oxidation state and the second is to form chloride complexes, which will have higher mobility in the system. Determination of oxidation state and the subsequent metal chloride complex are left for future research.

Electrokinetics is also proposed to improve acidizing operations, i.e., increase the penetration distance. Aqueous solutions of hydrochloric acid (usually 15%) are pumped into the carbonate formations to enlarge the pores and pre-existing fractures. However, the penetration distance of acid is very short. By applying D.C. current, one can drive the acid for long distances into the formation being acidized. According to Professor Chilingar, this is a unique discovery which will lead to doubling the oil reserves in carbonate reservoirs (60 % of World oil reserves reside in carbonates).

Chapter 1

Introduction

Contaminated muds are a tremendous threat to water resources, i.e., the groundwater and seawater near the industrial areas. Huge volumes of offshore muds which are contaminated with heavy metals (toxicity) require restoration.

The present dissertation is the continuation of research work presented in Ph.D dissertation of Dr. Muhammad Haroun on the subject.

The writer worked six months at the electrokinetics laboratory of Dr. M. Haroun at the Petroleum Institute, Abu Dhabi, U.A.E, to improve the electrokinetics methodology and expand the experimental results. This resulted in publication of three articles. In addition to Arabian-Persian Gulf offshore muds, the writer is experimenting with offshore muds of California and Gulf coast, contaminated with heavy metals. The following discussion is heavily based on those presented by Anbah et al. (1963) and Haroun (2009). A review of theory behind the electrokinetics was presented by Haroun (2009).

1.1 Heavy Metals

"Heavy metals" are chemical elements with a specific gravity that is at least 5 times the specific gravity of water. Some well-known toxic metallic elements are arsenic, sp. gr. = 5.7; cadmium, sp. gr. = 8.65; iron, sp. gr. = 7.9; lead, sp. gr. = 11.34; and mercury, sp. gr. = 13.546 (Lide, 1992). Heavy metals become toxic when they are not metabolized by the body and accumulate in the soft tissues. They may enter the human body through food, water, air, or absorption through the skin when they come in contact with humans in agriculture and in manufacturing, pharmaceutical, industrial, or residential settings.

Offshore muds are composed of clays, which are predominantly negatively charged and, therefore, act as storage “sponges” for positively charged heavy metals, which can be absorbed and adsorbed in muds. Offshore muds are being deposited daily across the coastlines worldwide, acting as toxic supply to the marine environment. This is affecting the ecosystem due the suddenly significant concentrations of toxic and carcinogenic compounds, leading to adverse health effects to all the coastline communities. Whereas people whose diet is heavily focused on seafood are the most affected, epidemiological studies conducted are showing evidence that water sources and agriculture are affected by the sudden increase in the heavy metal concentration, leading to detrimental health effects (Haroun, 2009).

Most of the presence of heavy metals present in the offshore muds is due to unregulated industrial discharges and lack of environmental proactive technology. For example, as pointed out by Haroun (2009), in the Arabian-Persian Gulf area there is a

very heavy oil/gas traffic, which contributes heavily to both organic and inorganic contaminations. The increasing health concerns are due to both the industrial toxic and carcinogenic heavy metals. Complex combinations of heavy metals, e.g., strontium plus chromium, leads to bone cancer among other diseases.

1.2 Electrokinetics

The theoretical development of electrokinetic phenomena and electrochemical transport has been studied historically as far back as 1879 by Helmholtz that led to the introduction of the first analytical equation. Helmholtz described the motion of the charged ionic solution from the anode to the cathode and explained it by the presence of a double layer. This double-layer theory is illustrated in Figure 1-1, where the negatively-charged surface of the clays attracts the positive ions of aqueous medium, forming the *immobile* double layer. This immobile double layer is followed by a thick *mobile* layer with a predominanance of positively-charged ions (cations), with a few diffused negatively-charged ions (anions).

Later, the analytical solution was further modified by Smoluchowski in 1921 to arrive at the Helmholtz-Smoluchowski's equation (electrokinetic permeability, k_θ):

$$k_\theta = \frac{D\,\xi}{4\,\pi\,\eta} \tag{1-1}$$

where: D = dielectric constant

ξ = zeta potential

η = viscosity of the fluid

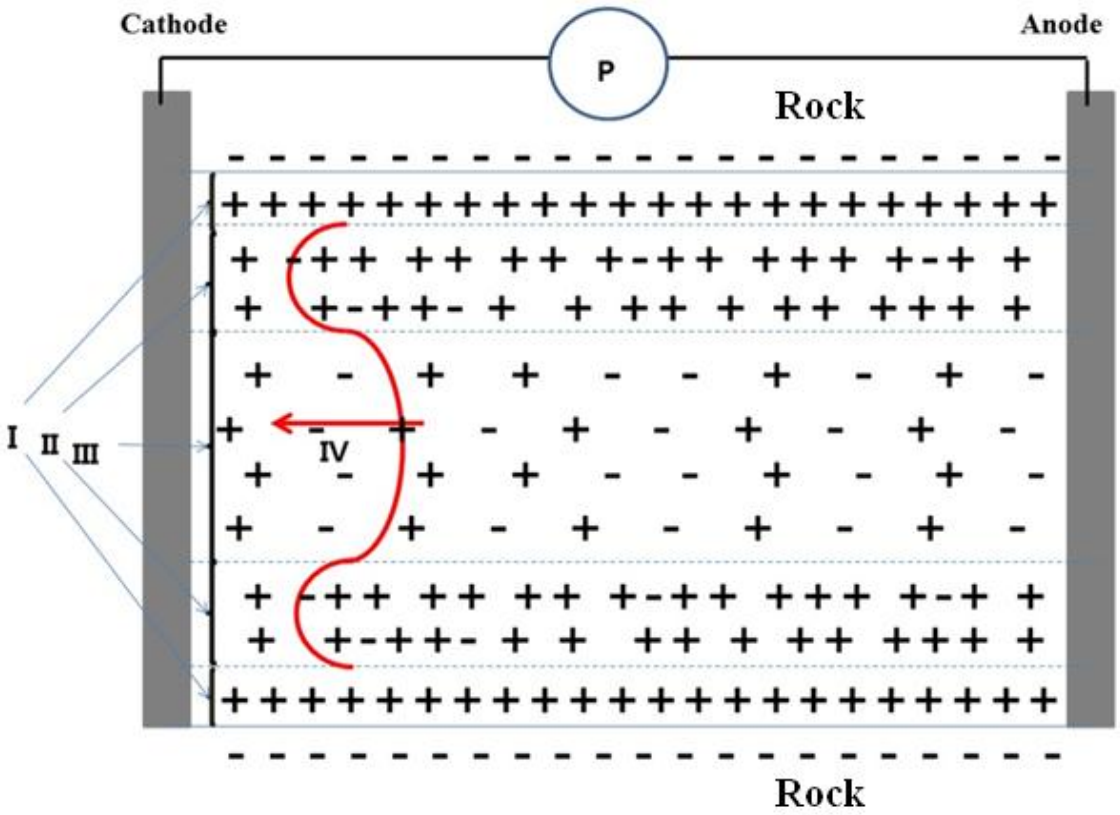

Figure 1-1: Schematic diagram of electrokinetic double layer (I: Immobile Double Layer, II: Mobile Double layer, III: Free water, IV: Velocity Profile) as envisioned by Dr. George V. Chilingar (personal communication). Solid curved line – velocity profile in a capillary. P = D.C. current power supply. Rock is negatively charged.

The proportionality constant, *D*, has been verified by several investigators for various types of liquid--solid interfaces. However, extreme sensitivity and complexity of these phenomena have lead to reports of discrepancies in the relative constancy of this term. Probstein and Hicks (1993) have shown the effects of concentration of ionic species within the pore fluid, electric potential, and pH on the zeta potential (ξ). Thus, it doesn't remain constant throughout the electrically- induced transport in soils that is governed by zeta potential.

Counterions from the water solution balance the charges at the solid surface and form the immobile Stern layer, Figure 1-2. The thickness of the Stern layer is only one or two molecular diameters consisting of ions that are adsorbed strongly enough to form an immobile layer. The outer edge of the Stern layer where the ions are mobile is known as the shear plane. There is a linear potential drop across the width of the Stern layer $(\psi_s - \psi_\zeta)$, followed by an exponential potential difference across the diffuse layer between the shear plane and the bulk solution $(\psi_\zeta - \psi_\infty)$; the bulk solution is designated as the reference zero potential. The potential difference between the shear plane and the bulk fluid is known as the zeta potential (Donaldson and Alam, 2008).

The thickness of the Helmholtz layers thus reflects the size of the adsorbed anions and counter-ions within the Stern layer and is observed by the differences of the measured linear potential differences within the Stern layer.

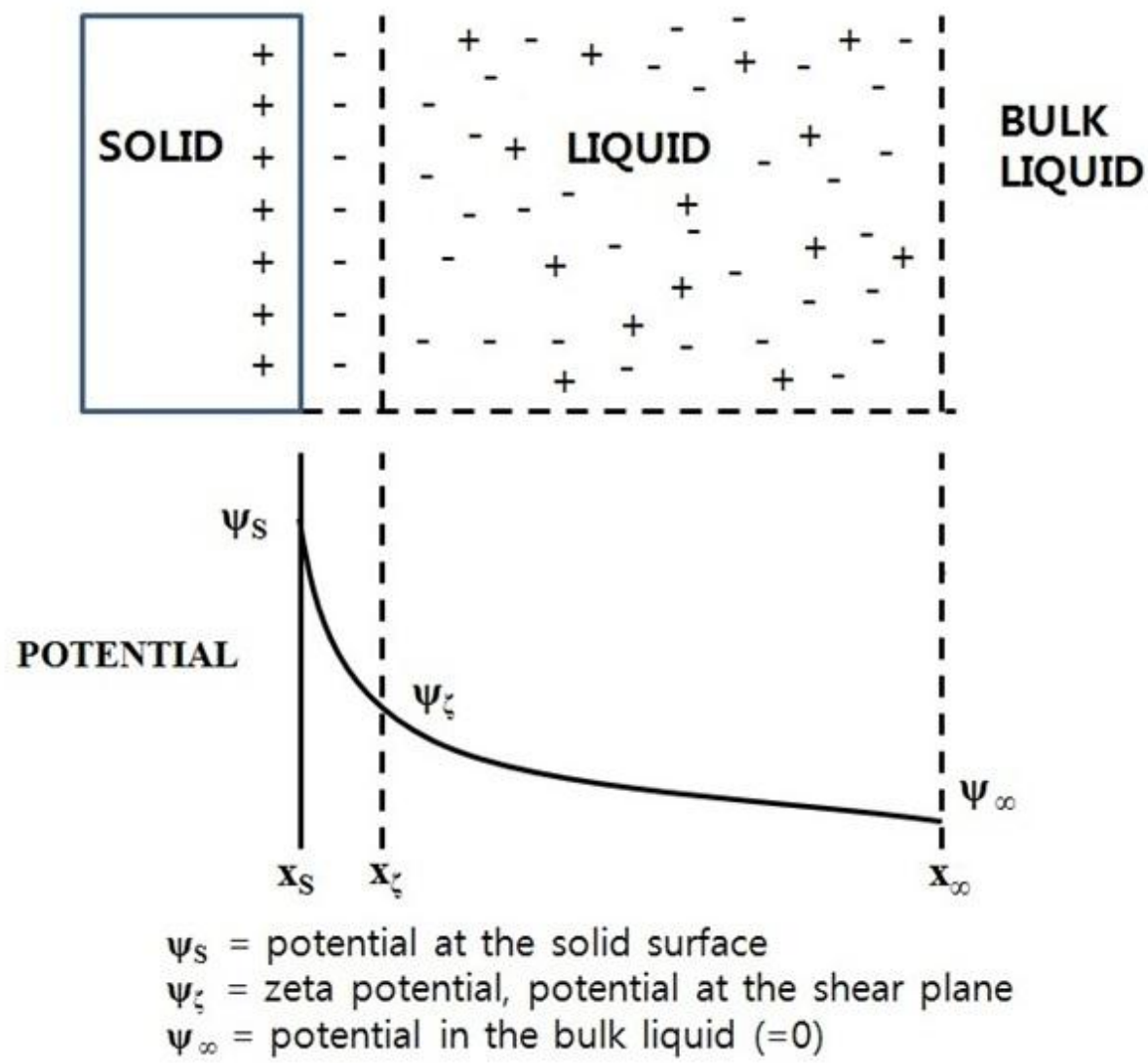

Figure 1-2: Electric double layer at the interface between a solid and liquid: x_s = surface of the solid, x_ζ = shear plane, x_∞ = bulk liquid, $x_\zeta - x_s$ = Stern layer, $x_\infty - x_\zeta$ = electrical diffuse layer. (Debye length). (Modified after Donaldson and Alam, 2008.) Note that the surface of the solid in this case is positively charged.

The length of the exponential electrical field decay (from the shear plane to the bulk fluid) is known as the Debye length ($\frac{1}{k}$). For example, if the plates of a capacitor have equal charge densities, the zeta potential is the potential difference from the center of the separation to one of the plates (Donaldson and Alam, 2008):

$$\frac{1}{k} = x_o - x_s = \varepsilon\varepsilon_o \frac{\psi_s}{\sigma_c} = \sqrt{\frac{\varepsilon\varepsilon_o KT}{\rho_i Z^2 \varepsilon^2}} \quad (1\text{-}2)$$

$$(m \text{ (mass)} = [\frac{c^2}{jm} * \frac{j}{c} * \frac{m^2}{c}])$$

where, ρ_i is the number density of ions in the solution; Eq. 1-2 also shows that the charge density of the surface (σ_c) is proportional to the surface potential (ψ_s). ε is the dielectric constant. ε_o is the permittivity of free space [8.854 * 10 $^{-12}$ C^2/ J*m = C^2 / N*m^2]. *KT* is the constant, 4.144 * 10 $^{-21}$ J at 25 ^{o}C; 4.045 * 10 $^{-21}$ J at 20 ^{o}C. *Z* is vertical distance.

With respect to an ionic solution, the Debye length is the distance from the shear plane of the Stern layer to the bulk fluid. The Debye length depends on the specific properties of the ionic solution. For aqueous solutions (Donaldson and Alam, 2008):

$$\frac{1}{k} = \frac{B}{\sqrt{M}} \quad (1\text{-}3)$$

where *B* is a constant specific to the type of electrolyte. *B* is equal to 0.304 for monovalent cations and anions (NaCl); 0.176 where either the cation or the anion has a valency of two ($CaCl_2$ or $NaCO_3$); and 0.152 when both ions have a valency equal to two

($CaCO_3$). *M* is the molaritry of the pore solution.

The composition of the Stern layer varies with respect to the nature of the surface charge and ionic constituents of the electrolyte (Castellan, 1971).

The zeta potential of mineral surfaces in contact with aqueous solutions is a function of pH. In general, acidic solutions promote positive charges at the surface with an attendant positive zeta potential and basic solutions produce an excess of negative charges at the surface from an increase of the hydroxide ion. The *pH* at which the zeta potential is equal to zero is defined as the zero point charge *(zpc).* When the negative and positive charges of ions in a solution are equally balanced, the solution is electrically neutral and this condition is defined as the isoelectric point *(iep)* (Castellan, 1971).

The significance of zeta potential is that its value can be related to the stability of colloidal dispersions. The zeta potential indicates the degree of repulsion between adjacent, similarly charged particles in dispersion. For molecules and particles that are small enough, a high zeta potential will confer stability, *i.e*., the solution or dispersion will resist aggregation because the surface charge disperency of the particles are highly satisfied. When the potential is low, attraction exceeds repulsion and the dispersion will break and flocculate. Thus, colloids with high zeta potential (negative or positive) are electrically stabilized, whereas colloids with low zeta potentials tend to coagulate or flocculate:

Zeta potential is widely used for quantification of the magnitude of the electrical charge at the double layer. However, zeta potential is not equal to the Stern potential or electric surface potential in the double layer. Such assumptions of equality should be

applied with caution. Nevertheless, zeta potential is often the only available path for characterization of double-layer properties.

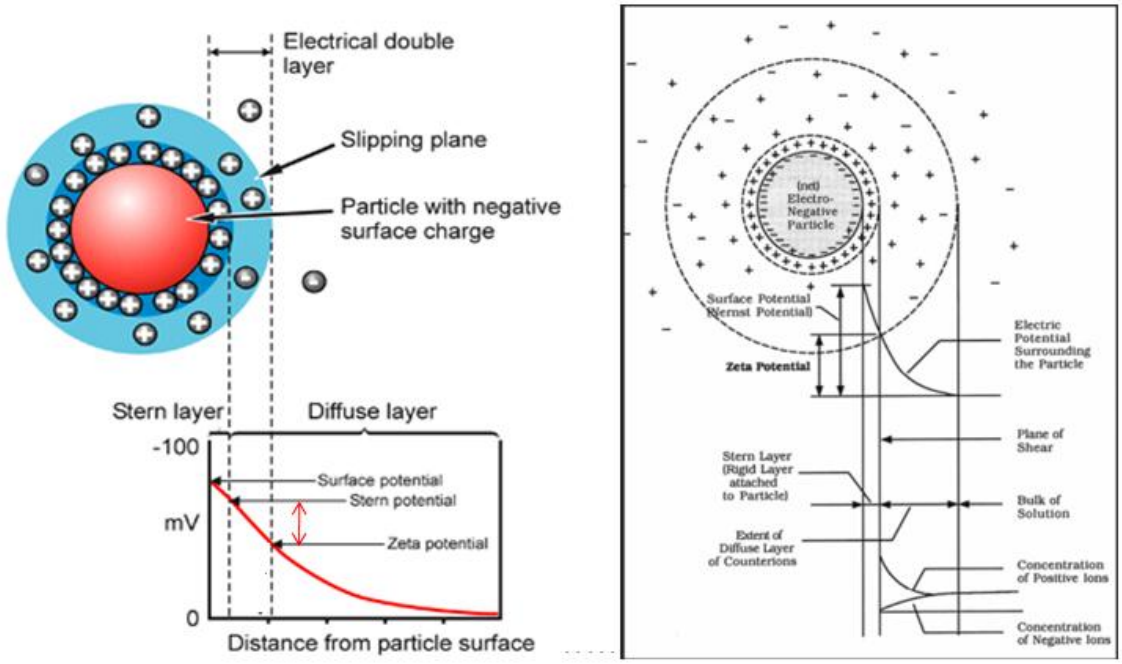

Figure 1-3: Schematic representation of zeta potential (ξ) (Modified after Zetasizer Nano series technical note, Malvern Instruments)

There is a surface of shear (slipping plane) between the fixed and mobile sub-regions. The zeta potential (ξ) is the potential difference between this plane and the bulk liquid. This zeta potential (ξ) is smaller than the total or thermodynamic potential (after Butler et al., 1951). The classical zeta potential (ξ) equation is as follows (after Street et al., 1961):

$$\xi = \frac{4\,\pi\,\eta\,(EM)}{D} \tag{1-4}$$

where, η is the viscosity of mass,

EM is the electrophoretic mobility.

D is the dielectric constant.

Anbah (1963) stated that the larger the ionic charge on the clay particle, the larger the electric potential between the diffuse and inner fixed layer. Thus, fewer ions are able to move in an external field. Overbeek and Liklema (1969) have shown that the higher the ion concentration, the smaller the double layer thickness and, hence, the smaller the zeta potential.

With decreasing pH, however, the zeta potential (ξ) decreases until a critical pH is reached at which time a reversal in the sign of zeta potential occurs (Hunter and James, 1992). This is caused by the accumulation of H^+ ions in low--pH environments, resulting

in a compression of the Helmholtz double layer due to the cation build up. As the concentration of hydrolyzable metal ions increase, the compression of the electric double layers occurs. This may lead to a reduction in electrokinetic flow in soils with high pore fluid electrolyte concentrations, making electromigration the dominant mechanism of electrochemical transport (Pamukcu et al., 2008). This reversal of sign of the zeta potential (ξ) has been found due to the accumulation of cations and the compression of the electric double layer. The largest effect of zeta potential ξ) occurs during the intermediate pH, slightly higher than the value needed for precipitation of the metal hydroxide. It has been shown to be influenced by the type and concentration of electrolytes added to the suspension (Kruyt, 1952).

As mentioned earlier, the pH is one of the most important factors affecting the zeta potential (ξ). Thus, the zeta potential value alone is actually meaningless without defining the solution conditions (Zetasizer Nano Series Technical Note, Malvern Instruments, www.nbtc.cornell.edu).

1) On assuming a negative value zeta potential, if acid is added to this suspension, a point will be reached where the charge will be neutralized. The further addition of acid will cause a buildup of positive charge. Consequently, the zeta potential (ξ) versus pH curve will be positive at low pH and lower or negative at high pH.

2) On the other hand, if more alkali is added to the system, then the accumulation and buildup of negative charge on particle will prevail. The point where the plot of the zeta potential versus pH passes through the zero zeta potential is called the

isoelectric point. Usually, a colloidal system is least stable at this point.

1.3 Theoretical Analysis

A modern concept of the liquid-solid interface introduced by Gouy (1910) led to the concept of the diffuse double layer. The solid-liquid interface is the seat of a double layer in which the ions of one kind are adsorbed and tightly held to the surface, thus leaving an excess of the other kind of ions in solution. The ions arrange themselves in a diffuse layer in which the excess of concentration of the second kind over the first dimishes toward the center of the capillary – from a maximum at the wall to zero at an outer boundary.

Helmholtz (1879) was the first to attack this phenomenon analytically, and assumed that: (a) the hydrodynamic equations for viscous liquids are valid for the entire region of the double layer; and (b) laminar flow conditions prevail.

Later modifications by Smoluchowski (1921) led to the famous Helmholtz-Smoluchowski equations:

$$v = \frac{\zeta\ D\ E}{4\ \pi\ \eta} \tag{1-5}$$

$$Q_e = \frac{A\ \zeta\ D\ E}{4\ \pi\ \eta} \tag{1-6}$$

where A = the cross-sectional area, D = dielectric constant, ξ = zeta potential, E = potential difference, and Q_e = electrokinetic flow rate. Smoluchowski also proved the

validity of these equations for porous plugs where A was eliminated by the application of Ohm's law and by assuming no surface conductance:

$$A \bullet E = \frac{i}{\lambda} \tag{1-7}$$

$$\therefore Q_e = \frac{D\,E\,i}{4\,\pi\,\eta\,\lambda} \tag{1-8}$$

where λ is the specific conductivity and i is the current through capillaries. It was proved later that these equations still hold true for turbulent flow (Rutgers, 1957).

If there is surface conductance in the capillaries

$$AE + SE = I \tag{1-9}$$

$$\therefore Q_e = \frac{D\,\zeta\,i}{4\,\pi\,\eta\,(\lambda + \frac{S}{A}\lambda_s)} \tag{1-10}$$

where S = circumference of the capillary and λ_s = specific surface conductance.

The necessary corrections, however, could be made by measuring the conductivity or the resistivity of the liquid while it is present in the capillaries:

$$\therefore Q_e = \frac{D\,\zeta\,i}{4\,\pi\,\eta\,\lambda'} \tag{1-11}$$

where $\lambda'$is the corrected specific conductivity. Thus, it includes bulk conductivity, λ , and surface conductivity λ_s. λ' is determined experimentally from the measured resistance, *R*, across the core and its cell constant (*C*):

$$\lambda' = \frac{C}{R} \tag{1-12}$$

According to Manegold and Solf (1931)

$$C = \frac{L}{A\,(1-f)\,\sigma} \tag{1-13}$$

where, *L* = length of the core, *A* = cross-sectional area, $(1-f)$= volume fraction available for ionic migration, and σ = shape factor.

$$\therefore Q_e = \frac{A\,D\,\zeta\,R\,i\,(1-f)\sigma}{4\,\pi\,\eta\,L} = \frac{A\,D\,\zeta\,\sigma(1-f)}{4\,\pi\,\eta} \bullet \frac{E}{L} \tag{1-14}$$

1.4 Transport of Contaminants in Soils on Application of D.C. Current

If the direction of hydraulic pressure gradient coincides with the direction of DC electric field current, i.e., Darcy's flow and the electrokinetic transport occur in the same direction, a one-dimensional mathematical model can be used to show the main mechanisms of the species' transport. In this case, redistribution of the species concentration in space can be described as a result of combined influence of three mechanisms: Darcy flow, electrokinetics and diffusion. The first two relate to the contaminants' solution flow with respect to the solid soil matrix, whereas the last redistributes the species inside the flowing fluids (Chilingar et al., 1997).

For the purpose of simplified analysis, it is reasonable to consider a one-dimensional fluid flow in the direction from anode to cathode. Denoting the distance from the anode by x and the distance between anode and cathode by 1, one can consider $0 \leq x \leq 1$. The total fluid flow rate $q_t(x)$ at the point x can be expressed for this case in the form:

$$q_t(x) = q_h(x) + q_e(x) \tag{1-15}$$

where, q_h is the hydraulic component of the flow and q_e is electrokinetic component

of the total flow q_t.

To define $q_h(x)$ one can use the Darcy's Law (e.g., Bear, 1973):

$$q_h(x) = A\, k_h\, \mu^{-1}\, \frac{dp}{dx} = A\, k_h\, \mu^{-1}\, \nabla p \tag{1-16}$$

where *A* is the cross-sectional area perpendicular to the direction of fluid flow, k_h is the Darcy's permeability of porous medium in the direction of flow, μ is the viscosity of fluid, and $\frac{dp}{dx} = \nabla p$ is the pressure derivative in the direction of flow at point *x*.

For the electrokinetic flow rate $q_e(x)$, one may use the Helmholtz-Smoluchowski equation version of the following form (Smoluchowski, 1921):

$$q_e(x) = A\, k_e\, \mu^{-1}\, \frac{d\Phi}{dx} = A\, k_e\, \mu^{-1}\, \nabla \Phi \tag{1-17}$$

for which electrokinetic permeability k_e is defined by

$$k_e = (4\, \pi\, F\,)^{-1}\, D\, \zeta \tag{1-18}$$

where F is the formation factor, D is the dielectric constant, ζ is the zeta-potential, Φ is the potential of electric field, and $\frac{d\Phi}{dx} = \nabla\Phi$ is the potential derivative in the direction of flow at the point x.

Chilingar et al. (1968) conducted a simple analysis of conditions that are responsible for relationship between hydrodynamic and electrokinetic components of the flow. Based on Eqs. 1-16 and 1-17, they presented the ratio:

$$\frac{q_t - q_h}{q_h} = \frac{k_e \nabla\Phi}{k_h p} \tag{1-19}$$

This ratio shows that an increase in the electrokinetic flow rate is proportional to the zeta-potential, dielectric constant, and potential gradient (Chilingar et al., 1997).

The direct conclusion from the Eq. 1-19 is that the electrokinetic technique is especially effective in cases when hydraulic permeability k_h is very small, which is valid, for example, for clays or clayey sands. Electrokinetic flow rate increases with increasing clay content in sands. For sands it is possible to raise the hydrodynamic component of the total flow by injection of special purging solutions (Shapiro and Probstein, 1993).

Electrical field application in situ, as a rule, leads to an increase in temperature. In turn, the temperature increase reduces the viscosity of hydrocarbon-containing fluids that, according to Eqs. 1-16 and 1-17 would result in an increase of the total flow rate

(Chilingar et al., 1968). Analyzing the results of "in situ" trials and verifying corresponding mathematical models, one should keep in mind this additional positive side- effect to avoid possible misinterpretations of electrokinetic efficiency. This effect is insignificant for the dissolved gaseous hydrocarbons (like butane and methane). For crude oils (e.g., California crude oils), however, the viscosity can be reduced more than twenty times upon heating from 50 to 100 ^{o}C (Ungerer et al., 1990). This (at least in theory) would increase the total fluids flow twenty times. Discussing an electrical field application for the acceleration of fluids transport in situ, one needs to consider also electr1cal propert1es of soils (electrical resistivity, for example) and ionization rate of the flowing fluids that can considerably affect the total flow rate. In addition, Chilingar and his associates (Chilingar et al., 1970) discovered that application of D.C. field to some soils leads to an increase of their hydraulic permeability that, in turn, can considerably accelerate the fluids transport. In addition, some clays are destroyed (become amorphous) upon application of direct electric current, possibly as a result of driving the interlayer water out (do not swell any longer).

1.5 Multicomponent Cleanup Technologies and Examples of Their Application *in situ*

There is a wide variety of mechanical, physical, chemical, and bioremediation cleaning methods that are applied in contemporary practice for the restoration of contaminated site. It is even difficult to name all of them and give their characteristics. Good classification of the bioremediation methods with general recommendations of their applications was presented by Pollard et al. (1994).

For any particular contaminated site, one should select the most appropriate cleanup technology (or the most appropriate combination of different technologies). The choice of a concrete technology (or technologies) depends on many factors, e.g., the site size, type of predominant contamination, the site's future use, and available resources (time and money). Examples of such an approach to the selection of cleanup strategy were presented by Blacker and Goodman (1994) and Fairless (1990). They developed some reasonable selection methodology of cleaning technologies, based on the principles of system analysis: from the final goal, through the quantitative characterization of the problem, to the choice of preferable alternatives.

Many good examples of successful application of the combined technologies were presented by W. Loo and his associates. Loo (1994) used a combined system,

including primarily passive cometabolic biotreatment and electrokinetic transport of amendments and contaminants in solution for degradation of gasoline and diesel in the soil and groundwater. In one case, spills of gasoline and diesel from an underground storage tank caused soil and groundwater contamination in the clayey Bay Mud, City of Hayward, California. The soil contamination extended to a depth of about 10 ft with a total petroleum hydrocarbons (TPH) concentration of 100 to 3,900 ppm. The gasoline and diesel in the soil were degraded to less than 100 ppm of TPH, and to less than 10 ppm in groundwater. The remediation process was completed in four weeks.

A combination of biodegradation and electrokinetic transport with a hot air venting system and ultraviolet light biocontrol system was used by Loo et al. (1994) for degradation of gasoline in the clayey soil. The gasoline soil plume covered an area of about 2,400 sq. ft, to a depth of about 30 ft. The upper 15 ft of sediments were composed of highly-conductive marine clay, whereas the lower 15 ft consisted of well-cemented conglomeratic sandstone. The gasoline concentration ranged from 100 to 2,200 ppm. The process of remediation was completed after about 90 days of treatment. The concentration of gasoline in the soil after treatment was far below the proposed cleanup level of 100 ppm. The cost of treatment was about $50 per ton of soil for this advanced soil treatment process, which provided a cost effective remediation with minimum disruption to business operations at the site (Chilingar et al., 1997).

A closed recovery system for soil and groundwater for a site contaminated with gasoline in Greenville, North Carolina, was developed by Burnett and Loo (1994). The

dissolved contaminant plume covered an area of 18,000 sq ft and penetrated to the depth of about 15 ft. The total volume of spill was estimated at 300,000 gallons. The initial concentration of gasoline in the plume averaged about 40 mg/l of total BTEX (Benzene, Toluene, Ethylbenzene, and Xylenes).

Special enhanced bioremediation system was designed to clean this site. The system consisted of two groundwater recovery wells, a treatment unit and an infiltration gallery. The treatment unit consisted of transfer pumps, pressure filters, granulated activated carbon filters, air sprayers, holding tanks, chemical feed system, water heater and monitoring means. The bioenhancement process included heating, addition of nutrient amendments (monoammonium phosphate and trisodium phosphate), and oxygen addition (dilute hydrogen peroxide). In six months of operations, BTEX in the plume had been reduced to a level less than 6.5 mg/l with the passage of 11 pore volumes of displacement.

1.6 Dewatering of Soils

Electrokinetics has long been applied in soil engineering. Several patents on the removal of water from clayey and silty soils by electrokinetic were issued in Germany before World War II. Later, the method was widely and successfully used in Germany, England, the U.S.S.R., and Canada in drying water-logged soils for heavy construction. The development of these practical applications has been largely due to the work of Casagrande (1937-1960) who has carried on a continuous research on their feasibility in relation to various soil characteristics.

The literature of civil engineering, soil mechanics, and highway research has reported investigations made by Winterkorn (1947-1958), Casagrande (1937-1960), and others on the nature and scope of the electrical treatment of soils.

Some examples of electrokinetics treatment in civil engineering are described here for the purpose of illustration.

1.6.1 Field Applications of Electrokinetics

Railway cut, Salzgitter, Germany (Casagrande, 1947). Difficulties which arose during the construction of a double-track railway cutting, in a loose-loam deposit due to the flow of soft soil, were overcome by a large-scale drying operation using electrokinetic. In sections of 100 meters, well electrodes 7.5 meters deep and 10 meters apart were used. Before the application of electrical potential, the average rate of flow of water was 0.4 cu.m. / day /20 wells. An electrical potential, with an average tension of 180 volts and average current of 19 amps/well, was applied. During an eight-week period, the flow continued at an almost constant rate of 60 cu.m./day/20 wells, i.e., at 150 times the flow rate before the application of potential.

U-boat pen, Trondheim, Norway. Several attempts to make an excavation about 14 meters deep in a very thick stratum of clayey silt interspersed by seams of sand in the proximity of the sea were doomed to failure because of the very active uplift phenomenon. The application of electrokinetics to cause water to flow away from the excavation site was next tried. The salt deposits, which increased the electrical conductivity of the soil, required high consumption of current.

Before the application of electrical potential, the flow rate varied from one to 50 liters per hour per well. A current of 26 amps at 40 volts tension was used. The application of current increased the flow rate up to 11-479 liters per hour per well. The average power consumed was estimated to be 0.4 Kw-hr per cubic meter of soil

excavated.

Lime sludge deposits. Some tests were made by Casagrande also on dewatering lime-sludge deposits (Wulprath, Germany) having a uniform water content of 120 per cent of dry weight. A 25 per cent decrease in moisture content was obtained by the application of electrical potential with 70-volt tension and a current of 50 amps for 14 days. The reduction lines of water content indicated that the electrokinetics dewatering process took place uniformly along the lines of equal potential strength.

1.7 Electrochemical Treatment of Soil and Weak Rocks

The first work along this line was carried out by Casagrande (1930) who noticed that a permanent stabilization of soil could be obtained by using aluminum electrodes. These aluminum electrodes were found to be greatly corroded and aluminum compound deposits were noticed around the electrodes. Encouraged by the model tests, Casagrande (1937) undertook a full scale experiment and came to the conclusion that electrochemical treatment could be used also for increasing the bearing capacity of piles.

A reduction in water saturation around the borehole (invaded zone by filtrate) may be accomplished by means of electrokinetics, thus increasing the relative oil permeability. This can be done over a very short period of time, and in the future may prove to be one of the most economical means of borehole treatment, particularly in the case of dirty formations.

Selective ion-drive. In many cases, whether during water flooding or primary production, it is desirable to add some surface-active agents in order to influence or change the surface-liquid properties. Usually this is accomplished by adding chemical to the injection fluid in the case of secondary recovery or by adding these chemicals through the producing well by means of back-flowing for specific zone treatment (Anbah et al., 1965).

The electrokinetics effect (ionic transport) can be used as an excellent ion-drive mechanism. Various kinds of ions can be driven selectively into the zones of interest by

the application of direct electric current for purposes of treatment. For example, in the case where the formation is desired to be oil-wet rather than water-wet in a specific zone, chemical additives such as ionizable organic amino-compounds may be driven into that particular zone by playing with the electrode arrangement. A simplified sketch of possible electrode arrangements is shown in Figure 1-4, where the wet ground is used as one of the terminals.

Generally speaking, however, it is always preferable to use old pipes or rods of any conducting material as anodes, which are inserted in the wet ground at a shallow depth around the treated well (Anbah et al., 1965). Inasmuch as the anodes will usually corrode, these rods or pipes can be replaced very easily in due time. In the cases where the anodes are lowered in the well to face the producing zone, it will be advisable to use nonelectrolyzable electrode material such as carbon, graphite, or noble metals. The initial cost for the noble metal electrodes may be decreased by using them as platings over base materials. In case it is feared that the casing or tubing of the injection well may corrode, an electrical potential can be superimposed on them in such a way that they will be cathodically protected. No such precautions are necessary in the case of the producing wells because the cathodes as a whole will be protected against corrosion.

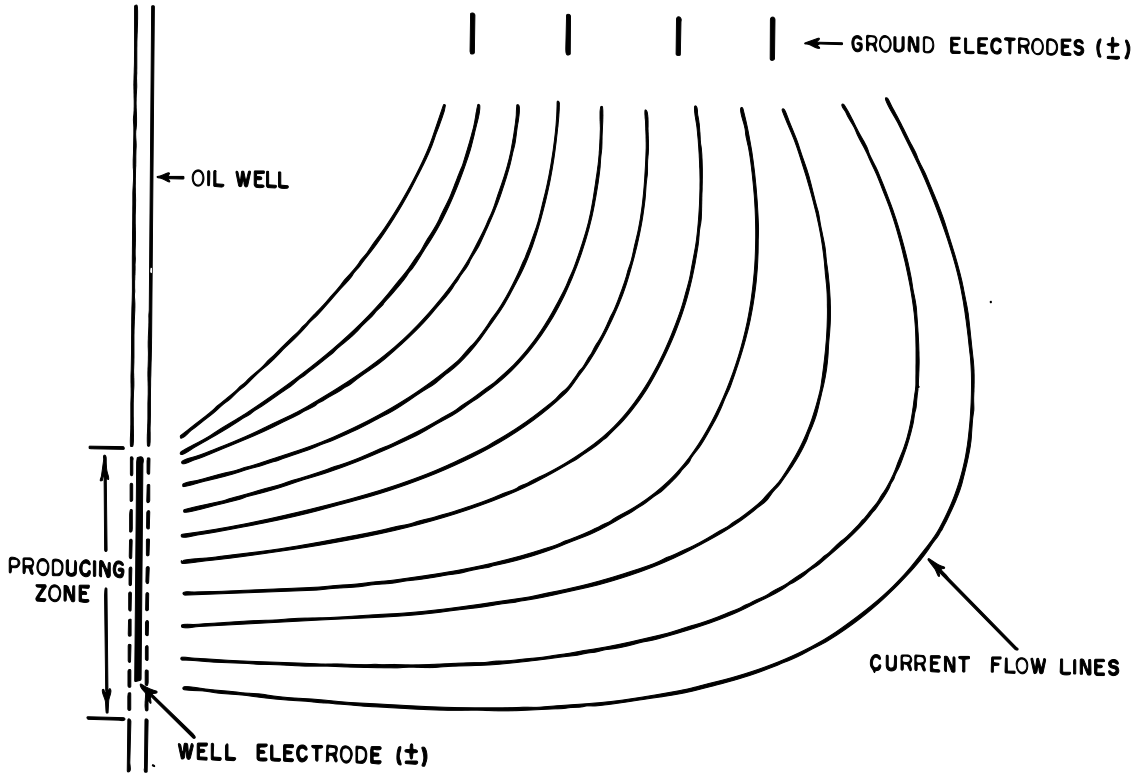

Figure 1-4: Electrode arrangement for selective ion-drive. Conducting pipes driven into the wet ground are used as anodes or cathodes. (After Anbah et al., 1965.)\

1.8 EEOR (Electrical Enhanced Oil Recovery)

In 1952, Tchilingarian suggested the possibility of using direct electric current for separation of fine sediments into grades on the basis of different cataphoretic velocity exhibited by clay particles of different size. This was achieved on treatment of clays with NaOH, because OH^- ions impart greater negative change to clays and, consequently, greater velocity towards the positive electrode. He started this research because he was questioning the statement in textbooks that "cataphoretic velocity is independent of size and shape of colloids" (personal communication with Professor G.V. Chilingar, 2010).

Also, knowing the success in dewatering of clays by soil engineers, he started research on EEOR together with his students at the Petroleum Engineering Laboratories of the University of Southern California (e.g., Anbah, 1963).

G. V. Chilingar and his students at the University of Southern California (Ace, 1955; Amba et al., 1964, 1965; Chilingar et al., 1968a,b, 1970,1997) conducted numerous laboratory tests involving electrokinetics, which indicated that this low-power drain mechanism could be used for EOR. Tikhomolova (1993) described similar studies conducted at the University of St. Petersburg, also suggesting electrokinetics as a potential EOR technology. Hill et al. (1997) conducted bench-scale studies, which suggested that hydrocarbons could be transported via electrokinetic mechanisms. Pamukcu et al. (1995) and her students at Lehigh University, demonstrated electrokinetic transport of hydrocarbons (PAH), in clay-rich soils, as a method of remediating manufactured gas plant site contamination.

Upon application of DC current, the mobile Gouy layer migrates toward the (negative) cathode. This motion of the water molecules and cations within the Gouy layer drags the water molecules, cations, and anions, in the free fluid, as well as any non-wetting fluid, along with it (Hill et al., 1997). Extensive experimental work, conducted at The University of Southern California (Ace, 1955; Amba et. al., 1964, 1965; Chilingar et al., 1968a,b, 1970, 1997) showed up to six-fold volumetric fluid flow increases in cores containing clay minerals, compared to only 2-fold increases in pure silica cores (see Figure 1-5). Chilingar et al. (1970) speculated that in pure silica core fluid flow might be, at least partly, due to a thermal effect. Mitchell (1993) maintained that all silicate minerals show this increased flow effect, to some extent. Those with high cation exchange capacity (CEC) exhibit the greatest flow increases.

Electro-enhanced oil recovery (EEOR) is an emerging technology that could significantly improve oil recovery, at costs below other secondary and tertiary oil recovery technologies, in environments where other technologies either do not work or are not attractive. EEOR has a nonexistent water demand, a smaller carbon footprint than traditional EOR technologies, such as steam injection, and does not involve injection of hazardous liquids, as is the case for caustic and/or co-solvent flood. EEOR requires minimal surface facilities. No steam generators, compressors, surface working fluid pumps, and/or hazardous material storage tanks are required. EEOR involves passing direct current (DC) electricity between cathodes (negative electrodes) in the producing reservoir and anodes (positive electrodes) either at the surface and/or at depth. The use of DC electrical power as an EEOR process was originally proposed by Prof. George V.

Chilingar in 1955 and then developed and patented by General Electric (GE) (Bell and Titus, 1973, 1974). It is currently being developed by Electro Petroleum, Inc., (EPI) of Wayne, Pennsylvania, USA (Bell et al., 1985; Titus et al., 1985; Wittle and Bell, 2005a, 2005b). These two organizations, collectively, spent several years and millions of (US) dollars in R&D to overcome encountered field operational difficulties. Their combined efforts resulted in successful EEOR demonstrations at California and Alberta heavy oilfields. At the time of the original GE EEOR Joule heating research and development (R&D), Professor G. V. Chilingar, and his students at the University of Southern California (Ace, 1955; Amba et al., 1964, 1965; Anbah et al., 1965; Chilingar et al., 1968a,b, 1970), had been conducting laboratory research, which indicated that DC current could increase effective reservoir permeability and hydrocarbon recovery, via electrokinetic processes.

Successful EEOR field tests have been achieved lately (Wittle et al., 2008 and 2011) in California and Canada. Application of EEOR would return about 25 dollars per each dollar invested, considering the initial installation cost and that of electricity. Anbah et al. (1965) suggested a few electrode arrangements for waterflooding operations.

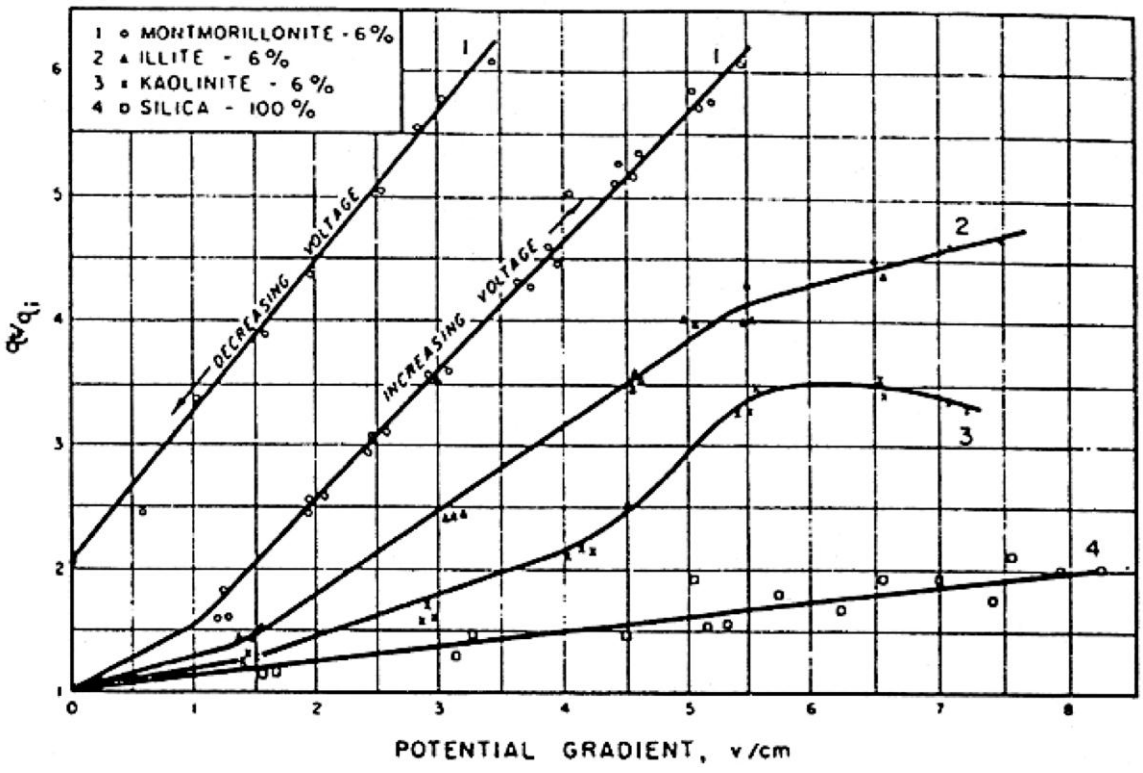

Figure 1-5: Relationship between potential gradient and normalized electrokinetically induced fluid flow, for different silica--clay mineral mixtures. Core No. 1: 94% silica sand and 6% montmorillonite clay. Core No. 2: 94% silica sand and 6% illite clay. Core No. 3: 94% silica sand and 6% kaolinite clay. Core No. 4: 100% 200-mesh silica sand. High cation-exchange capacity clays (montmorillonite and illite) exhibit greater sensitivity to DC electrical current stimulation. (After Chilingar et al., 1970.)

1.9 Economic Feasibility

Many assumptions should be' made in order to make rough calculation of economic feasibility of using D.C. current. The variables which will affect the economic considerations include: (1) thickness, depth, and resistivity of the pay zone, (2) arrangement of the electrodes, (3) duration of the electrical treatment, (4) labor cost, and (5) price of electricity at the site of application.

In general, the rock resistivity is a function of the amount of interstitial water present. This in turn is determined by the rock porosity and the amount of the pore space that is filled by interstitial water. The flow of electrical current in such a case is not a simple linear flow but follows an irregular path around the individual sand grains. This flow pattern will increase the length of the current flow lines and the resistivity of the rock. Inasmuch as the current is mainly transmitted through the rock in the form of electrolytic conduction, the resistivity of the interstitial formation water seems to be the deciding factor in the formation resistivity as a whole. The presence of clay, however, greatly affects the electrical resistivity of the formation, specially in the case of fresh formation water (Anbah et al., 1965).

Although the electrokinetics depends mainly on the imposed electrical potential gradient, yet the associated electrical current is conditioned by the type of formation under consideration and its electrolytic content. There is no simple relation between the amount of liquid transported by electrokinetics and the quantity of electricity consumed. The presence of expandable colloidal matter in a microporous media further complicates

the picture.

In field application, the energy consumption will depend on the dimensions of the electrodes, the applied electrical potential, and the underground condition. If these factors are known, the amount of transmitted electrical current can be estimated. Upon switching the current on, it will drop gradually because the over-all resistance will increase.

The total amount of current transmitted (I) for various electrode arrangement can be estimated (Rudenberg, 1945; Casagrande, 1949) by using equations such as those presented below:

(a) For two cylindrical electrodes of equal length and cross- sectional area:

$$I = \frac{2\,\Pi\,L\,E}{\rho\,ln\frac{d}{r}} \tag{1-20}$$

where ρ is the formation resistivity in ohm-meters; L and r are the length and radius of the electrode in meters, E is the imposed electrical potential in volts; and d is the distance between the anode and the cathode in meters.

(b) For two cylindrical electrodes with different radii:

$$I = \frac{\Pi\,L\,E}{\rho}\left(\frac{1}{ln\,\frac{d}{r_1}} + \frac{1}{ln\,\frac{d}{r_2}}\right) \tag{1-21}$$

(c) For a row of alternate anodes and cathodes the amount of electrical current can be given approximately by

$$I = \frac{N\,\Pi\,L\,E}{\rho}\left(\frac{1}{ln\,\frac{d}{r_1}} + \frac{1}{ln\,\frac{d}{r_2}}\right) \tag{1-22}$$

where *N* is the number of electrodes in each group.

(d) For spherical flow of current from a sphere with radius *a* to a distance *x* in the ground,

$$I = \frac{2\,\Pi\,E}{\rho}\left(\frac{1}{a} + \frac{1}{x}\right) \tag{1-23}$$

and when *x* approaches infinity, $\frac{1}{x}$ goes to zero and

$$I = \frac{2\,\Pi\,E}{\rho\,a} \tag{1-24}$$

Before one can proceed with estimating the consumption of power, some assumptions have to be made. The following estimation of the current application,

because it is very difficult to estimate the decrease in the current flow as a result of the increase in the overall resistance. On assuming that (1) the electrical current is available at the electrode; (2) the formation resistivity is constant and is equal to 10 ohm-meters; (3) the electrode-length and radius are equal to three and 0.1 meters, respectively; (4) the applied potential is equal to 100 volts, and (5) the distance between electrodes is equal to 40 meters (Anbah et al., 1965) and substituting the above values in Eq. 1-21:

$$\mathrm{I} = \frac{2*3.14*3*100}{10*\frac{\ln 40}{0.01}} = 31.4 \text{ amps}$$

Thus, the power consumption is then equal to

$$31.4 * \frac{100}{1000} = 3.14 \text{ Kw}$$

The approximate cost of electricity (at \$0.059/Kw.-hr.) = 3.14 x 24 x 0.059 = \$ 4.45 per day per well. If the labor cost is assumed to be \$50 per day per well, then the total cost becomes \$230.76 per well per day (See Handbook of Construction Cost, Halbert Powers Gillette, 2006.). It is assumed that the equipment needed (electronic power supply, electrodes, power cables, etc.) will cost approximately \$55,000 per well. If the estimated life of the equipment is five years and its salvage value is 11,000, then by using straight-line depreciation at 6 per cent average interest, the annual depreciation plus interest is equal to \$10,494 per well (Modified after Anbah et al. 1965).

According to laboratory experimental results and the application of electrokinetics in related engineering field, an average increase in the electrokinetics flow rate of water (corresponding to 3.14 KW-hr.) can be estimated as 0.75 cc./sec. or 41.7 B/D. If it is further assumed that a piston like displacement of water to oil (banking) takes places, an

average increase in the oil produced is estimated to be 13.9 B/D per well. The annual gross dollar return (at $70/Bbl) is equal to $355,145.00, and after CMR tax (at $6/Bbl) is equal to $324,704.00. This value minus the annual labor and electricity cost will give the net annual profit of: $324,704.00 - $84,227.40 = $240,476.60. The net profit is approximately equal to 240,476.60/10,494.00 ≈ $22.92 dollar returned per dollar invested (modified after Anbah et al., 1965).

These sample calculations are presented here in order to indicate the possibility of such application in the field. It should be kept in mind, however, that for field application the current is best applied in an interruptive manner which will cause a considerable saving in power consumption. For the purpose of well stimulation, the application of current may not exceed a period of one to two weeks. It is believed that such short electrical treatment may lead to 50 or even 100 per cent increase in the average flow rate of oil and water

The economic feasibility of using this technique in oil production will be more apparent in a large-scale field application. In order to ensure optimum results, it is strongly recommended that such large-scale application should be preceded by a flood pot test followed by a pilot test (Anbah et al., 1965).

Chapter 2

Apparatus

As an introduction, it is important to show the equipment initially used in the Petroleum Engineering Department of the University of Southern California (Figures 2-1 and 2-2) The equipment used by Dr. S. Pamukcu (Figures 2-3 and 2-4) and Dr. .M. Haroun (Figure 2-5) are also presented here. Figure 2-6 shows the equipment used by the writer.

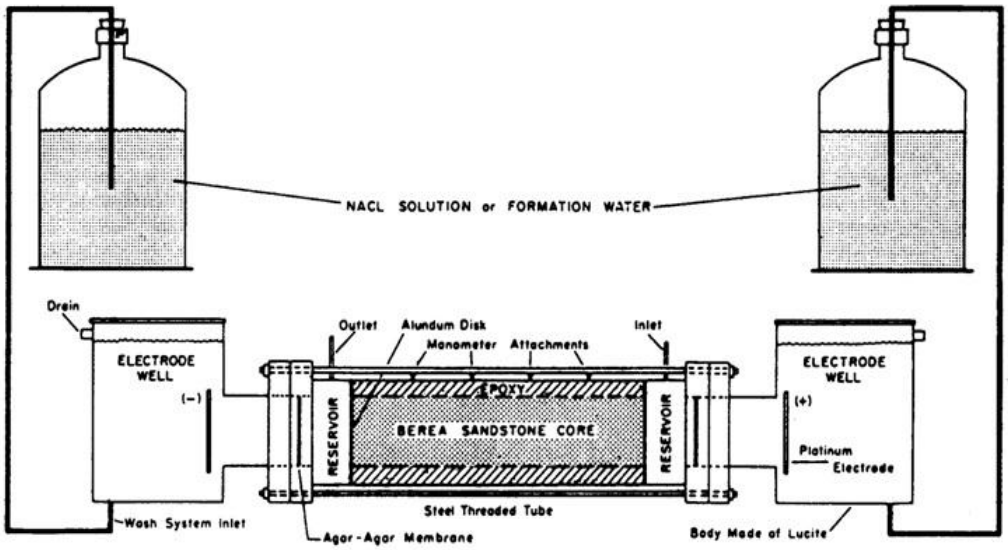

Figure 2-1: A schematic diagram showing the first apparatus and connections used in Petroleum Engineering Laboratories at the University of Southern California. (Personal communication with Dr. George V. Chilingar.)

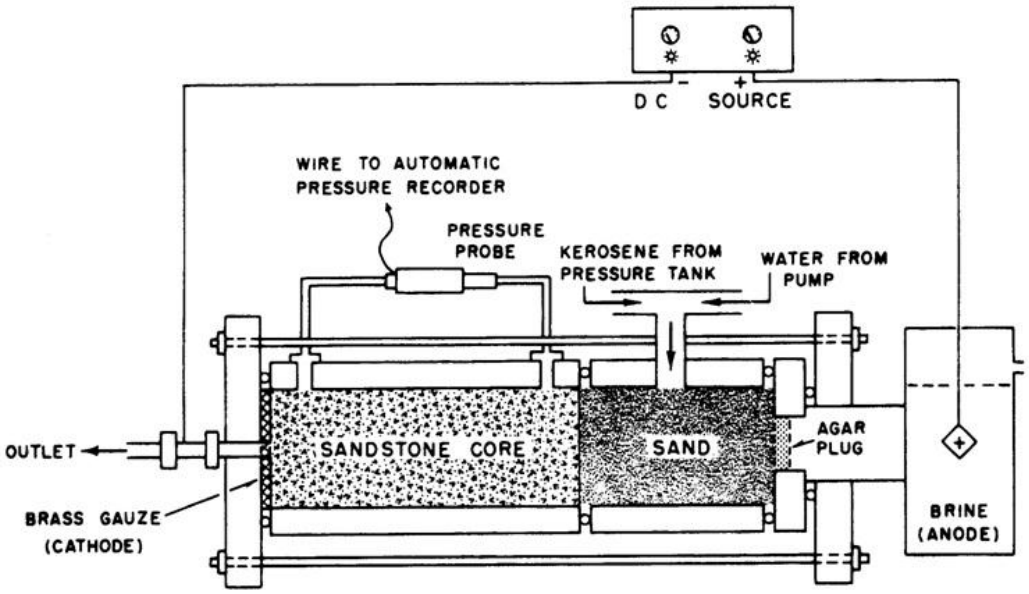

Figure 2-2: Schematic diagram of second apparatus and connections used in Petroleum Engineering Laboratories at the University of Southern California. (Personal communication with Dr. George V. Chilingar.)

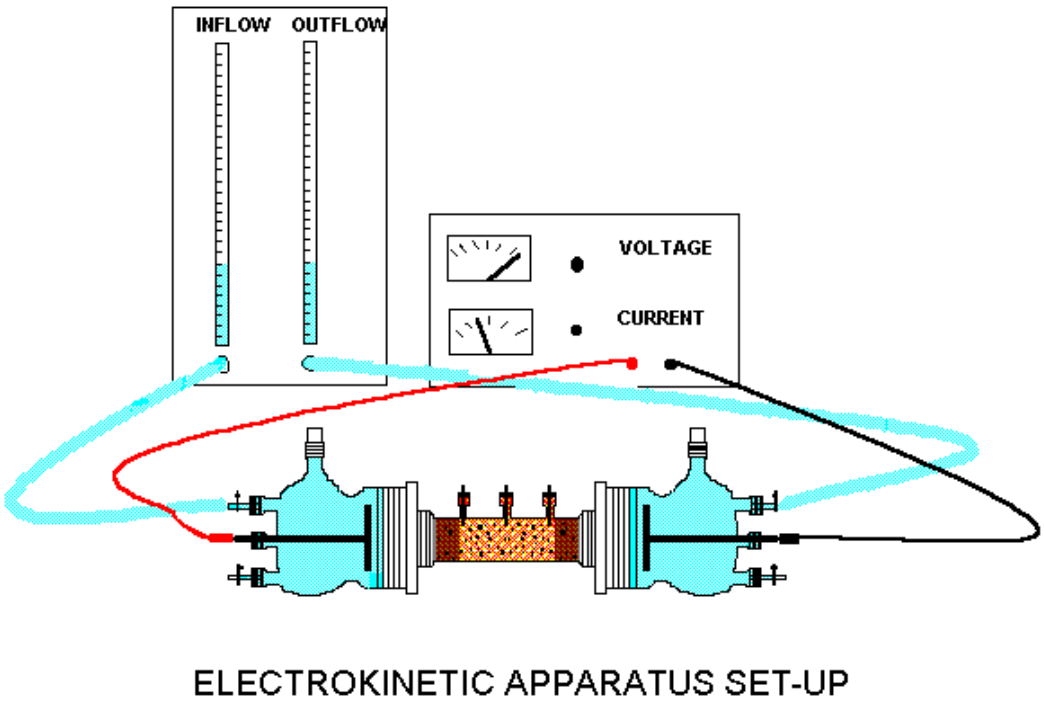

Figure 2-3: Electrokinetic apparatus, DC power source and graduated glass burettes to measure both inflow and outflow at each of the two electrode ends (anode and cathode). Apparatus used by Dr. S. Pamukcu at Lehigh University.

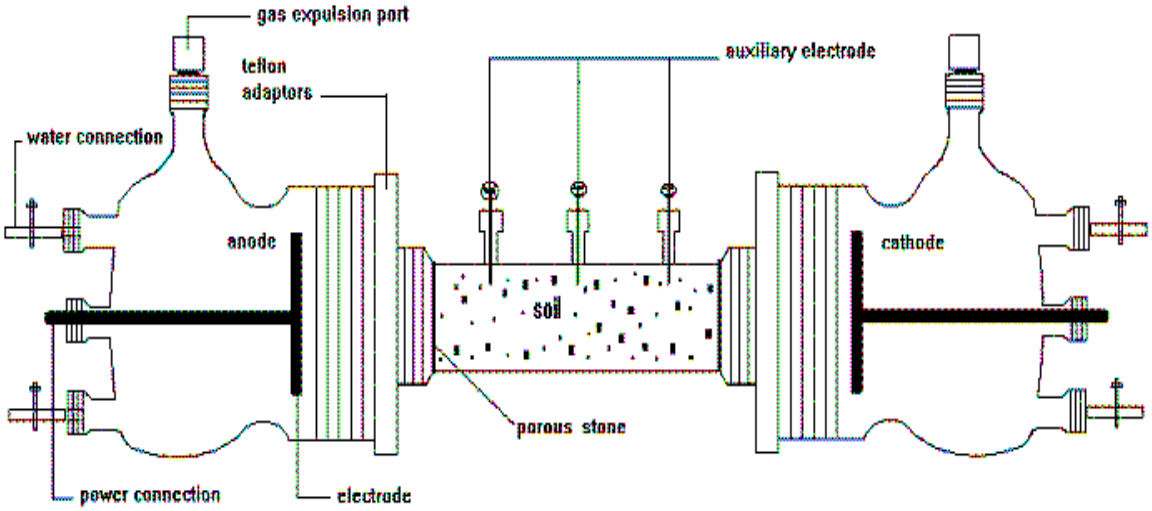

Figure 2-4: Schematic diagram of glass elektrokinetic cell. (After Pamukcu et al., 1993.)

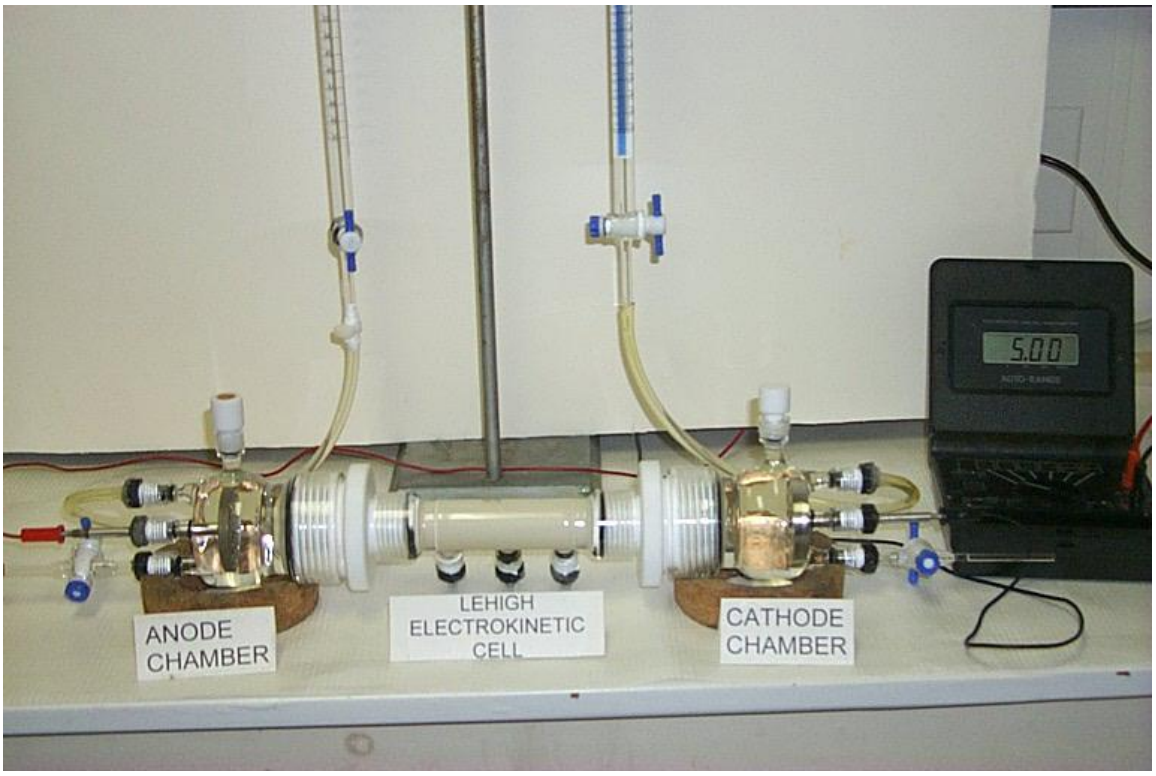

Figure 2-5: Photograph of electrokinetic apparatus and multimeter for measuring voltage, current and resistance used by Dr. M. Haroun.

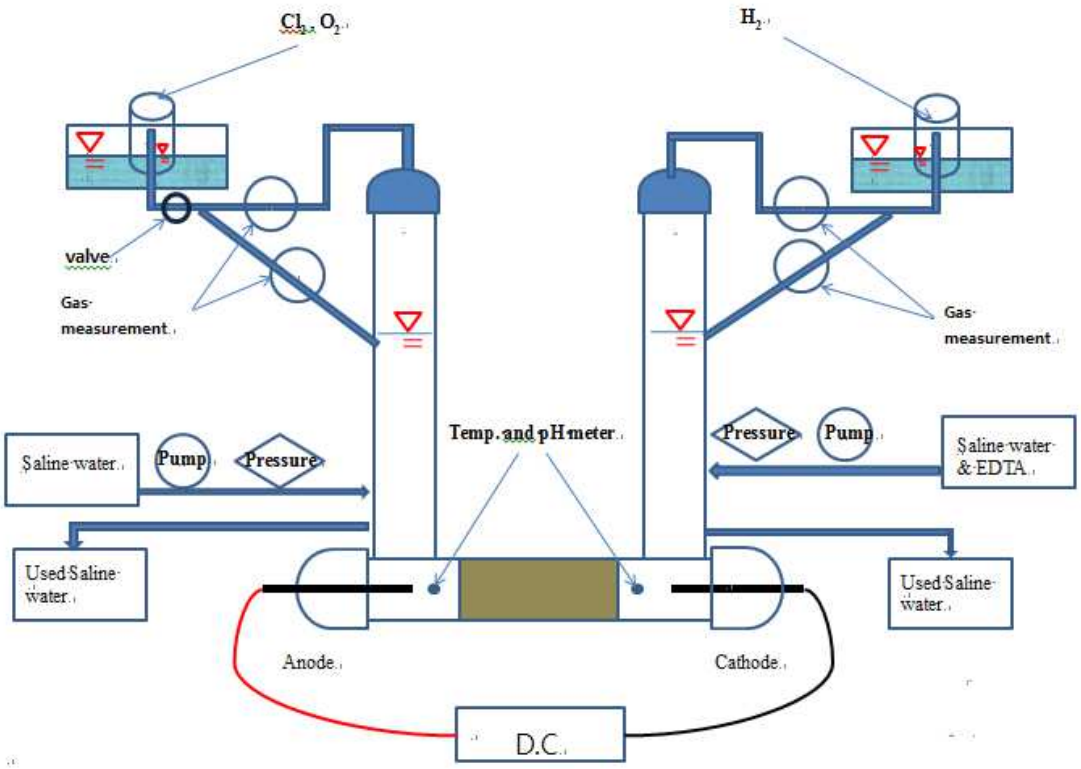

Figure 2-6: Apparatus used in electroremediation of heavy metals from offshore muds and sediments with partial chlorine gas removal equipment (controlling valve at left gas tank). Apparatus used by the writer.

2.1 Sampling Area in Abu Dhabi, U.A.E.

Samples were collected at three different locations: First Sample was collected near the refinery/ industrial area and bridge as shown in Figure 2-7, which was marked as 24^{o} 25’27” North, 54^{o} 29’ 30” East, Altitude 0 m. Second sample location is shown Figure 2-8; located near sewer -- 24^{o} 27’14” North, 54^{o} 24’ 19” East, Altitude 0 m. Sampling area near the port was selected as the third location (Figure 2-9); however, the size distribution of this sample was of sand size. All collected samples were sieved with 1-mm sieve for the removal of shells and other coarse materials before testing. All samples were collected by the writer.

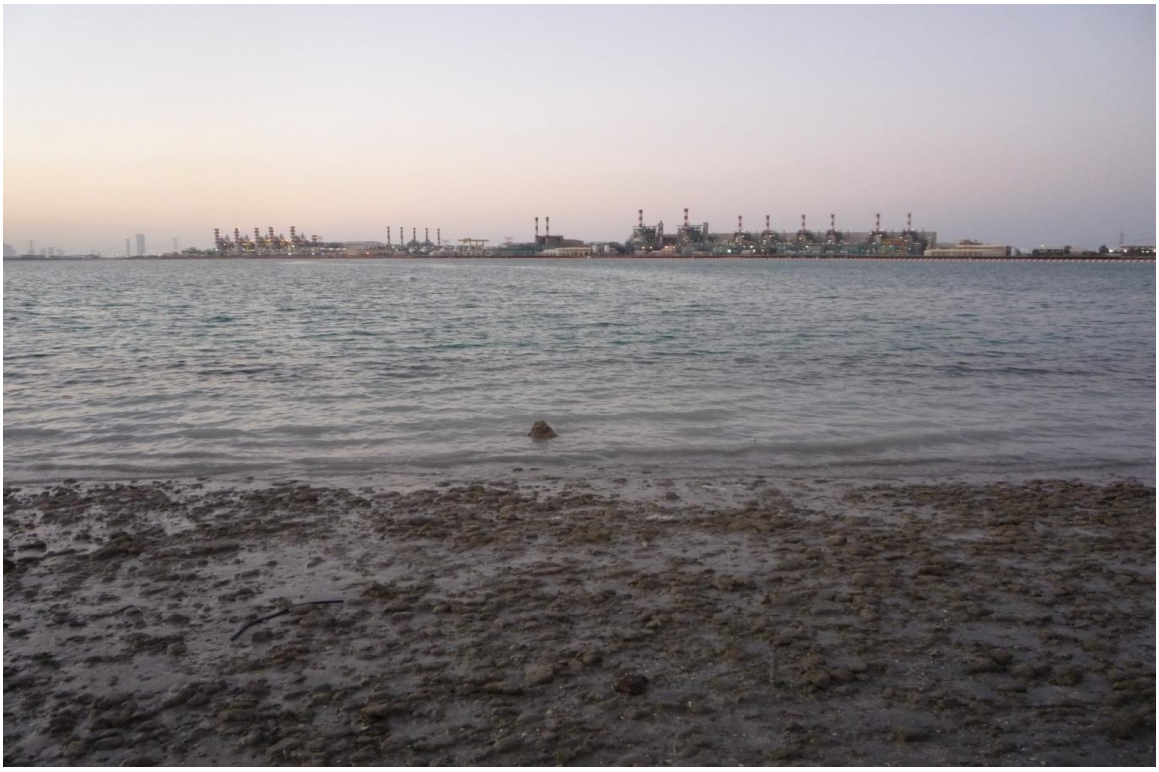

Figure 2-7: Sample location No. 1 near the refinery industrial area. (24^{o} 25’27” North, 54 ^{o} 29’ 30” East, Altitude 0 m)

Figure 2-8: Sample No. 2 location near the sewer outlet. (24^{o} 27’14” North, 54 ^{o} 24’ 19” East, Altitude 0 m)

Figure 2-9: Sampling area near the port (Sample No.3) in Abu Dhabi, U.A.E. (24^{o} 22’17” North, 54 ^{o} 28’ 2” East, Altitude 0 m)

2.2 Particle Size Distributions of Samples

The samples were sieved using the following procedures: ISO 3310-1:2000 (wet sieving) and BS ISO 11277:2009 (dry sieving). The water contents of samples were measured according to ASTM D2215-06. According to USDA, sediment size distribution was determined using the following classification: very coarse sand, coarse sand, medium sand, fine sand, very fine sand, silt and clay (See Table 2-I). Figure 2-10 shows the texture triangle proposed by USDA. Sieve analyses of samples are presented in Figs. 2-11 and 2-12.

Table 2-1: Sediment classification according to USDA sediment textural system (Modified)

Sediment	**Diameter limits (mm)** **(USDA Classification)**
very coarse sand	2.00 ~ 1.00
coarse sand	1.00 ~ 0.50
medium sand	0.50 ~ 0.25
fine sand	0.25 ~ 0.10
very fine sand	0.10 ~ 0.05
silt	0.05 ~ 0.002
clay	< 0.002

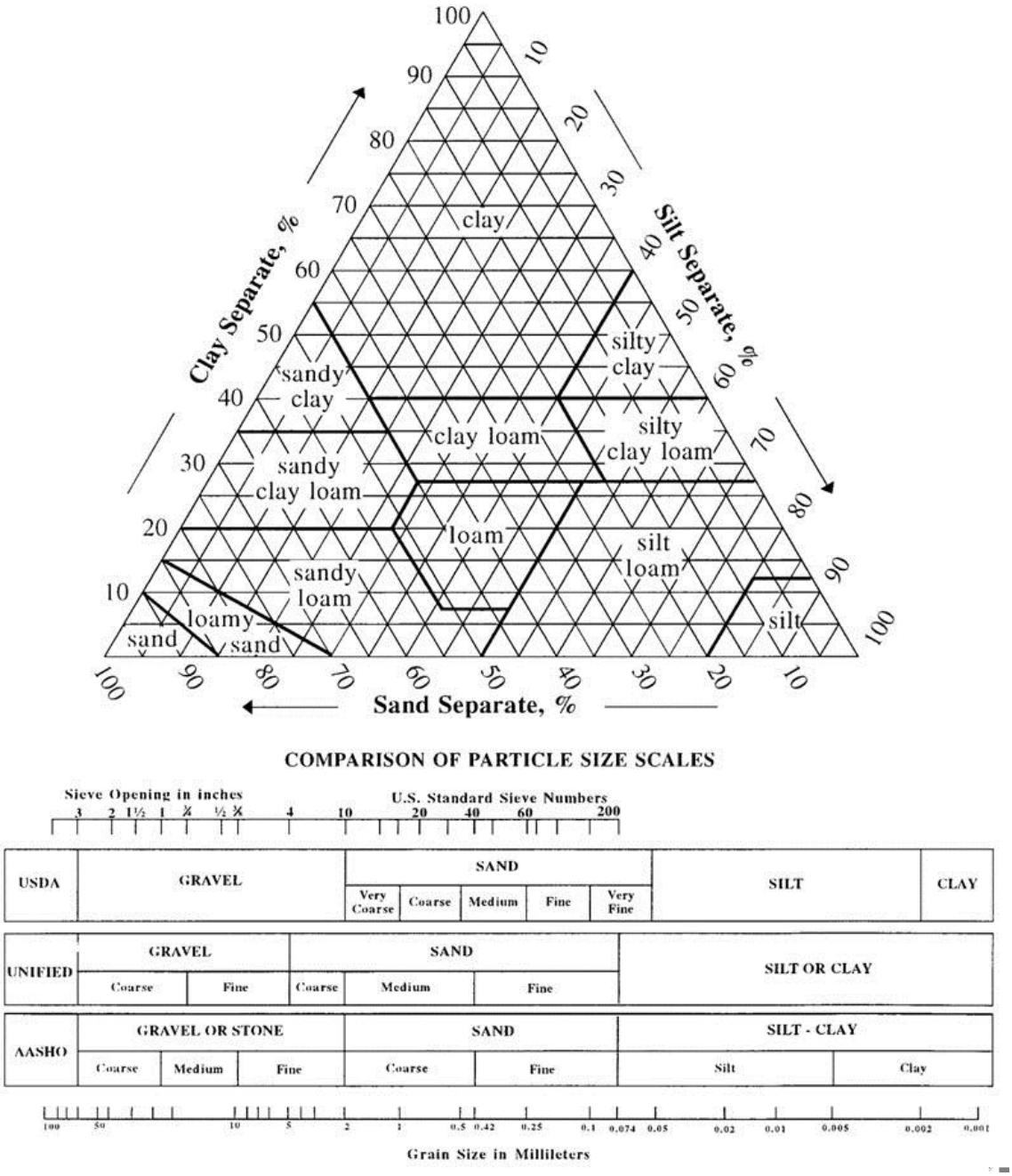

Figure 2-10: Sediment (soil) texture triangle (USDA).

Table 2-2: Particle size distribution of sample collected in Area No.1.

Opening (mm)	Sediment (g)	Cumulative Wt. (%)
2	1.72	0.688
0.5	10.26	4.792
0.25	28.65	16.252
0.125	66.72	49.94
0.063	105.23	85.032
Less < 0.063	37.42	100
-	250	-

Table 2-3: Particle size distribution of sample collected in Area No.2.

Opening (mm)	Sediment (g)	Cumulative Wt. (%)
2	2.2	0.215572
0.5	55.27	5.631332
0.25	86.22	14.0798
0.125	287.1	42.21197
0.063	438.11	85.1412
Less < 0.063	151.64	100
-	1020.54	-

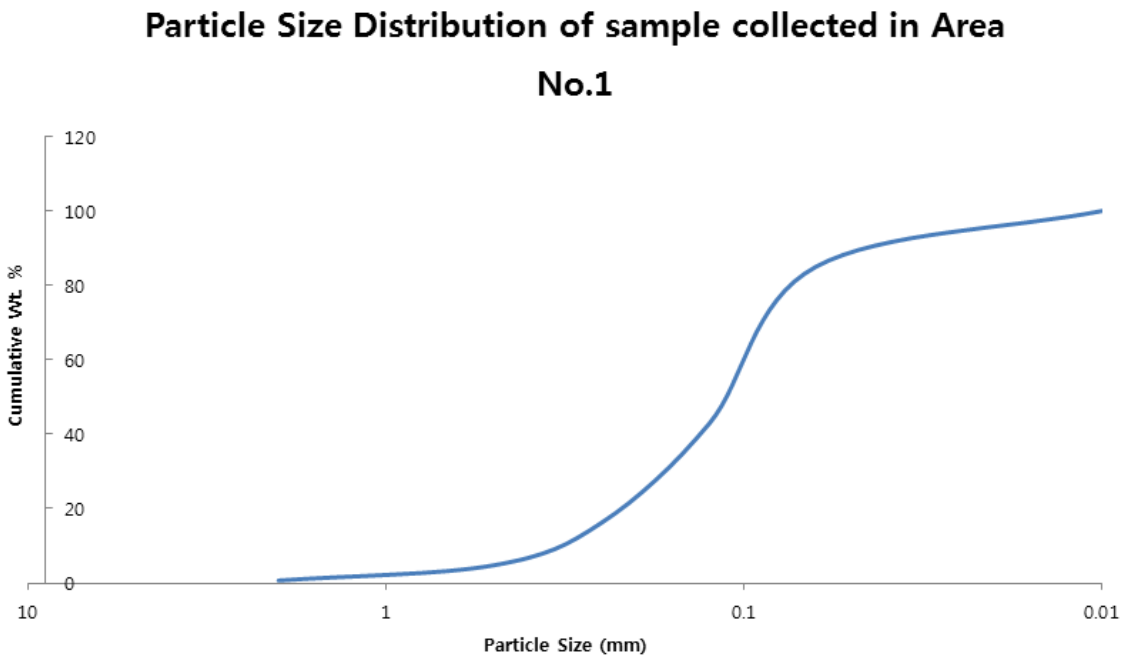

Figure 2-11: Particle size distribution curve of sample collected in Area No.1.

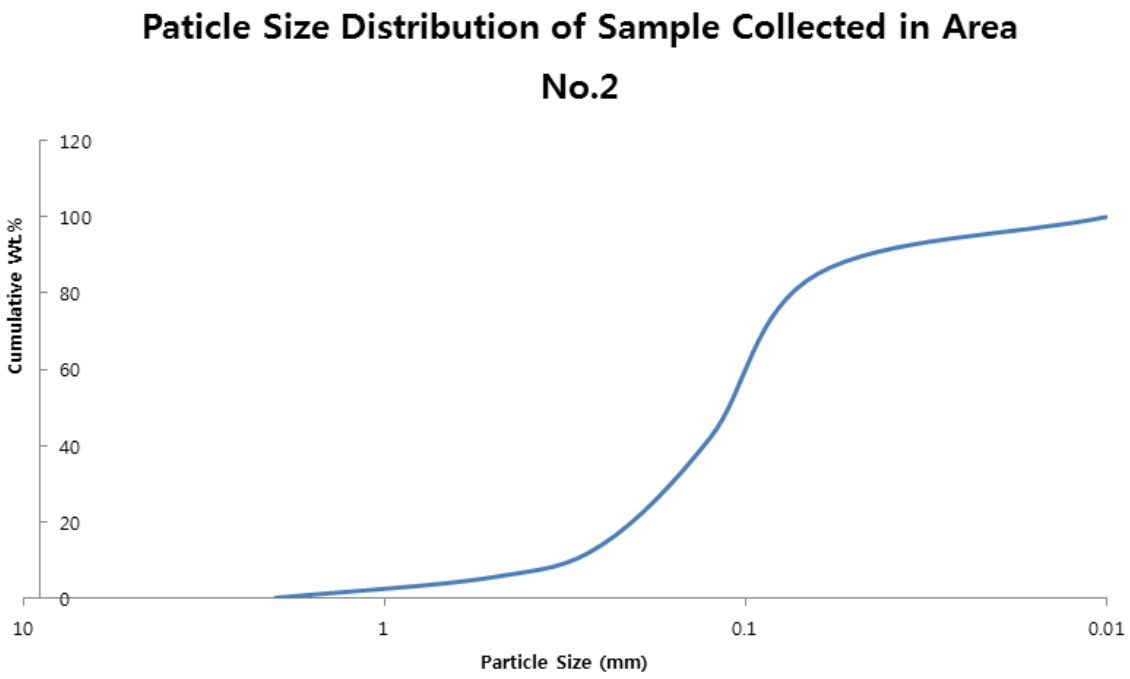

Figure 2-12: Particle size distribution of sample collected in Area No.2.

2.3 Preparation of Samples

The whole samples were consolidated for seven days at 30 psi pressure (Figure 2-13). The pressure was gradually increased until reaching 30 psi. After completion of tests, the EPA 3050b method was used to extract the heavy metals. Then, concentrations of metals were measured using ICP-MS equipment.

The diameter of the core pipe (P.V.C.) was 3.75 cm (1.5 inch). The length was 10 cm, 20 cm, and 30 cm. Silicon, teflon tape and rubber O-rings were used for connecting the sample chamber of consolidated sample to the anode chamber and cathode chamber.

The volumes of cathode and anode chambers were 1000 ml each. Cathode and anode chambers are at the same elevation.

Carborandum porous stones, which were installed in the end of the sample, had a permeability of 10^{-3} cm/sec. They are highly porous compared to the muds tested, which have hydraulic permeability ranging from 10^{-6} to 10^{-8} cm/sec (Haroun, 2009). The porous stones were cleaned with diluted strong acid such as hydrochloric acid, sulfuric acid, or nitric acid and then placed in the boiling de-ionized water before using them.

The diameter and length of electrodes, which were composed of graphite, was 0.635 cm and 12 cm. Total surface area calculated was 24.56 cm^2 ; however, the surface area reacted was approximately 20.56 cm^2 as 10 cm which is reached with the solution at each chamber.

Fluid connections: Teflon or stainless steel quick-connections were provided on the bottom of the back wall of the electrode chambers. These outlet or inlets are then

connected to volume measuring tubes and pumped via Teflon tubing. The advantage of the quick connections is that they close the connection upon detachment, which allows the electrokinetic (EK) cell to be detached from the control panel while the electrode chambers are still being charged with fluid.

Gas expulsion or sample extraction/injection ports: These ports are pressure valves provided on the cover plate over each electrode chamber. These valves have metal surfaces which are coated to control any deterioration by electrochemical reactions or metal ion deposition on them. Sample extractions or fluid injections are accomplished using a volumetric syringe which allows for accurate control of quantities of fluids.

Power supply: Variable direct current (DC) power supply was used capable of applying either constant voltage (0 to 105 volts), or constant current (0 to 2500 mA). These units also contain analog meters for measuring voltage and current.

Compaction Apparatus: A schematic diagram of the compaction apparatus used is shown in Fig. 2-13. The apparatus consists of a PVC sample cell (guide tube) measuring 45.72 cm in length by 2.67 cm in diameter, in to which the slurry sample is injected. The weight base with compacting column causes a piston - like displacement based on choice of several weights that allow for a varied pressure range of 5 psi to 30 psi. This is then placed on top of the injected slurry that's contained within the PVC sample cell with the porous stone placed at the bottom end. The weights are placed in the tray at the top of the compacting column in progressive increments, throughout a period of 24 hours reaching to a final pressure of 30 psi. During compaction, fluid is drained at the top and bottom of the sample via porous stones resting on both ends of the core.

Muds are prepared by mixing an aqueous solution of the desired contaminant with the mud. After the 24-hour period of compaction, all the samples had a water content of 40% recorded as the initial water content before the E-K test.

Electrokinetics Testing: In all experiments, a constant 20-volts DC potential was applied across the core samples. The current density was recorded. This is done using a multi-meter to read voltage across the E-K apparatus via power connections to each of the primary electrodes and on the secondary electrodes along the sample tube. Readings were taken at 0, 15 and 30 minutes and one and two hours after the start of the test (Pamukcu et al., 1993). During cell disassembly, the pH of the anode and cathode fluid was recorded and a sample was taken for analysis. Finally the mud was extruded from the core sample and measurements were made at 5 evenly spaced points along the length of core for pH, water content and redox-potential in volts (Pamukcu et al., 1993).

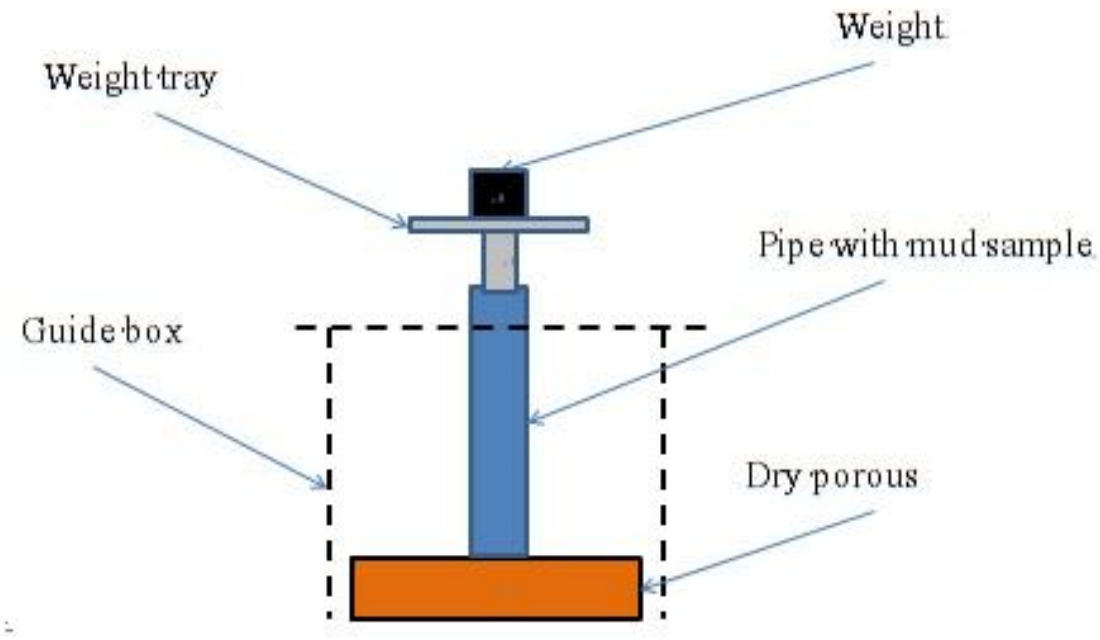

Figure 2-13: The consolidation equipment setup used to prepare samples.

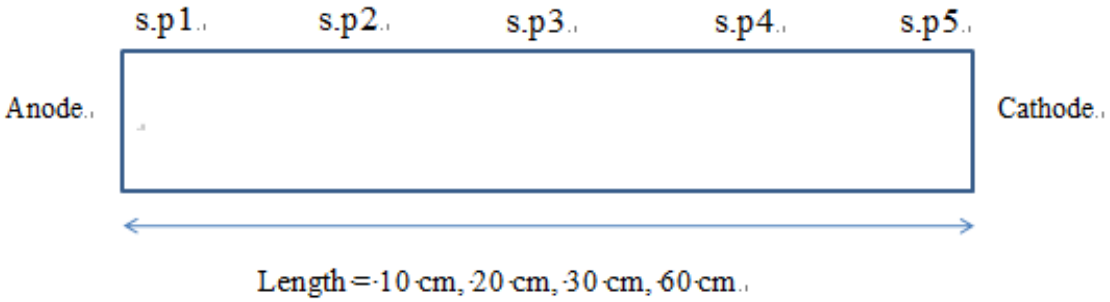

s.p1 = 1 cm from anode.

s.p5 = 1 cm from cathode.

s.p3 = mid-point.

s.p2 = middle between s.p1 & s.p3.

s.p4 = middle between s.p3 & s.p5.

Figure 2-14: Sampling locations

Chapter 3

Experiment Results

In order to determine the optimum voltage gradient required in electroremediation of various heavy metals, the following experiments were performed.

3.1Removal of Heavy Metals upon Application of D.C. Current Using Different Voltage Gradients for the Following Metals: Al: Aluminum, As: Arsenic, Cs: Cesium, Cr: Chromium, Se: Selenium, Pb: Lead and Zn: Zinc.

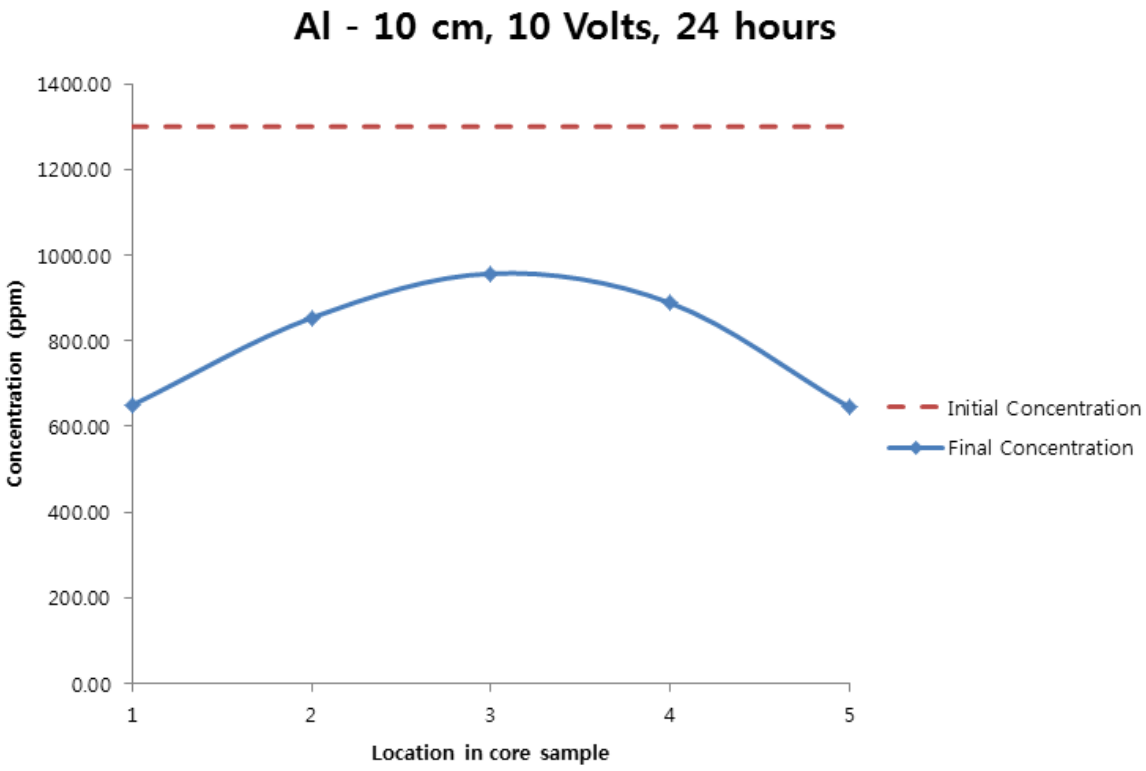

Figure 3-1: Concentration of Al upon EK treatment. – Length: 10 cm, 10 Vol., Treatment time: 24 hours.

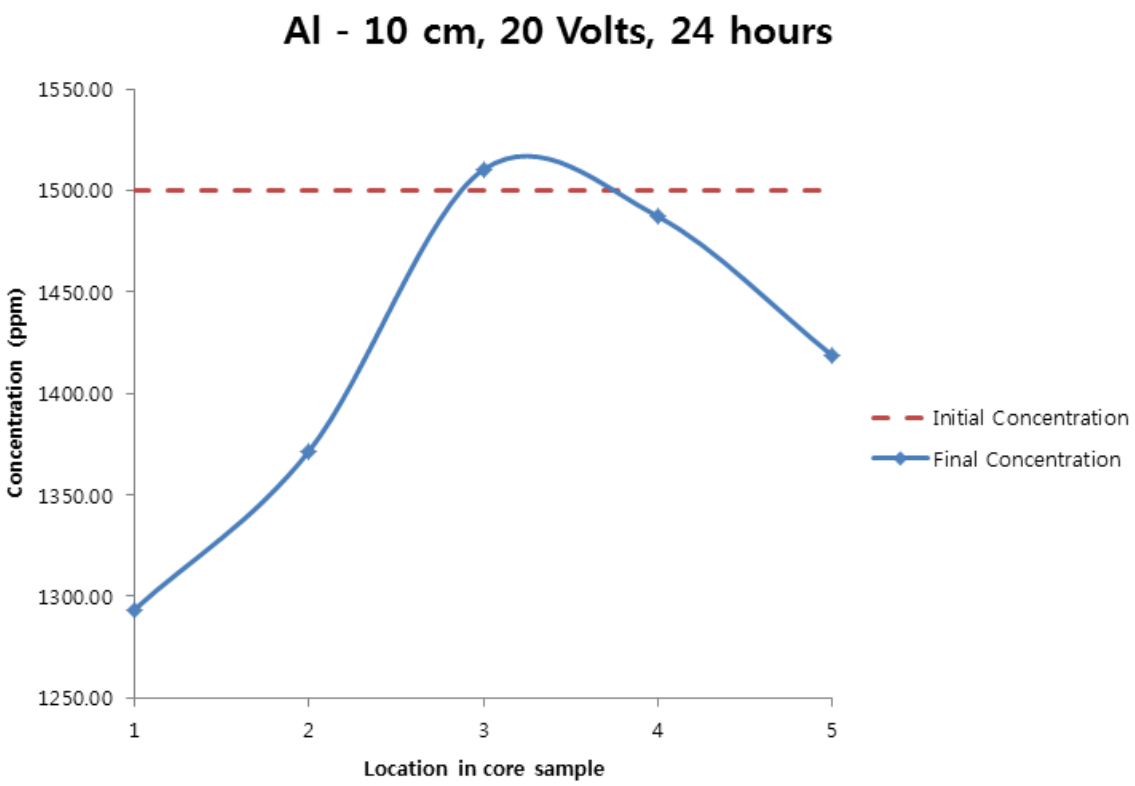

Figure 3-2: Concentration of Al upon EK treatment. – Length: 10 cm, 20 Vol., Treatment time: 24 hours.

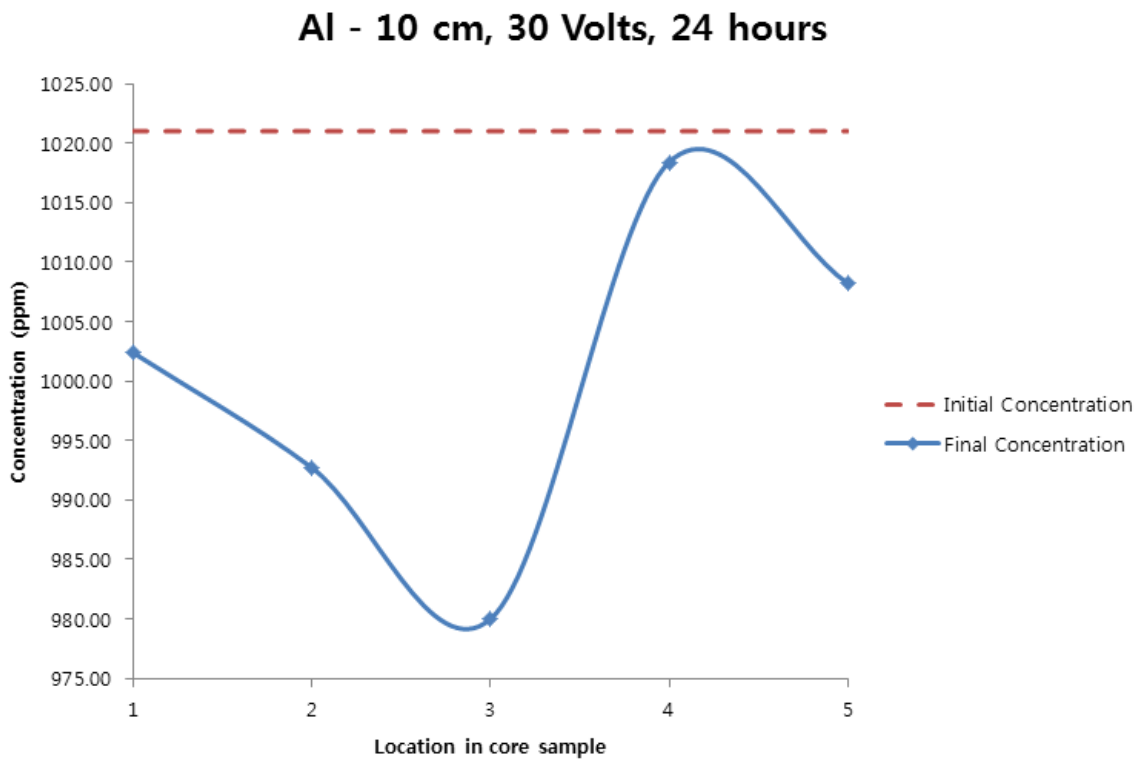

Figure 3-3: Concentration of Al upon EK treatment. – Length: 10 cm, 30 Vol., Treatment time: 24 hours.

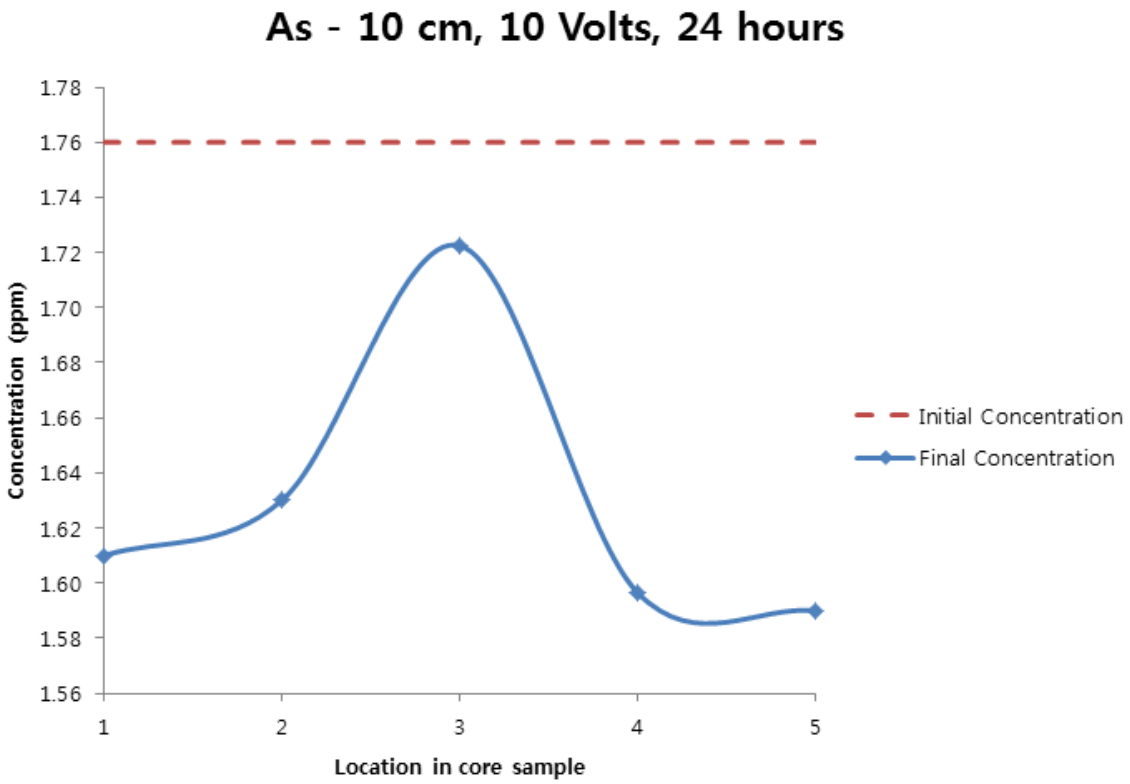

Figure 3-4: Concentration of As upon EK treatment. – Length: 10 cm, 10 Vol., Treatment time: 24 hours.

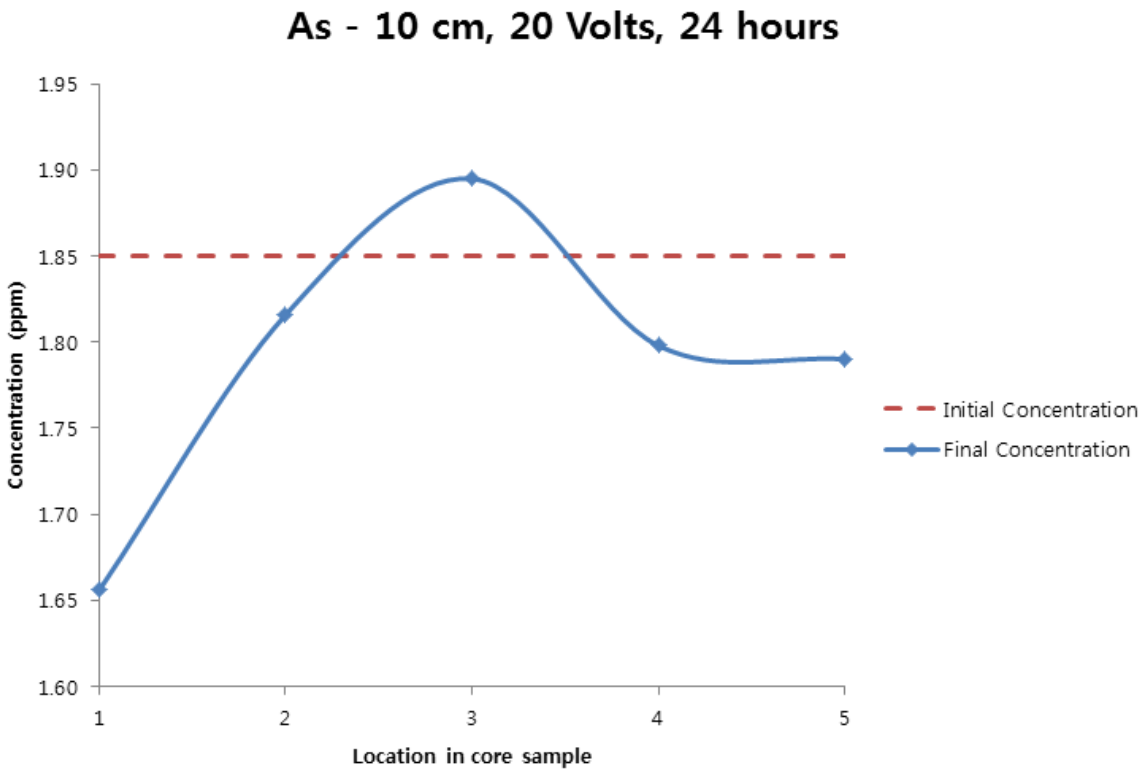

Figure 3-5: Concentration of As upon EK treatment. – Length: 10 cm, 20 Vol., Treatment time: 24 hours.

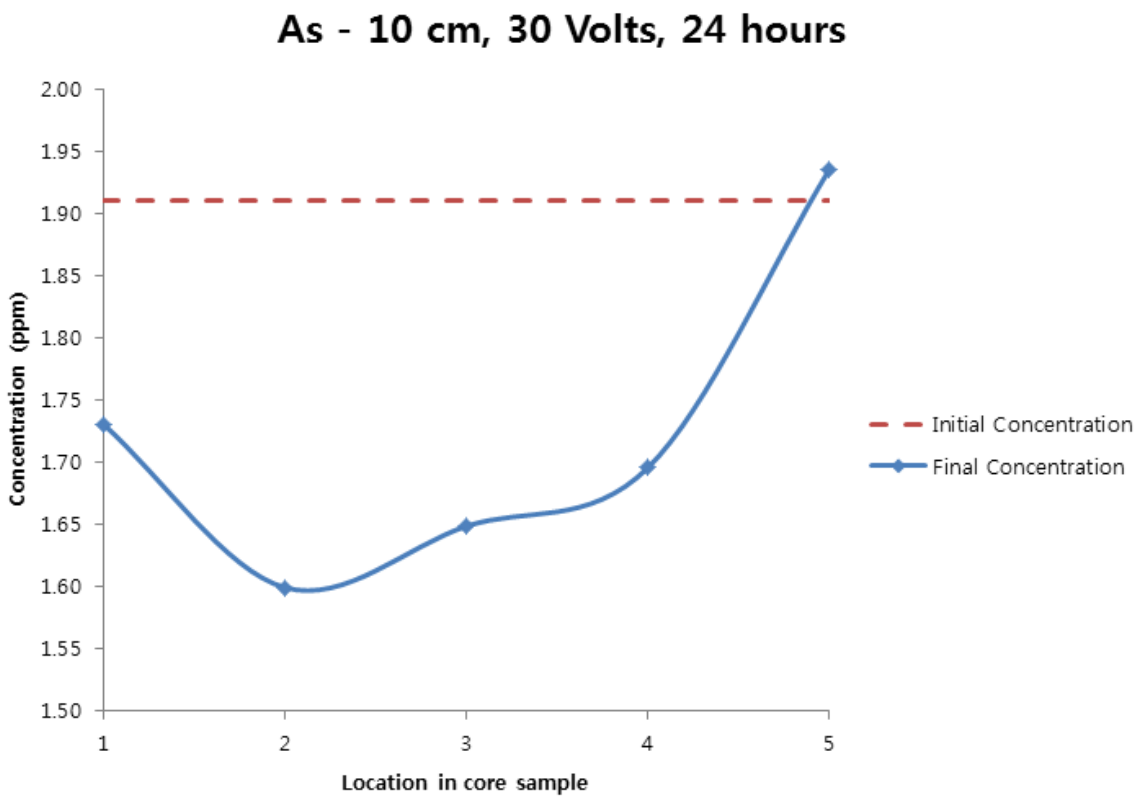

Figure 3-6: Concentration of As upon EK treatment. – Length: 10 cm, 30 Vol., Treatment time: 24 hours.

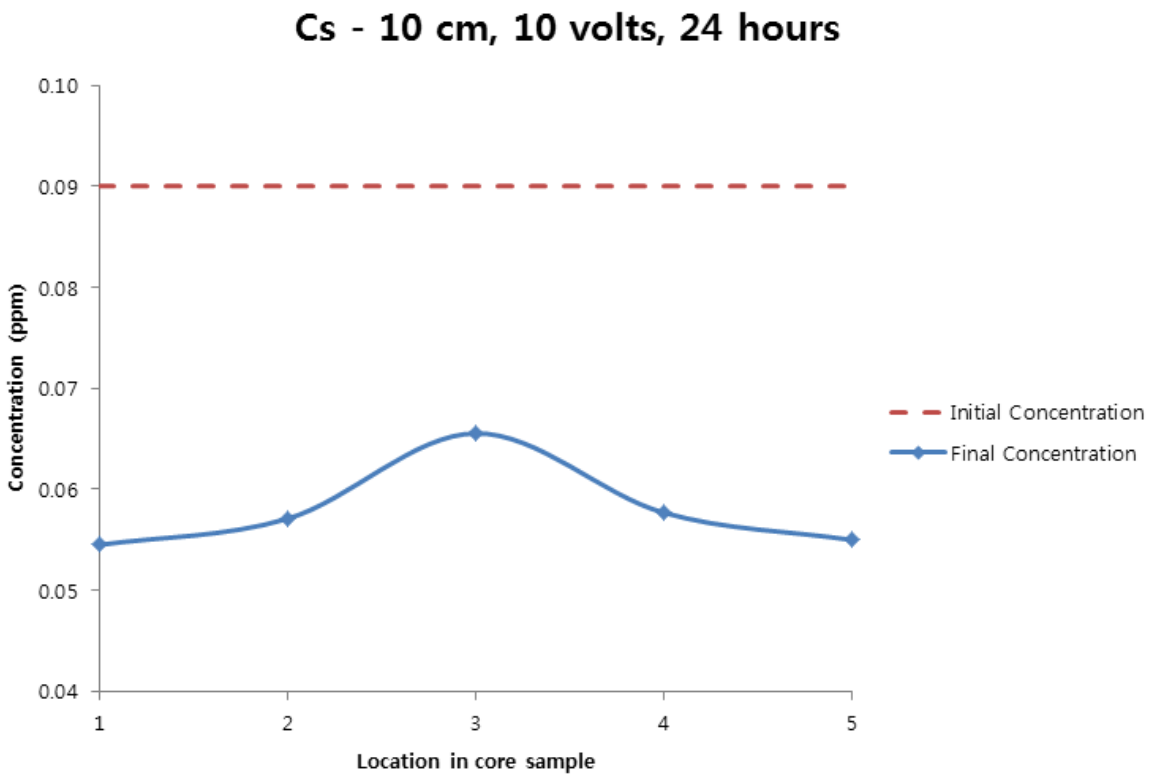

Figure 3-7: Concentration of Cs upon EK treatment. – Length: 10 cm, 10 Vol., Treatment time: 24 hours.

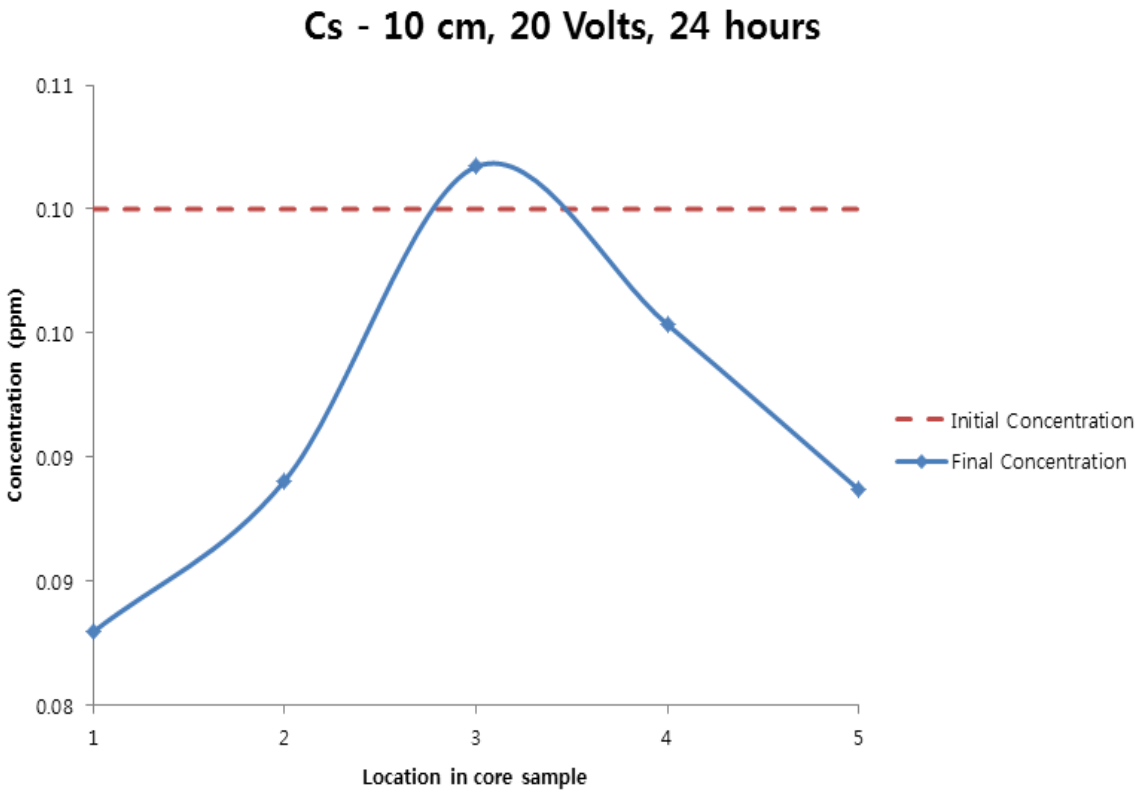

Figure 3-8: Concentration of Cs upon EK treatment. – Length: 10 cm, 20 Vol., Treatment time: 24 hours.

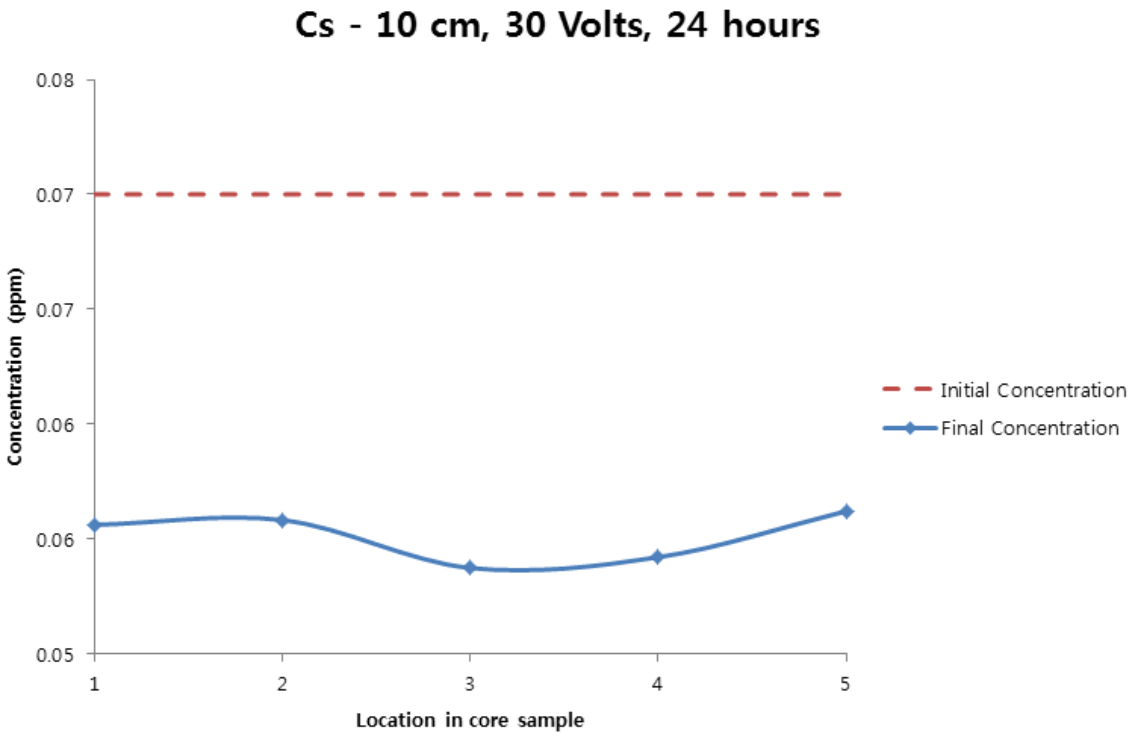

Figure 3-9: Concentration of Cs upon EK treatment. – Length: 10 cm, 30 Vol., Treatment time: 24 hours.

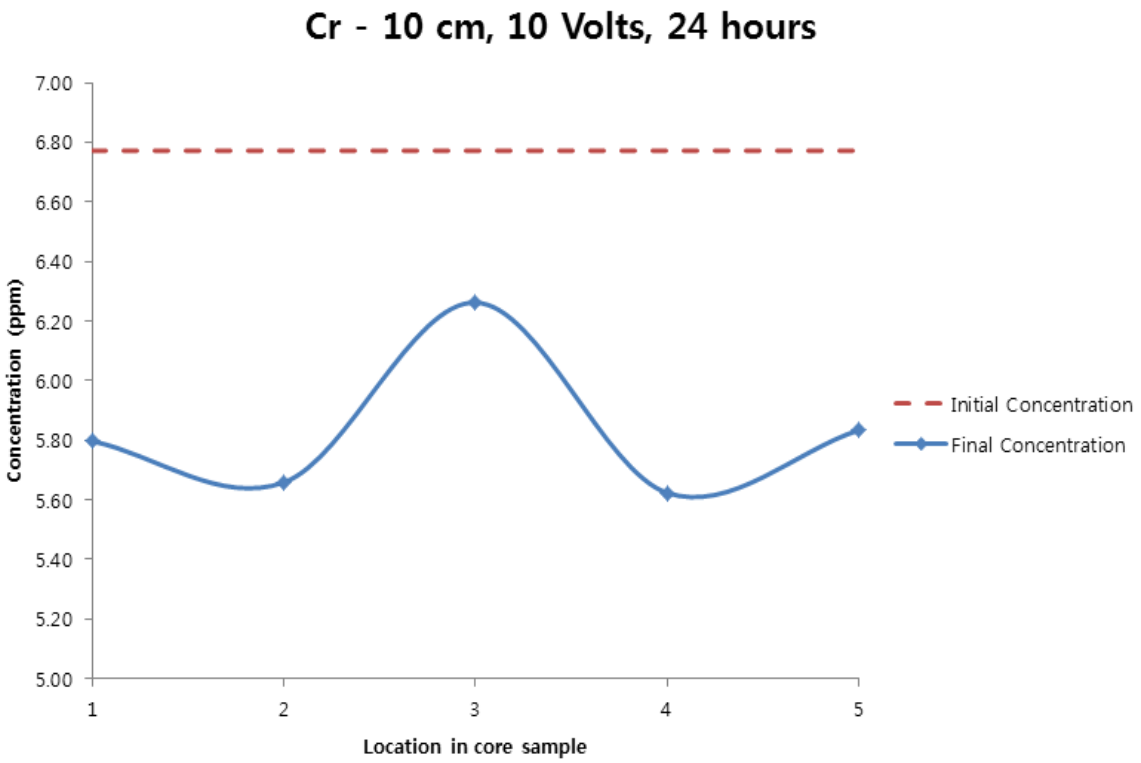

Figure 3-10: Concentration of Cr upon EK treatment – Length: 10 cm, 10 Vol., Treatment time: 24 hours.

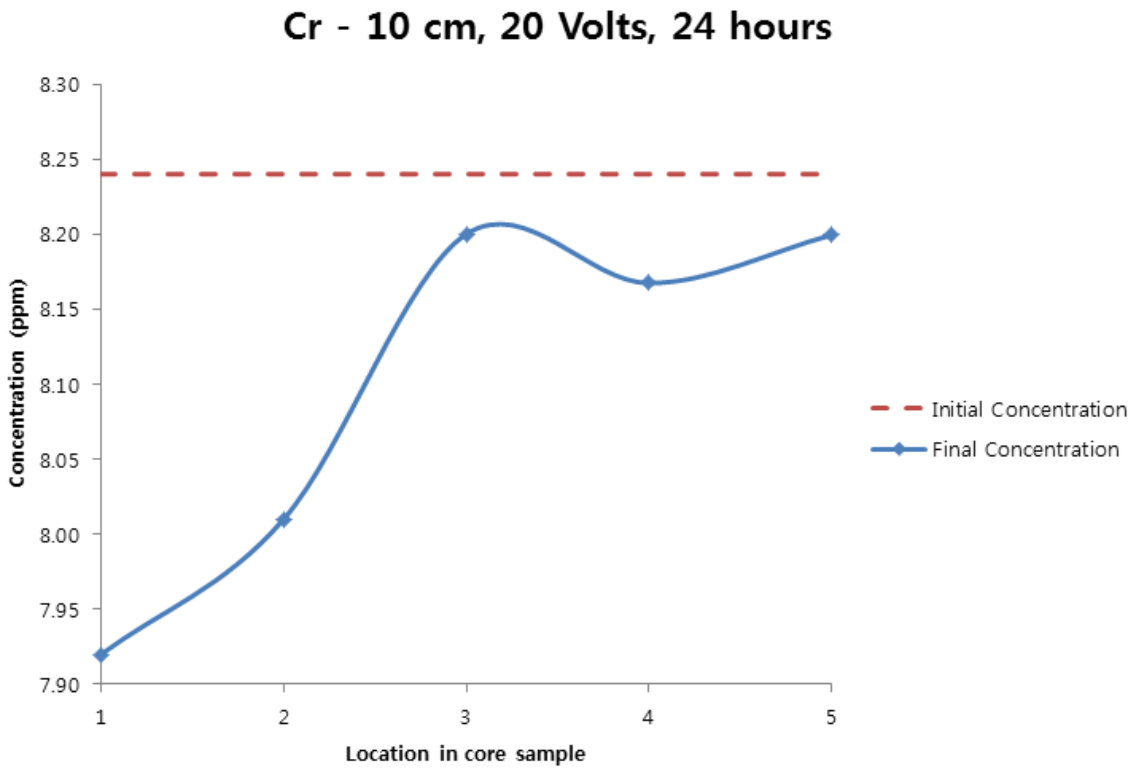

Figure 3-11: Concentration of Cr upon EK treatment – Length: 10 cm, 20 Vol., Treatment time: 24 hours.

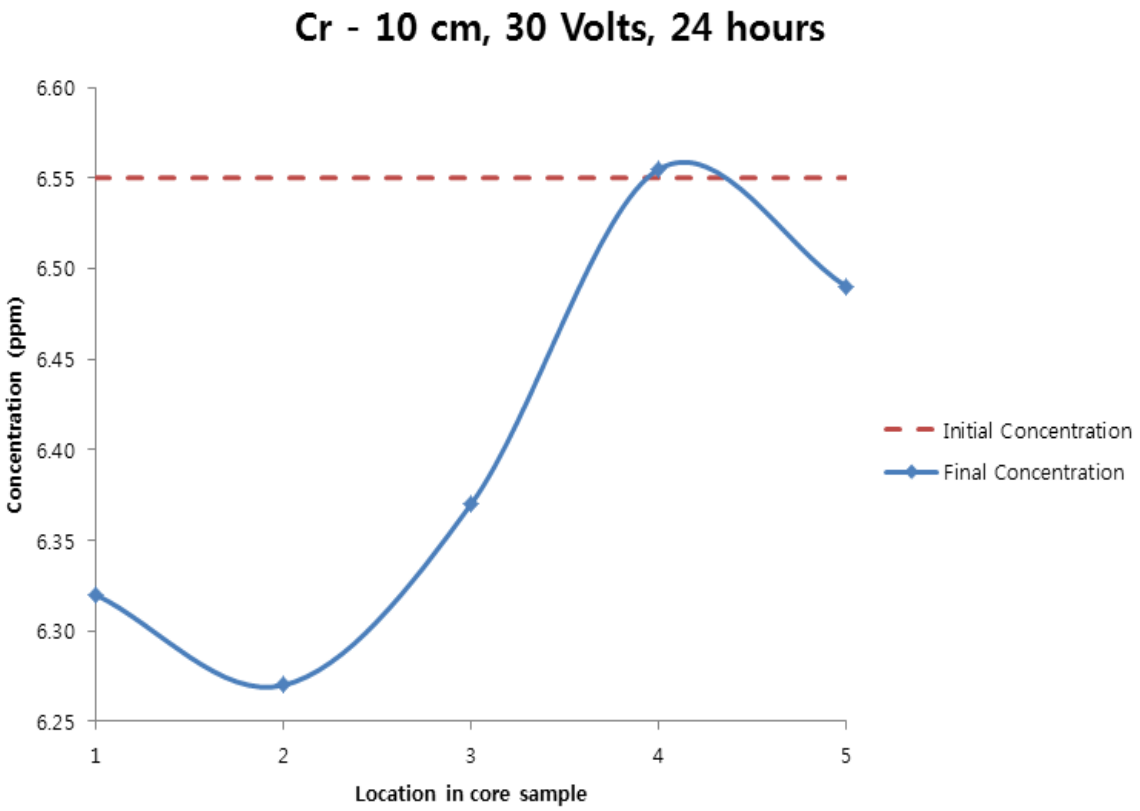

Figure 3-12: Concentration of Cr upon EK treatment.– Length: 10 cm, 30 Vol., Treatment time: 24 hours.

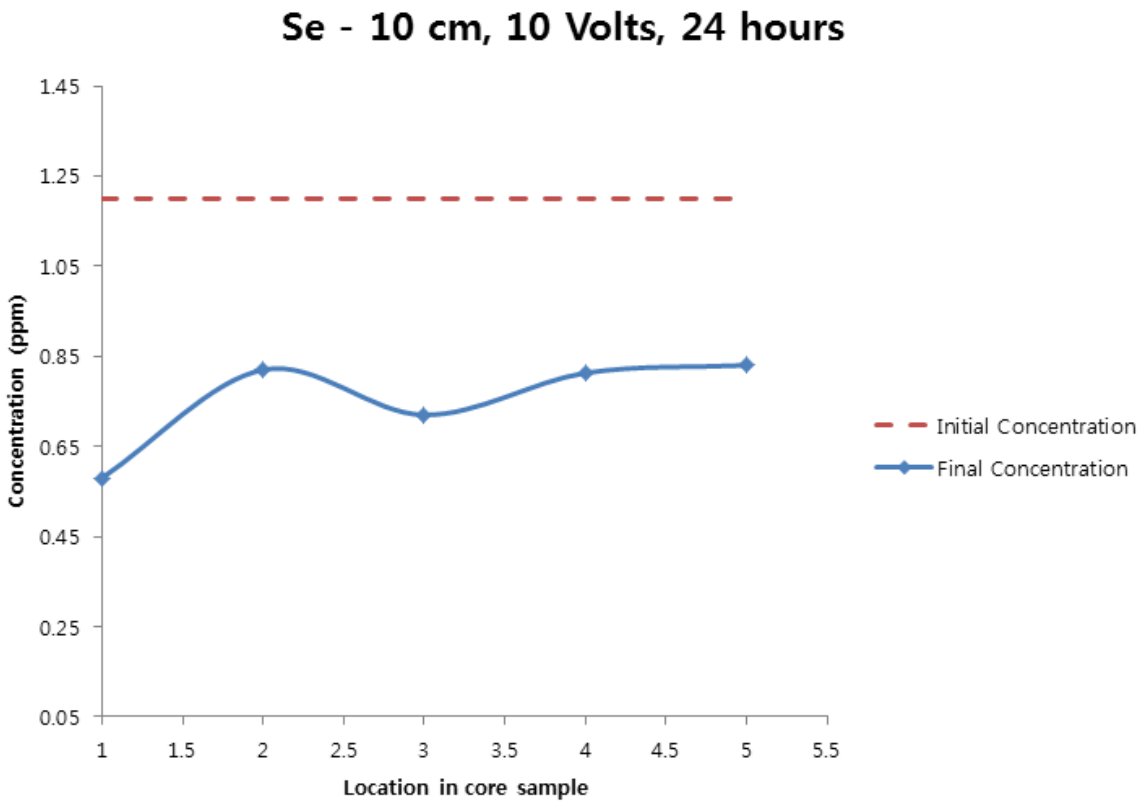

Figure 3-13: Concentration of Se upon EK treatment. – Length: 10 cm, 10 Vol., Treatment time: 24 hours.

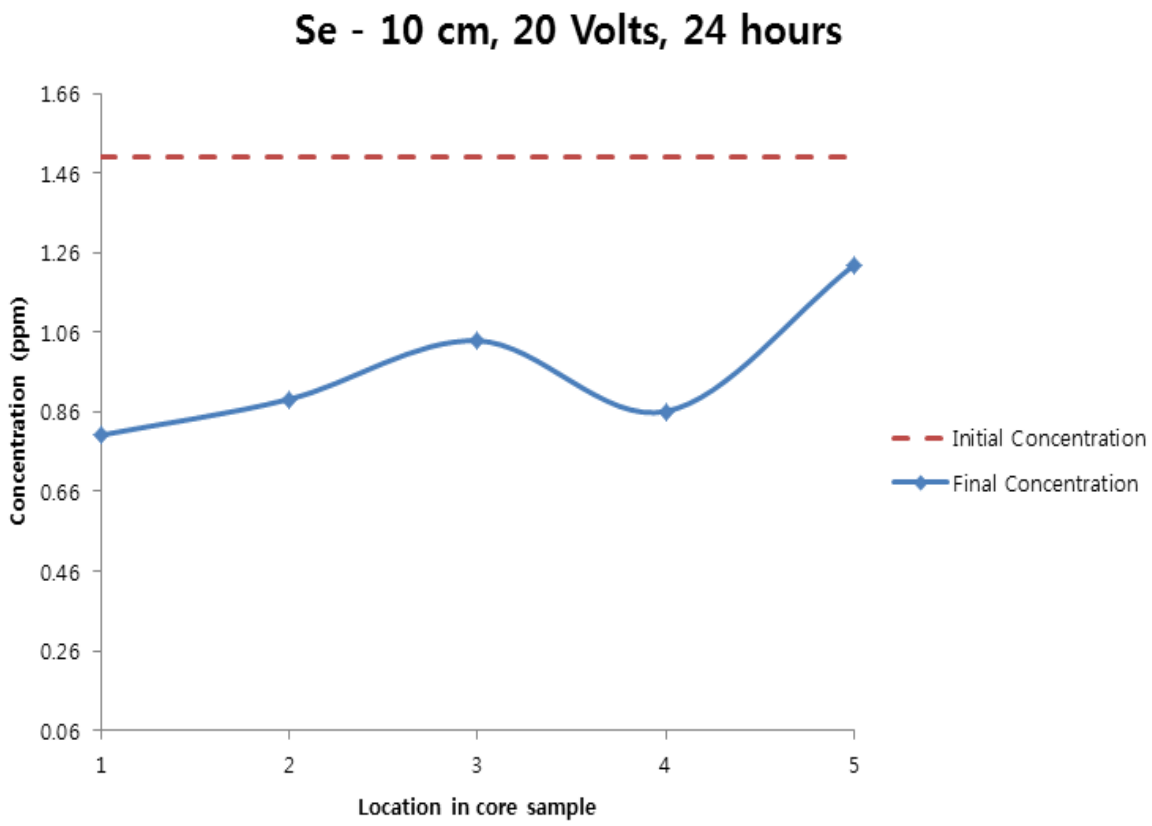

Figure 3-14: Concentration of Se upon EK treatment.– Length: 10 cm, 20 Vol., Treatment time: 24 hours.

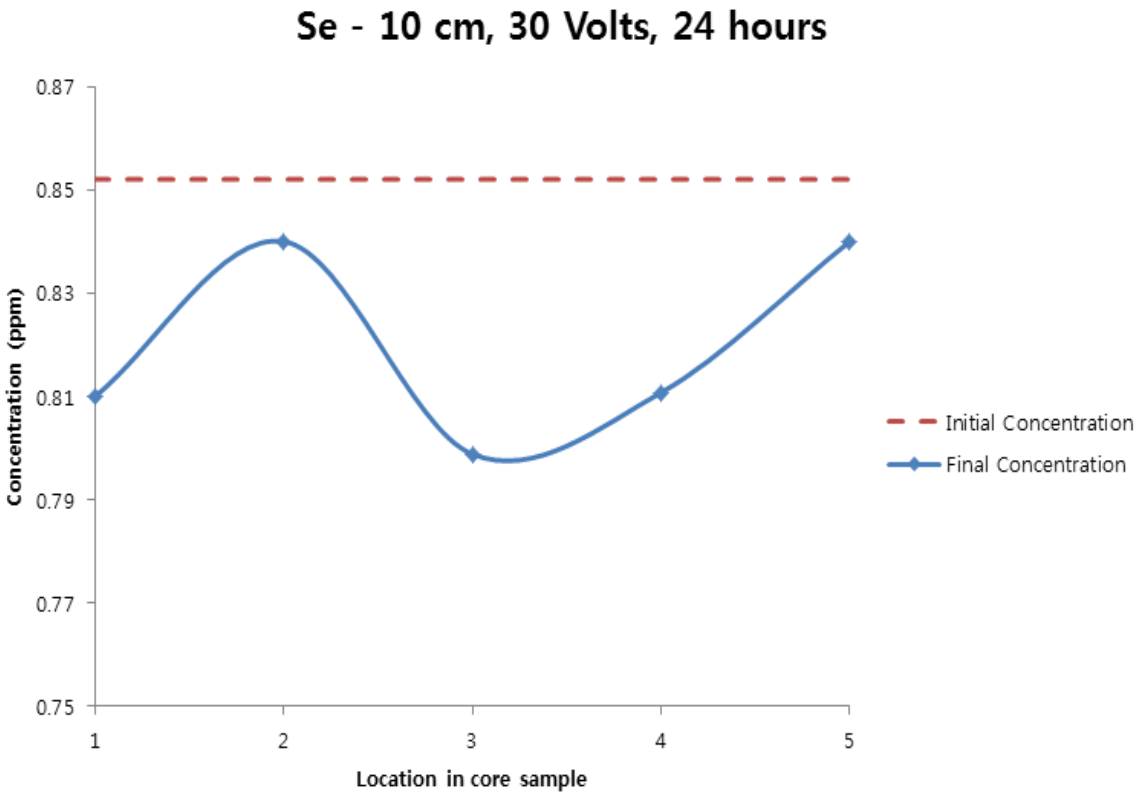

Figure 3-15: Concentration of Se upon EK treatment.– Length: 10 cm, 30 Vol., Treatment time: 24 hours.

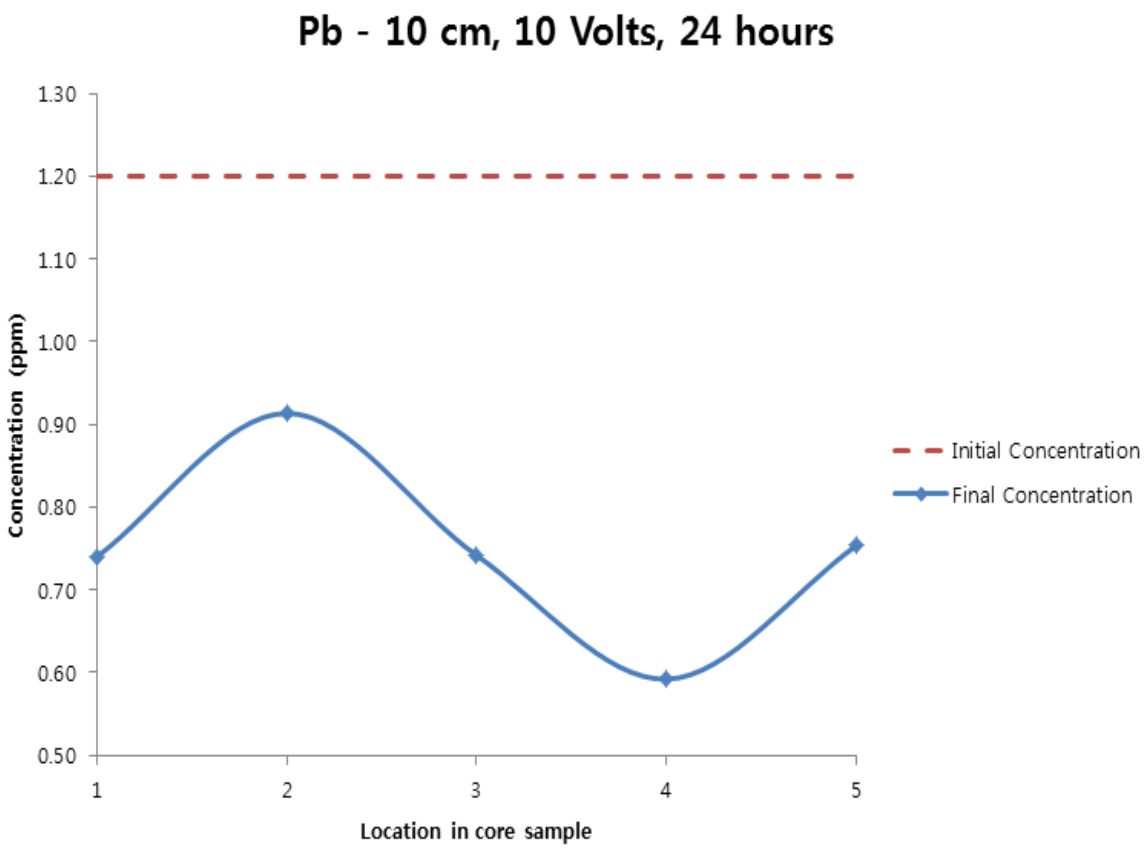

Figure 3-16: Concentration of Pb upon EK treatment.– Length: 10 cm, 10 Vol., Treatment time: 24 hours.

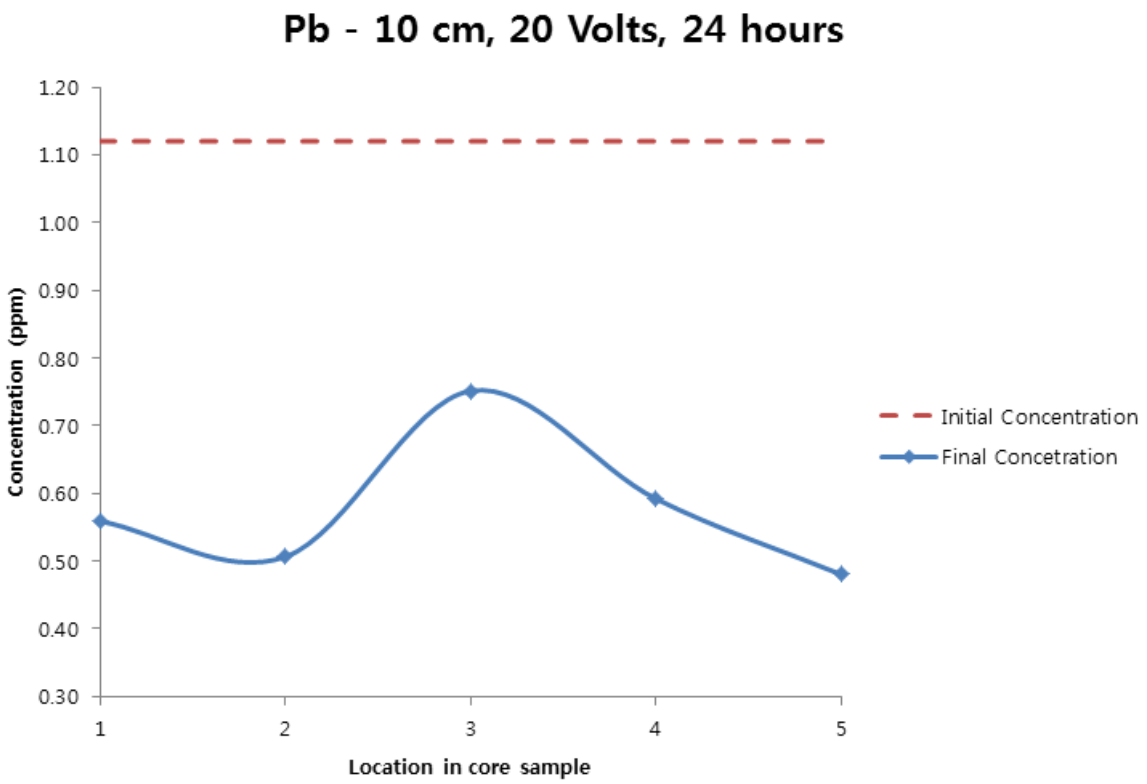

Figure 3-17: Concentration of Pb upon EK treatment. – Length: 10 cm, 20 Vol., Treatment time: 24 hours.

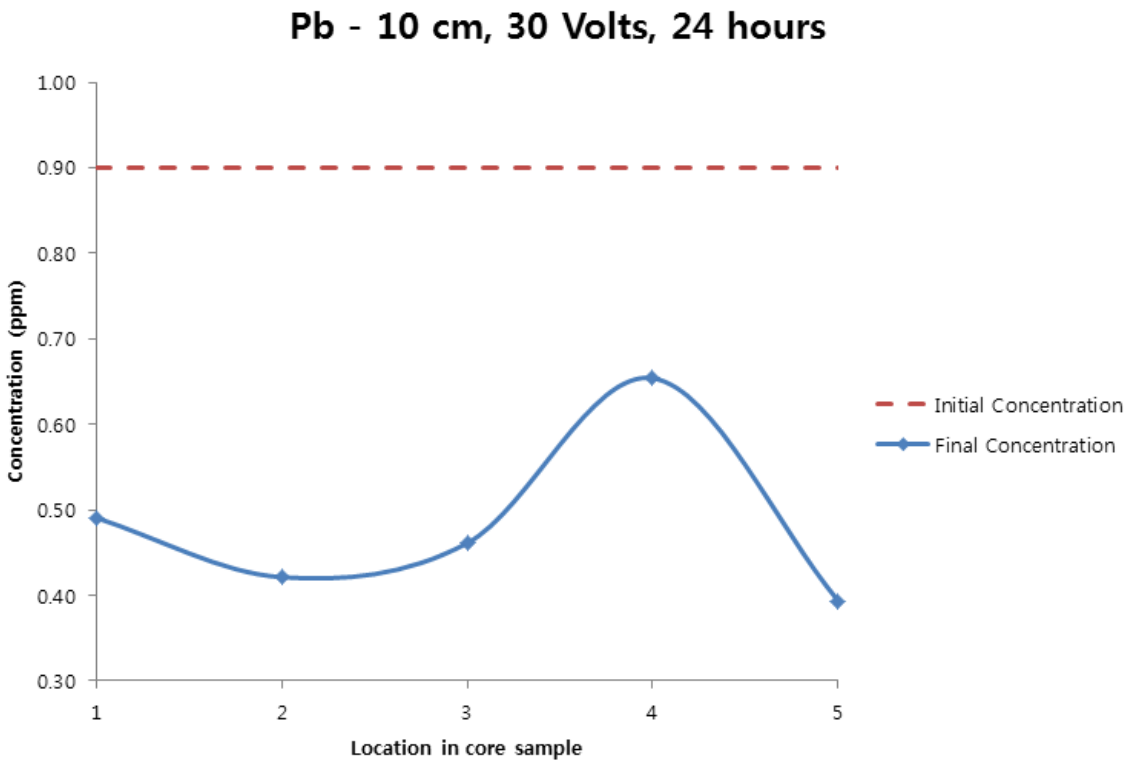

Figure 3-18: Concentration of Pb upon EK treatment. – Length: 10 cm, 30 Vol., Treatment time: 24 hours.

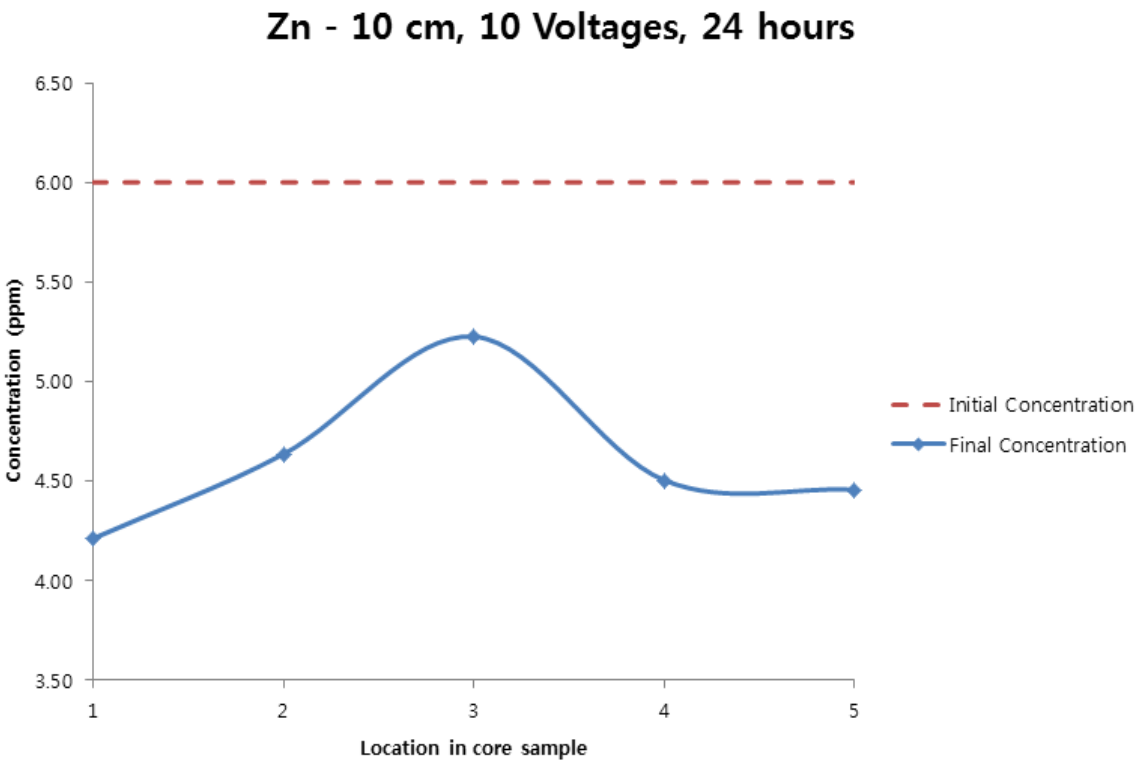

Figure 3-19: Concentration of Zn upon EK treatment. – Length: 10 cm, 10 Vol., Treatment time: 24 hours.

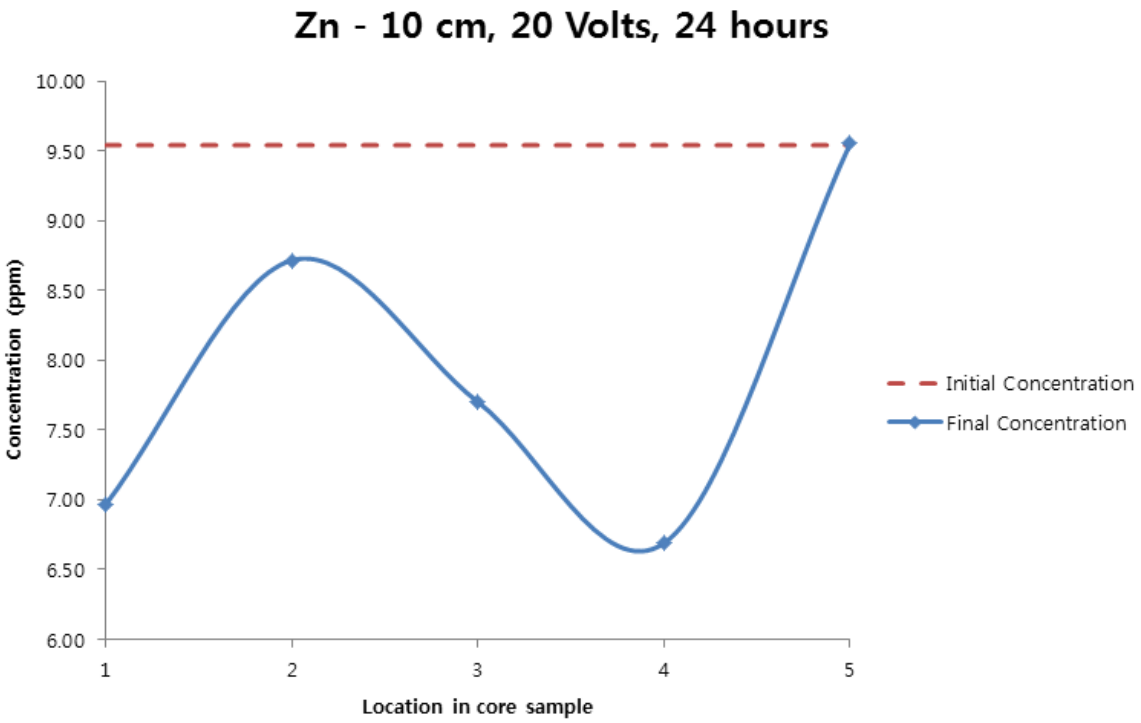

Figure 3-20: Concentration of Zn upon EK treatment. – Length: 10 cm, 20 Vol., Treatment time: 24 hours.

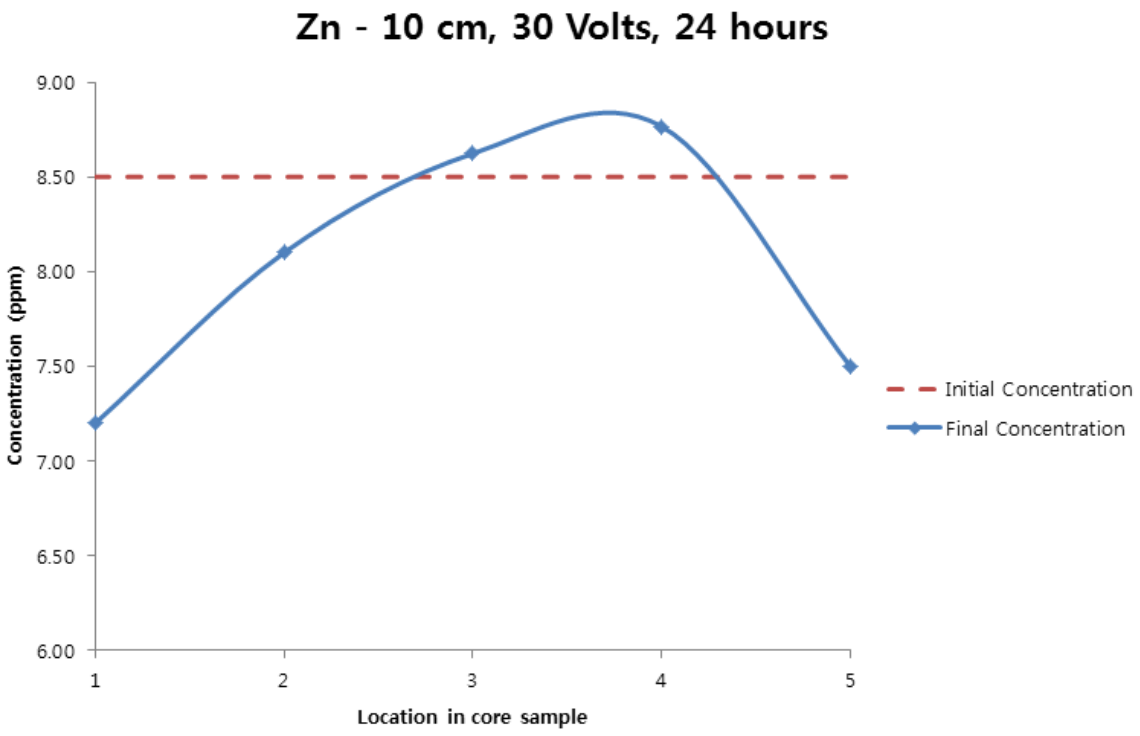

Figure 3-21: Concentration of Zn upon EK treatment. – Length: 10 cm, 30 Vol., Treatment time: 24 hours.

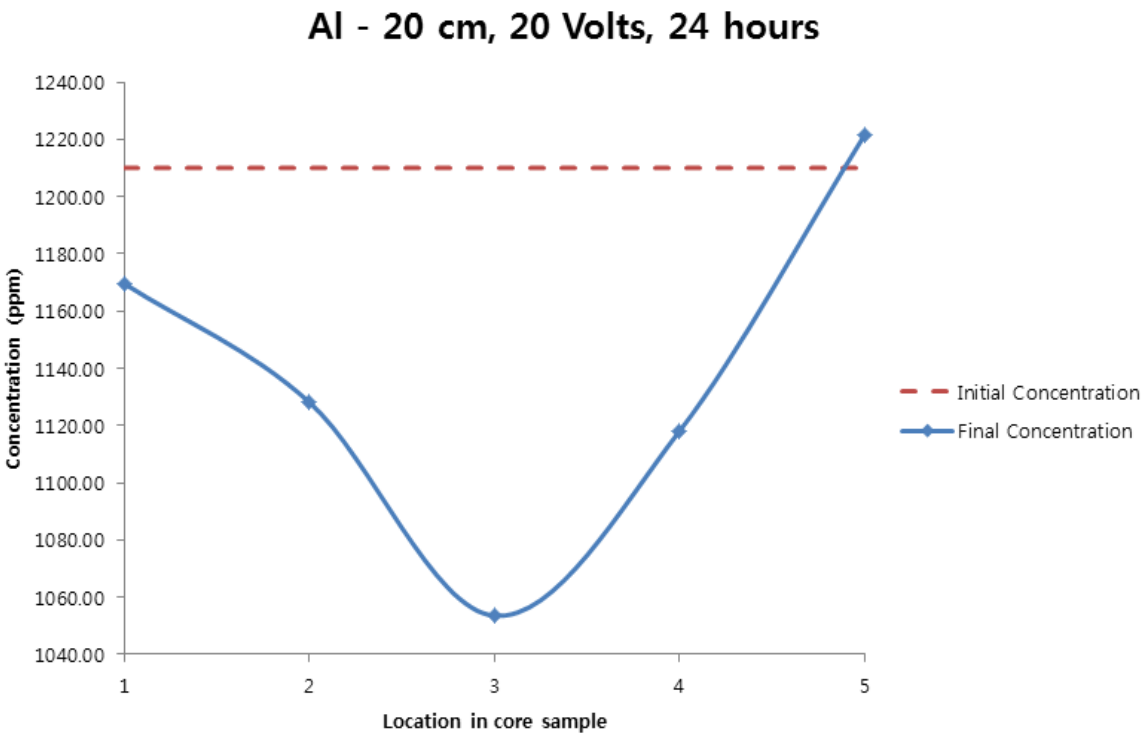

Figure 3-22: Concentration of Al upon EK treatment. – Length: 20 cm, 20 Vol., Treatment time: 24 hours.

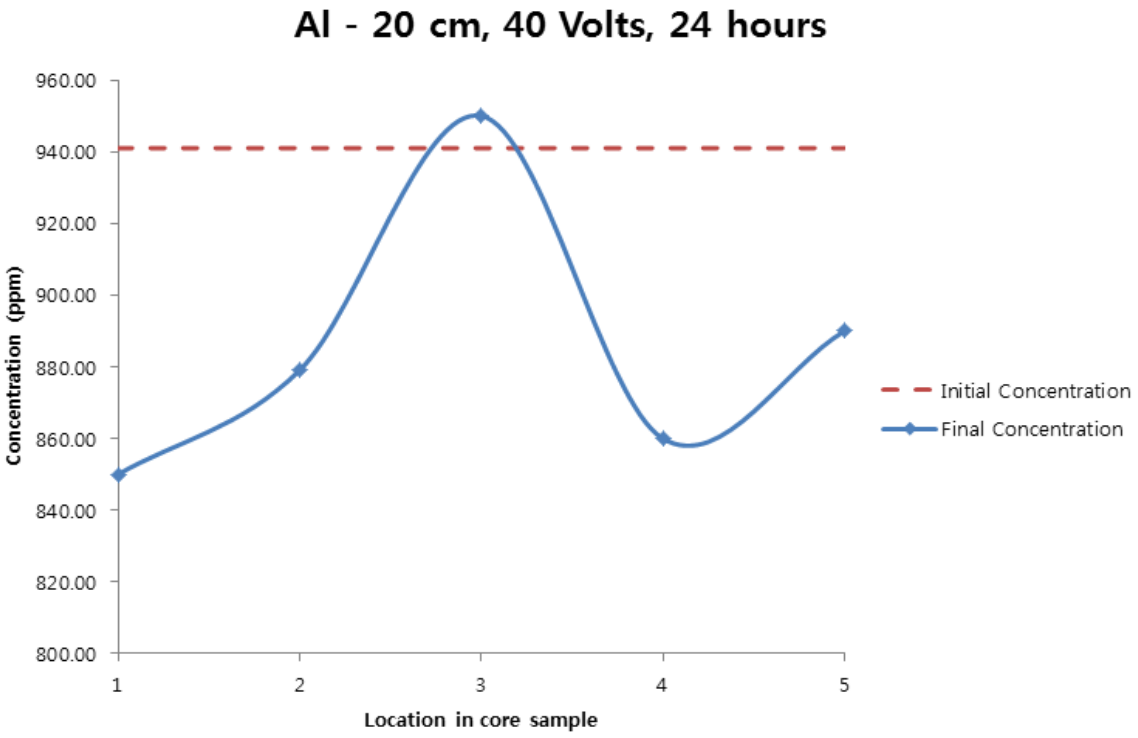

Figure 3-23: Concentration of Al upon EK treatment. – Length: 20 cm, 40 Vol., Treatment time: 24 hours.

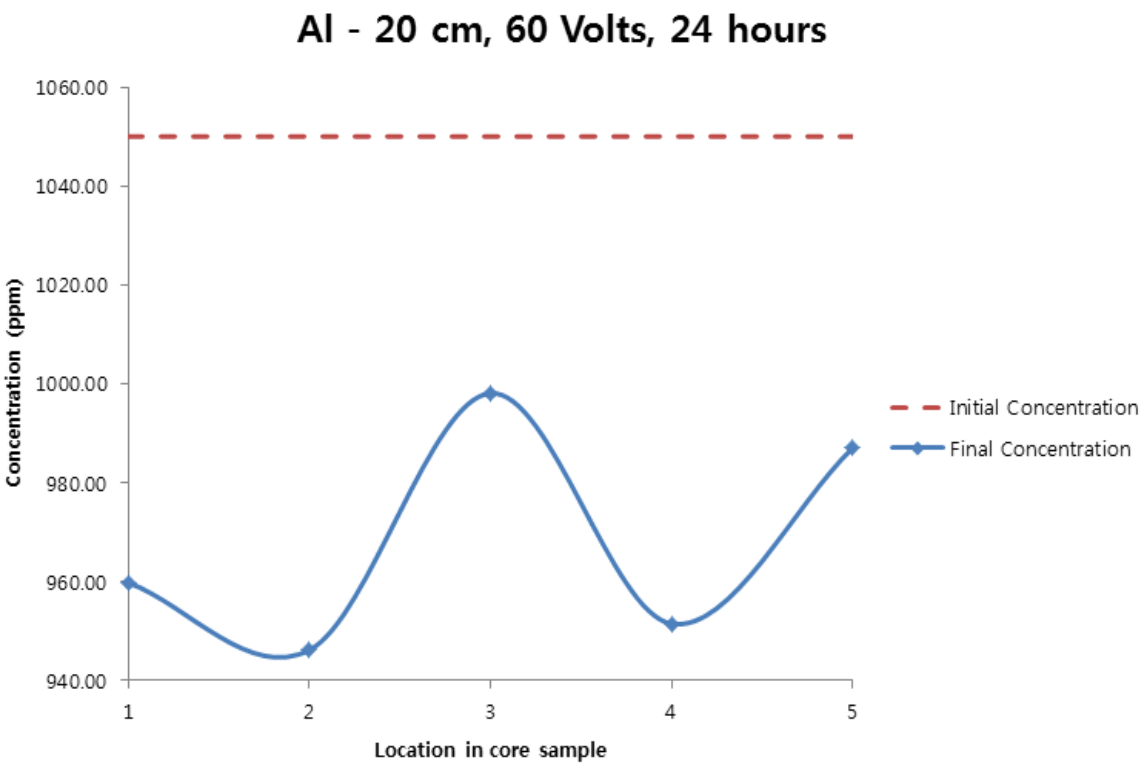

Figure 3-24: Concentration of Al upon EK treatment. – Length: 20 cm, 60 Vol., Treatment time: 24 hours.

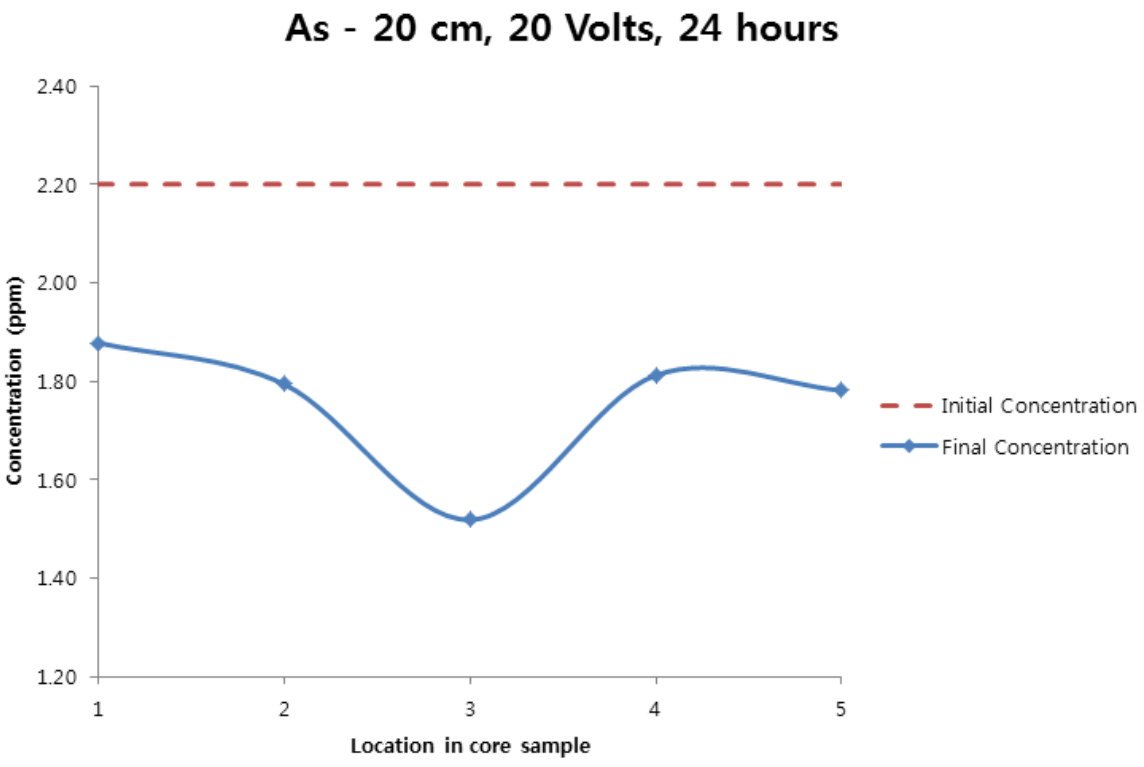

Figure 3-25: Concentration of As upon EK treatment. – Length: 20 cm, 20 Vol., Treatment time: 24 hours.

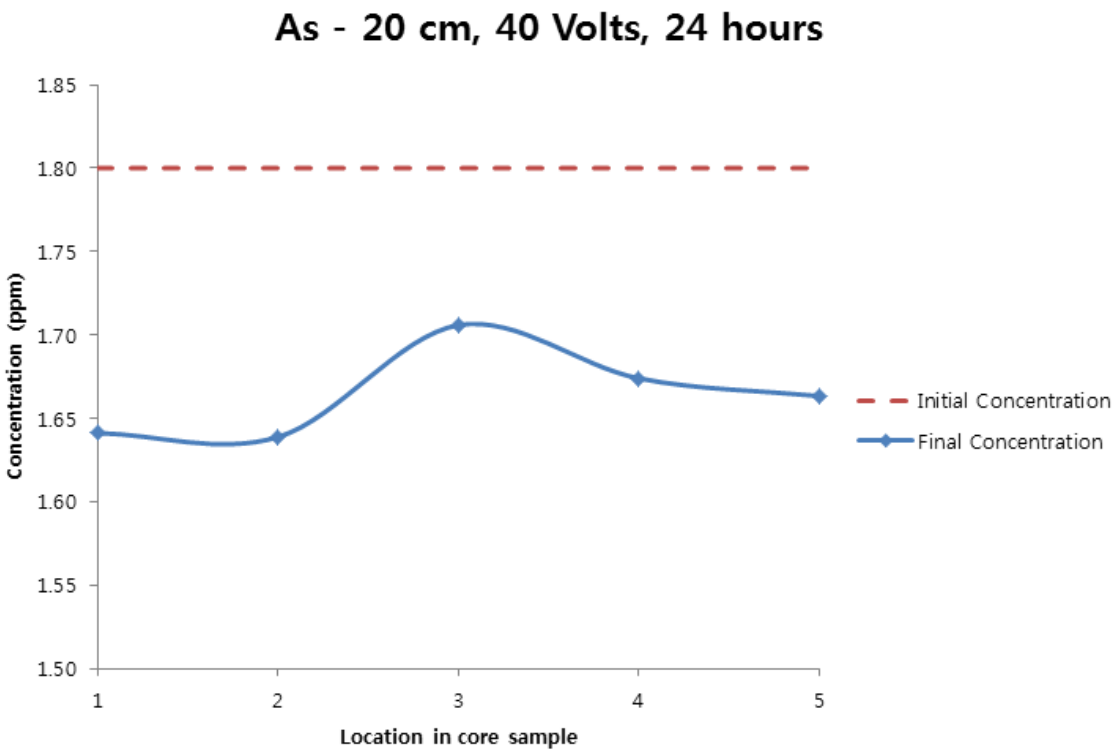

Figure 3-26: Concentration of As upon EK treatment. – Length: 20 cm, 40 Vol., Treatment time: 24 hours.

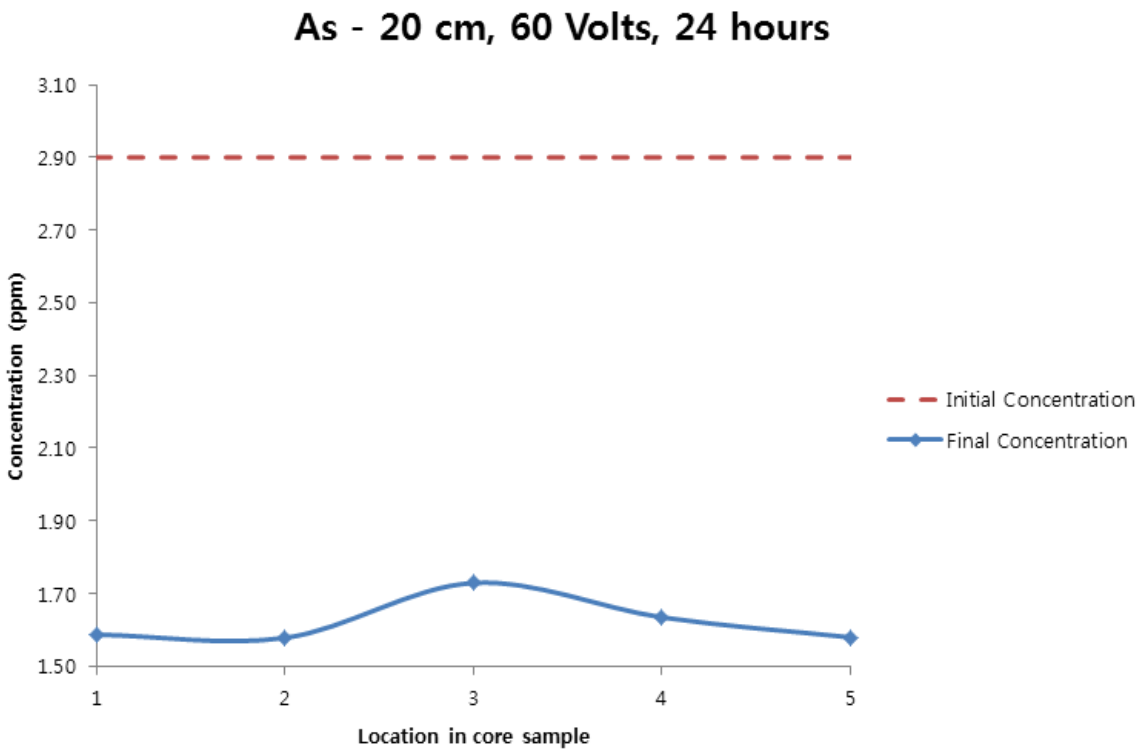

Figure 3-27: Concentration of As upon EK treatment.– Length: 20 cm, 60 Vol., Treatment time: 24 hours.

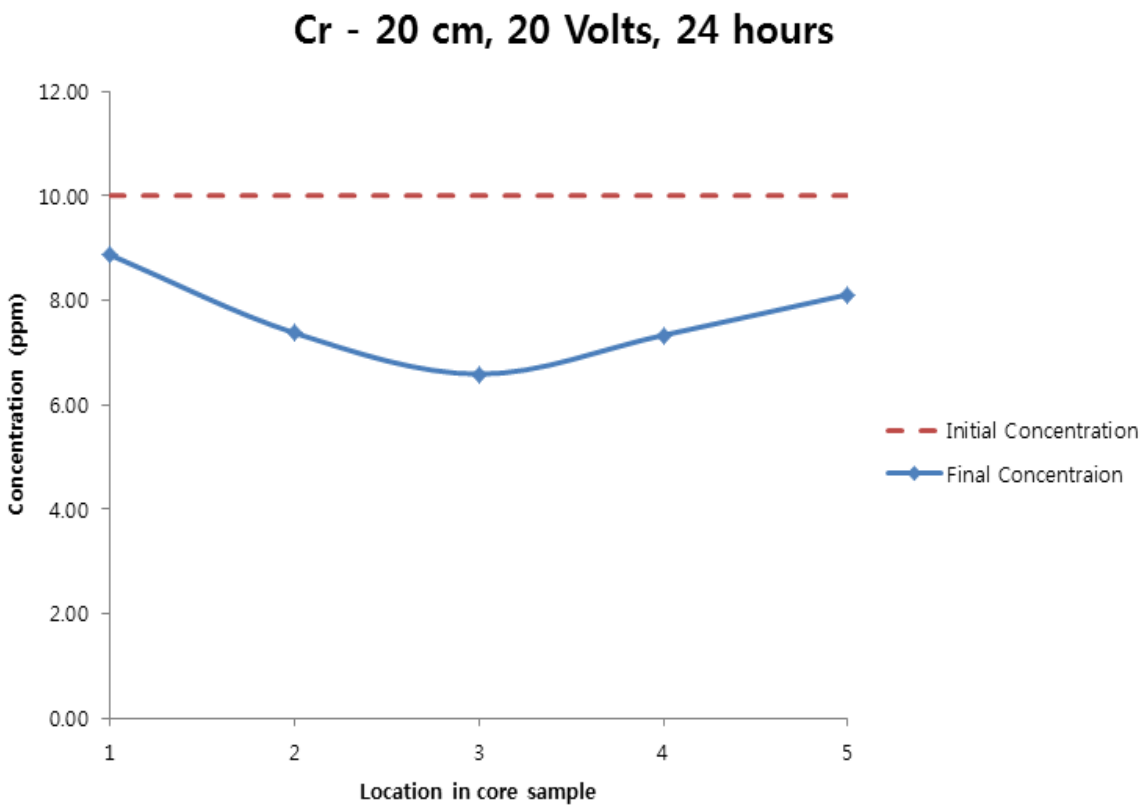

Figure 3-28: Concentration of Cr upon EK treatment.– Length: 20 cm, 20 Vol., Treatment time: 24 hours.

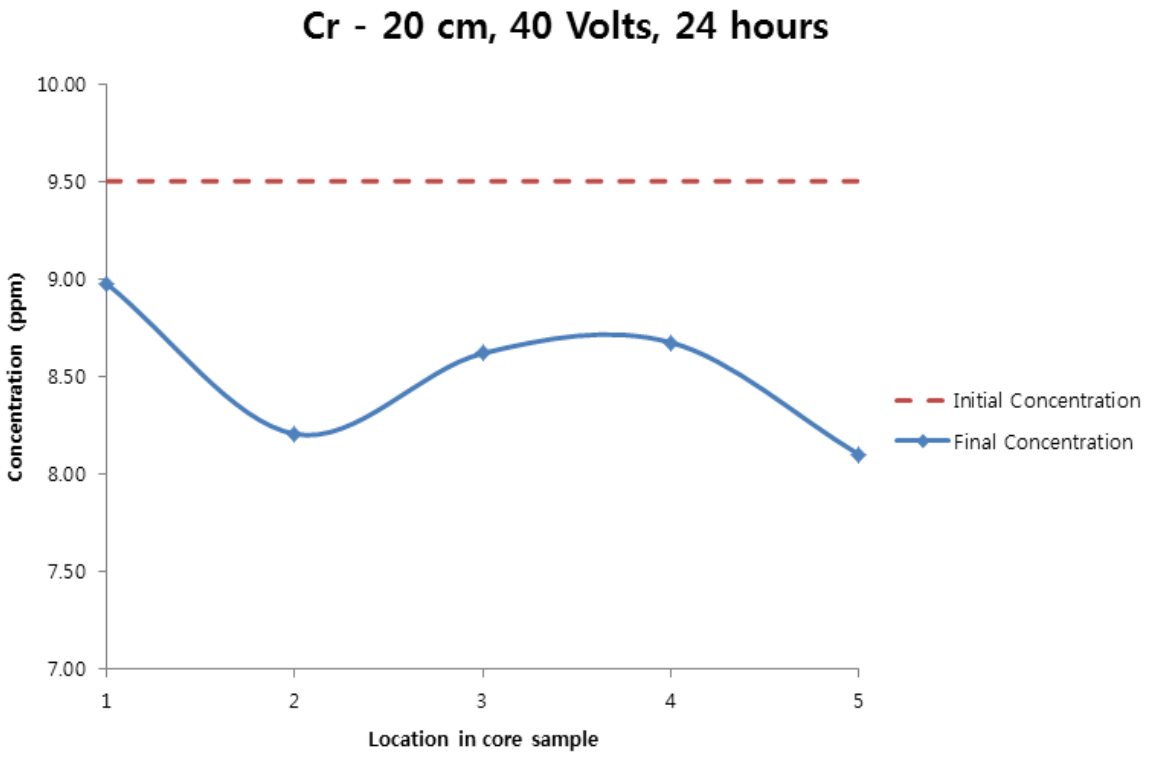

Figure 3-29: Concentration of Cr upon EK treatment.– Length: 20 cm, 40 Vol., Treatment time: 24 hours.

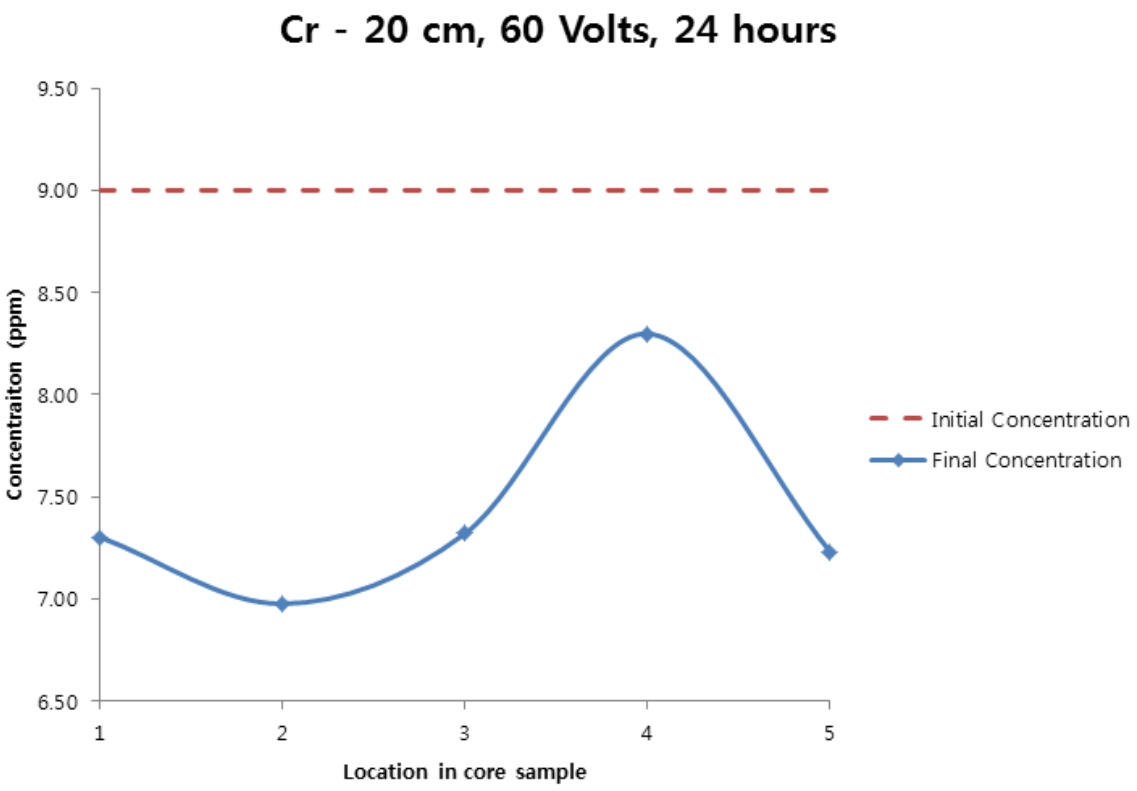

Figure 3-30: Concentration of Cr upon EK treatment.– Length: 20 cm, 60 Vol., Treatment time: 24 hours.

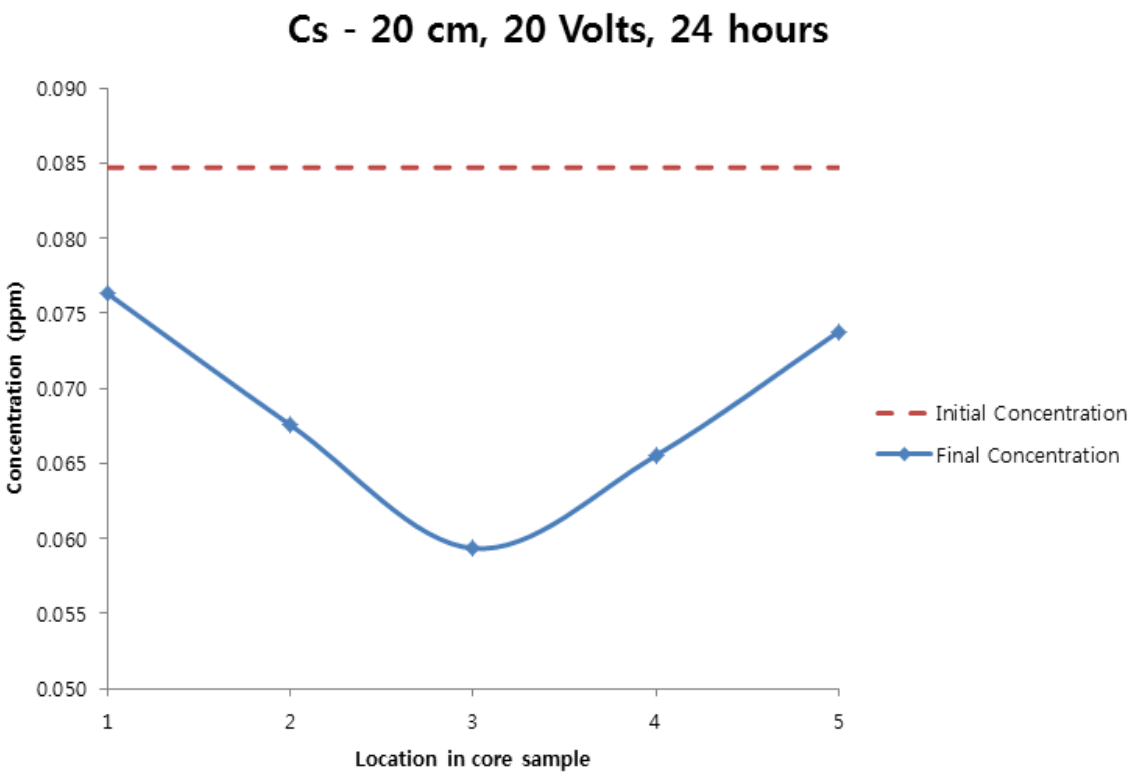

Figure 3-31: Concentration of Cs upon EK treatment.– Length: 20 cm, 20 Vol., Treatment time: 24 hours.

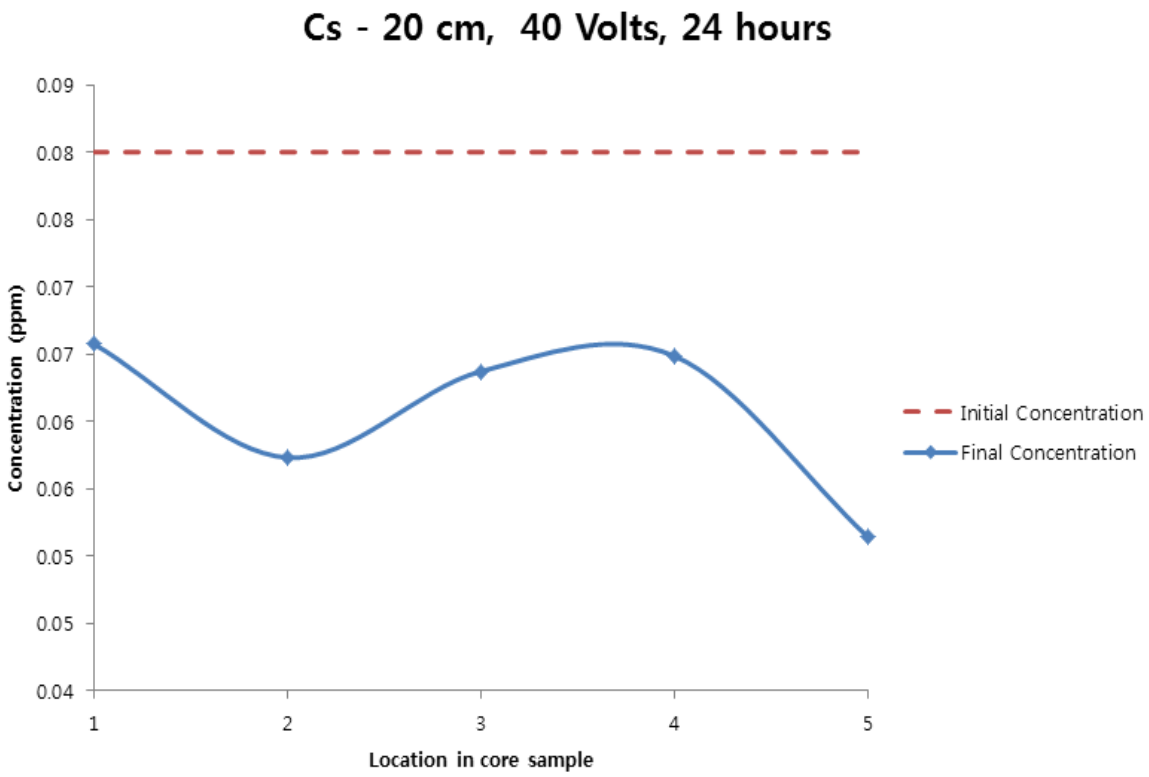

Figure 3-32: Concentration of Cs upon EK treatment.– Length: 20 cm, 40 Vol., Treatment time: 24 hours.

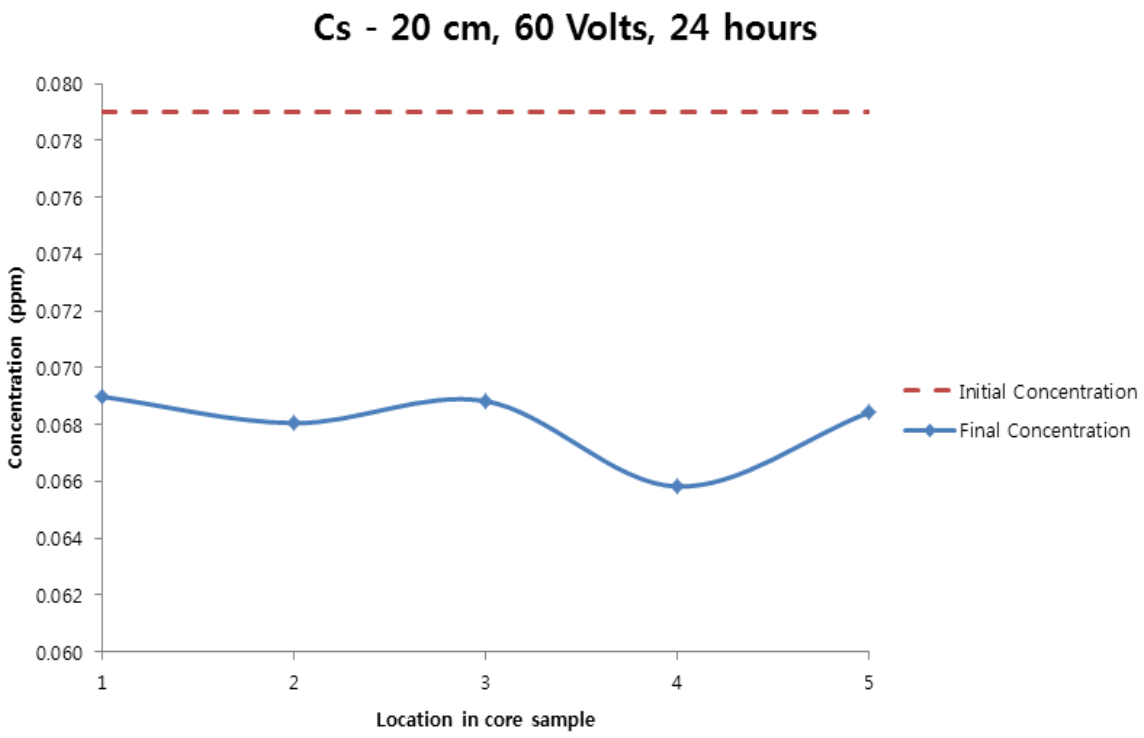

Figure 3-33: Concentration of Cs upon EK treatment.– Length: 20 cm, 60 Vol., Treatment time: 24 hours.

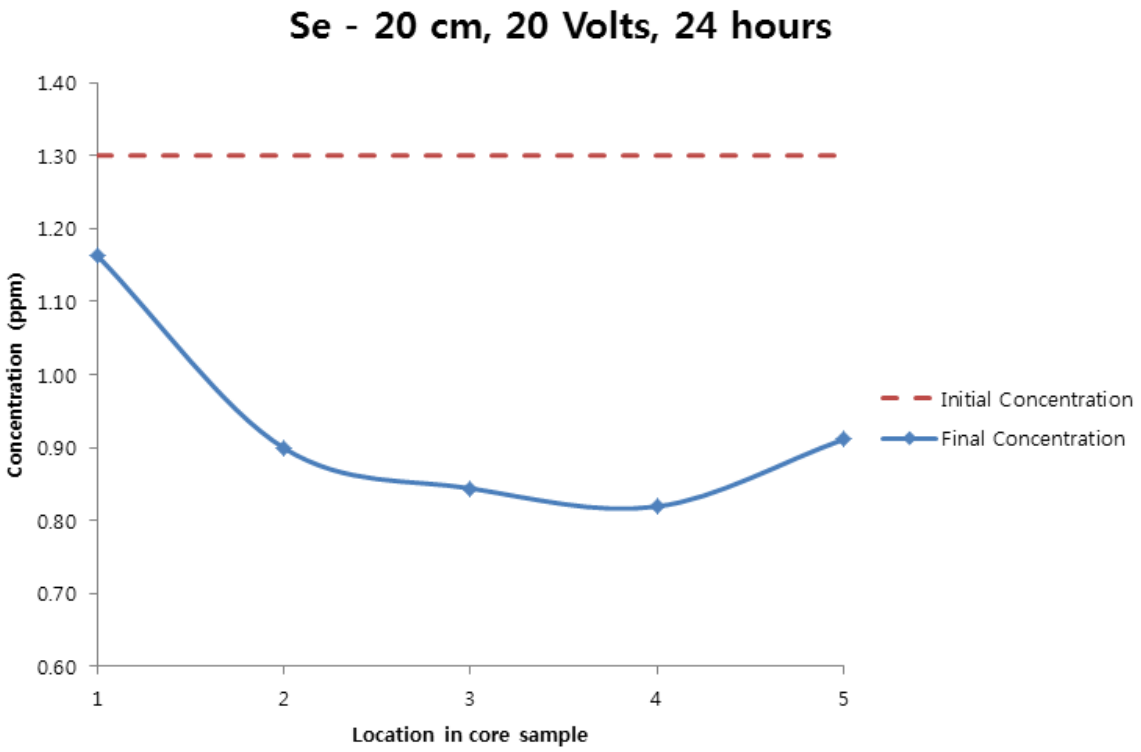

Figure 3-34: Concentration of Se upon EK treatment.– Length: 20 cm, 20 Vol., Treatment time: 24 hours.

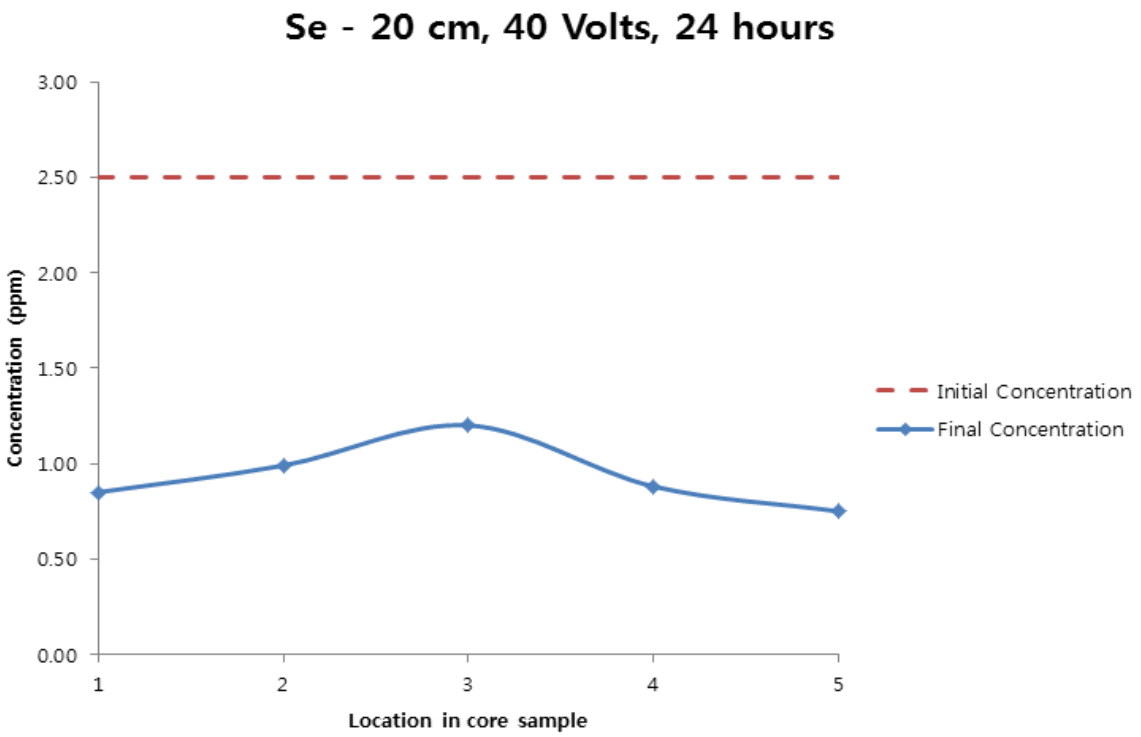

Figure 3-35: Concentration of Se upon EK treatment. – Length: 20 cm, 40 Vol., Treatment time: 24 hours.

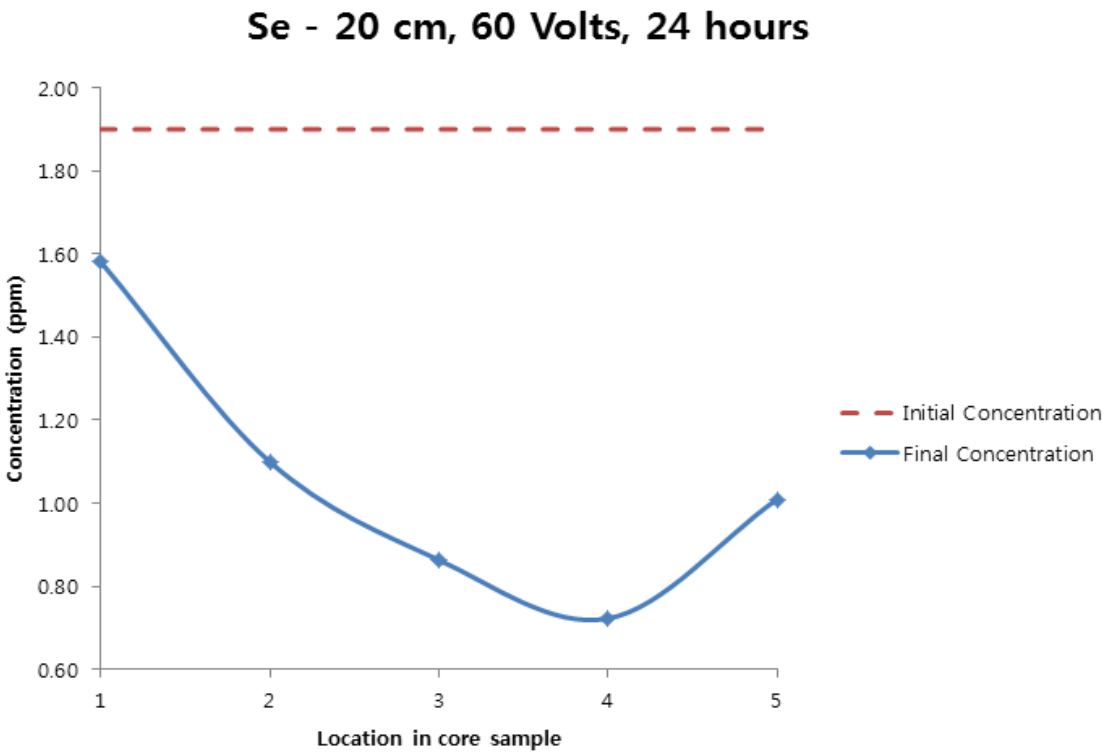

Figure 3-36: Concentration of Se upon EK treatment. – Length: 20 cm, 60 Vol., Treatment time: 24 hours.

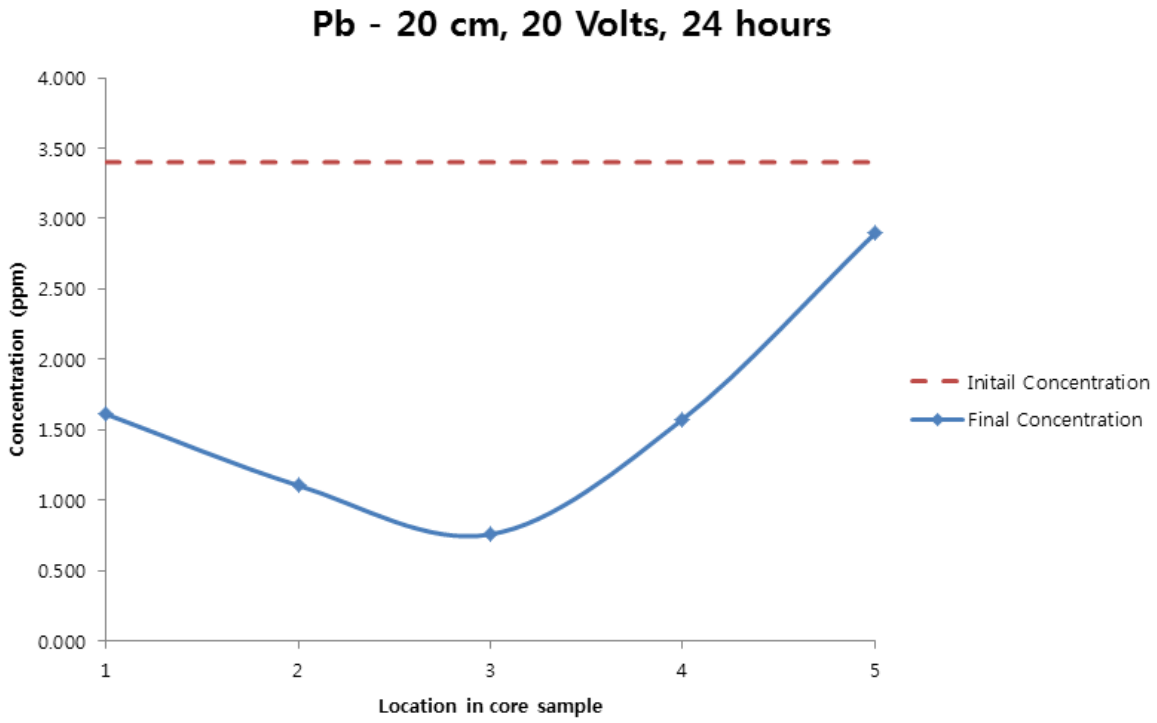

Figure 3-37: Concentration of Pb upon EK treatment.– Length: 20 cm, 20 Vol., Treatment time: 24 hours.

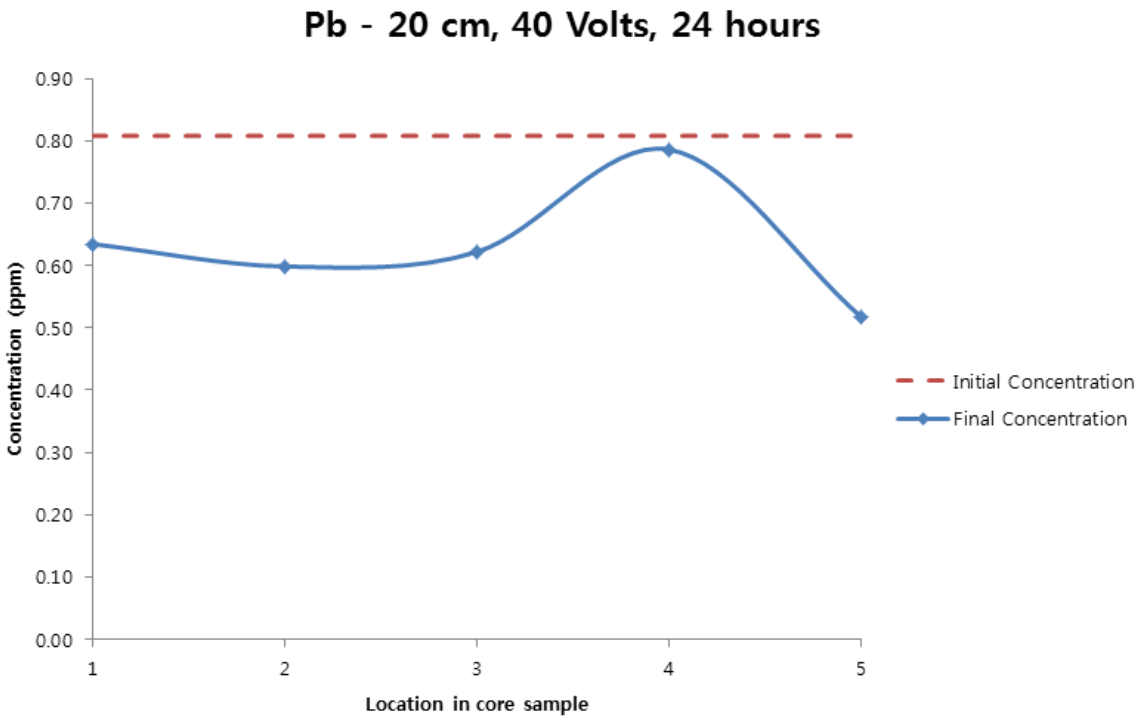

Figure 3-38: Concentration of Pb upon EK treatment. – Length: 20 cm, 40 Vol., Treatment time: 24 hours.

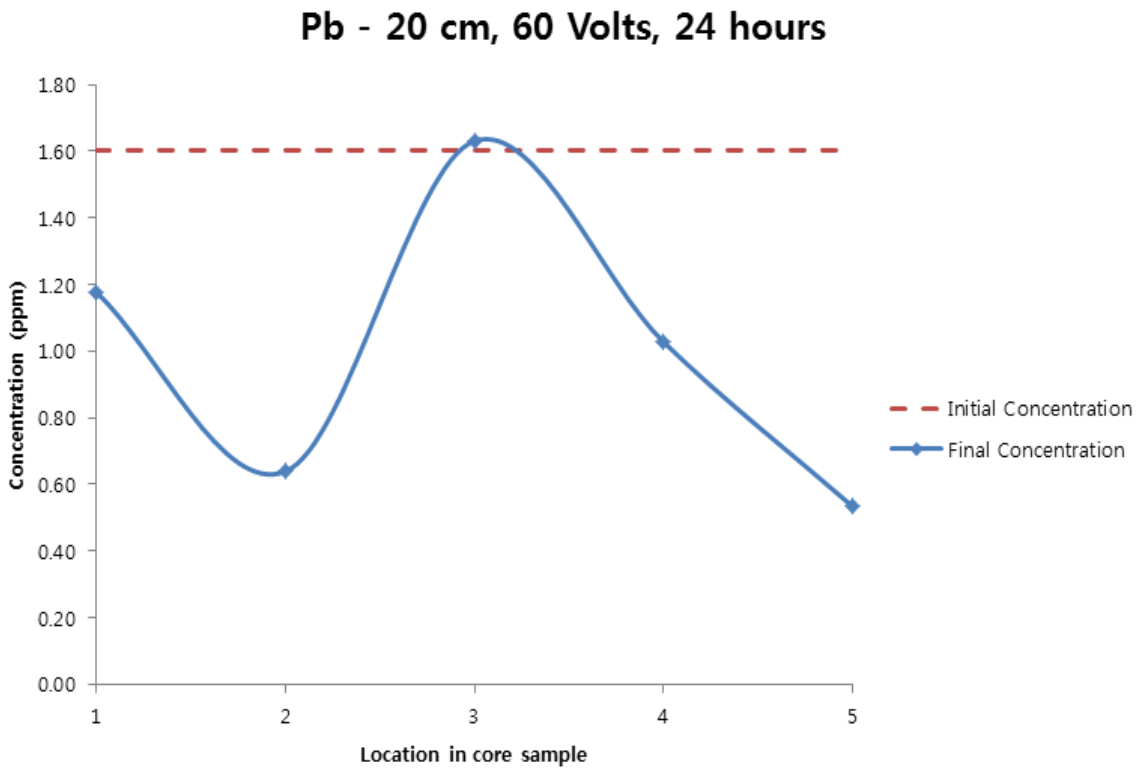

Figure 3-39: Concentration of Pb upon EK treatment. – Length: 20 cm, 60 Vol., Treatment time: 24 hours

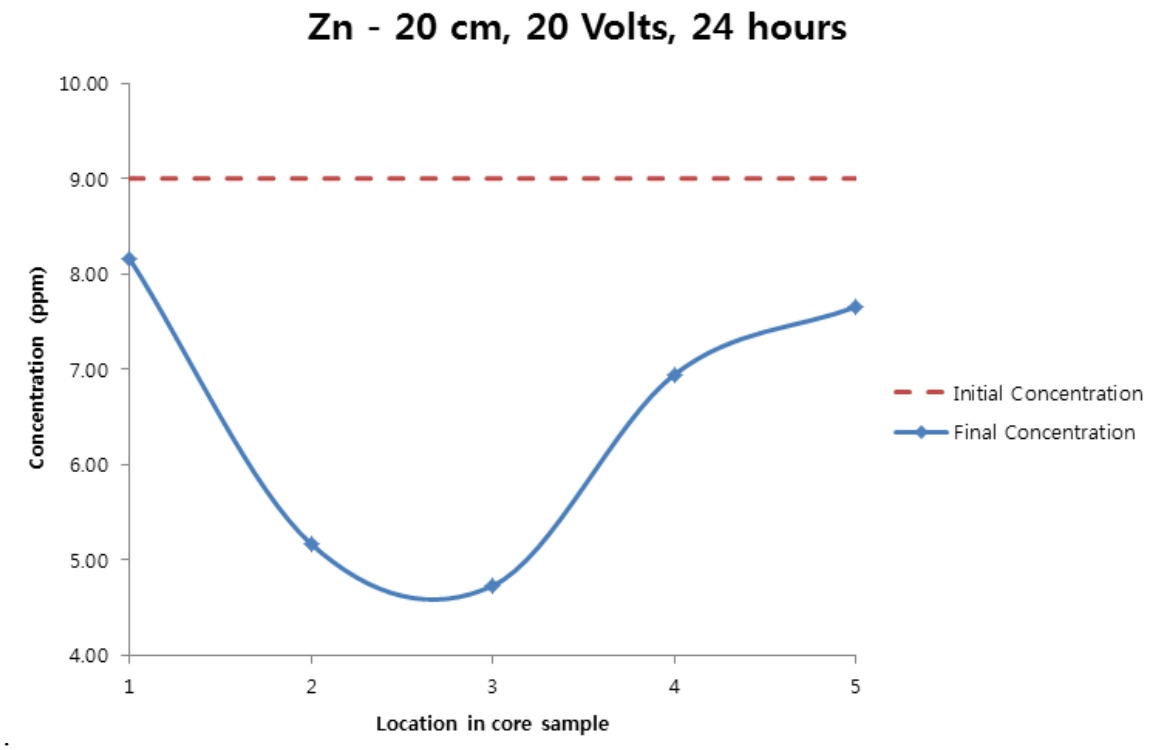

Figure 3-40: Concentration of Zn upon EK treatment. – Length: 20 cm, 20 Vol., Treatment time: 24 hours.

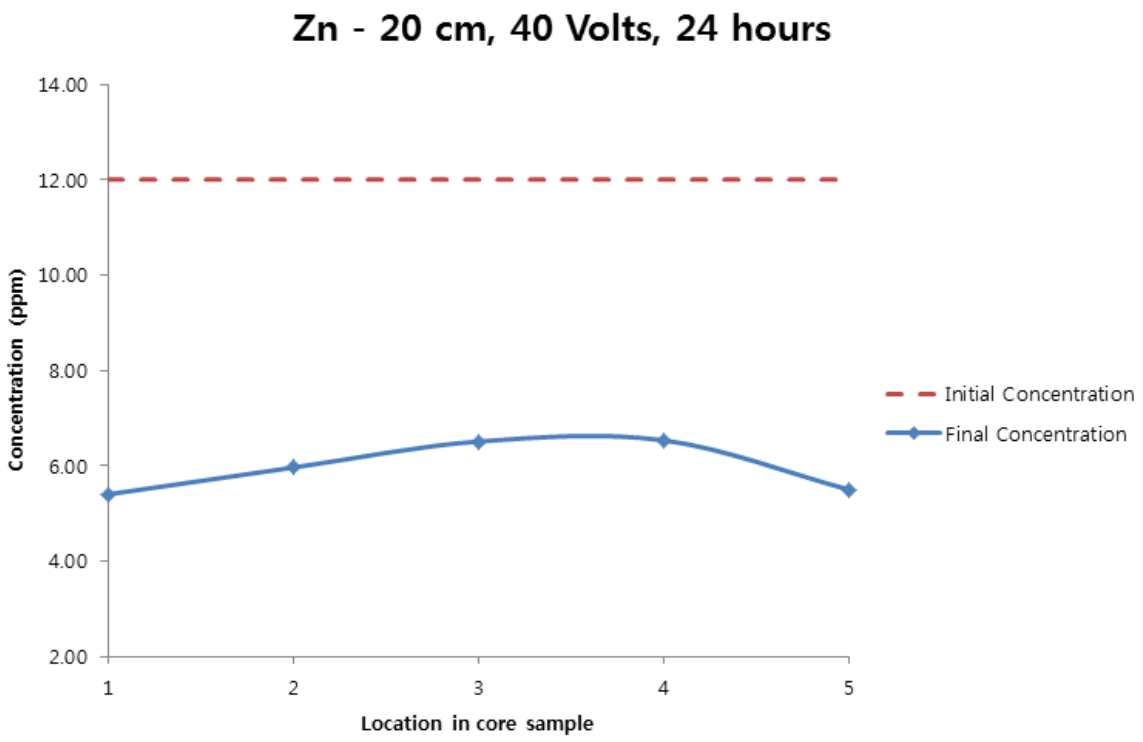

Figure 3-41: Concentration of Zn upon EK treatment.– Length: 20 cm, 40 Vol., Treatment time: 24 hours.

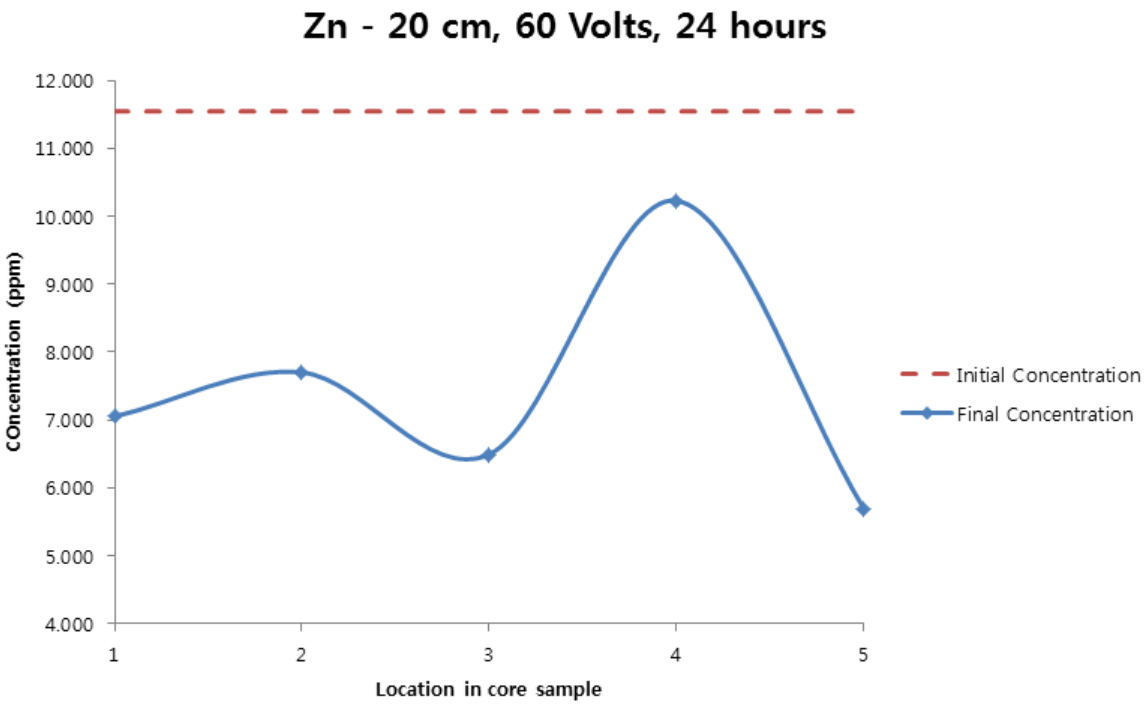

Figure 3-42: Concentration of Zn upon EK treatment.– Length: 20 cm, 60 Vol., Treatment time: 24 hours.

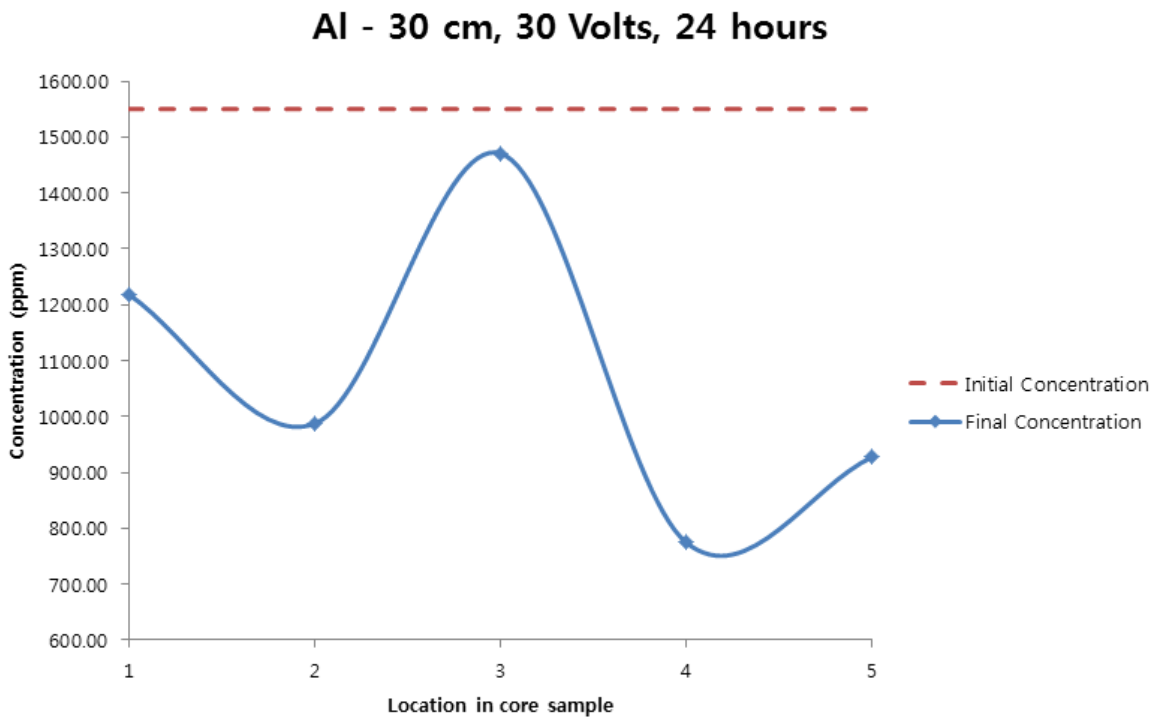

Figure 3-43: Concentration of Al upon EK treatment.– Length: 30 cm, 30 Vol., Treatment time: 24 hours.

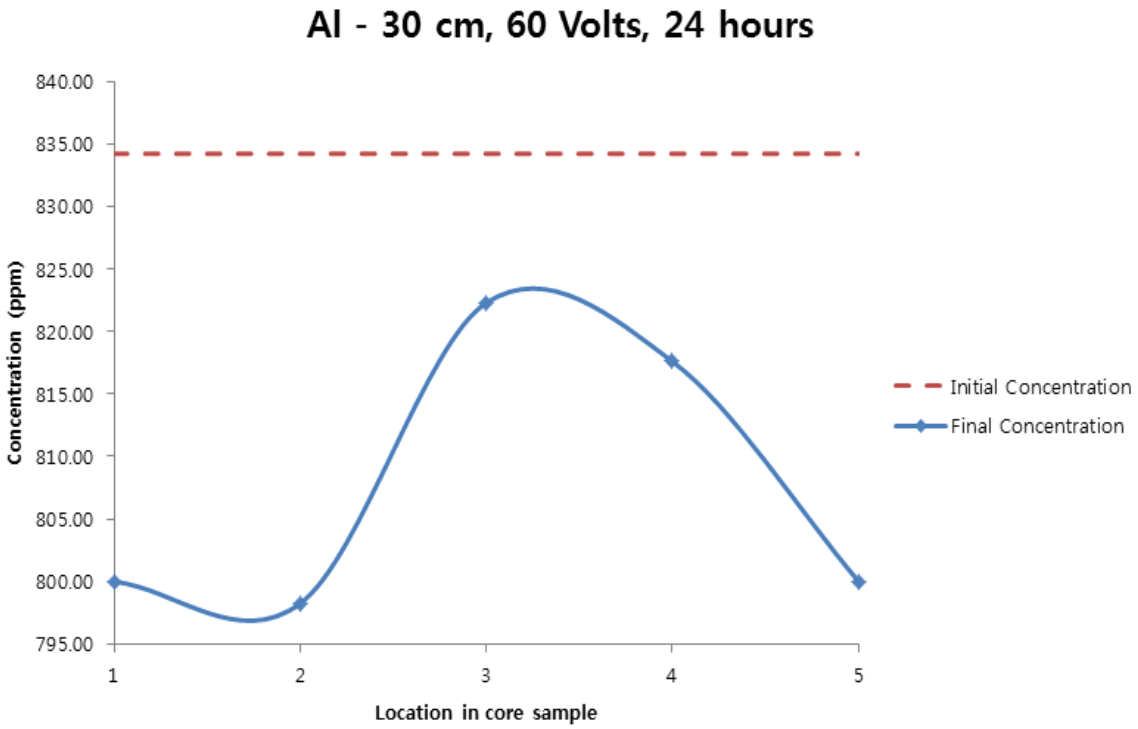

Figure 3-44: Concentration of Al upon EK treatment. – Length: 30 cm, 60 Vol., Treatment time: 24 hours.

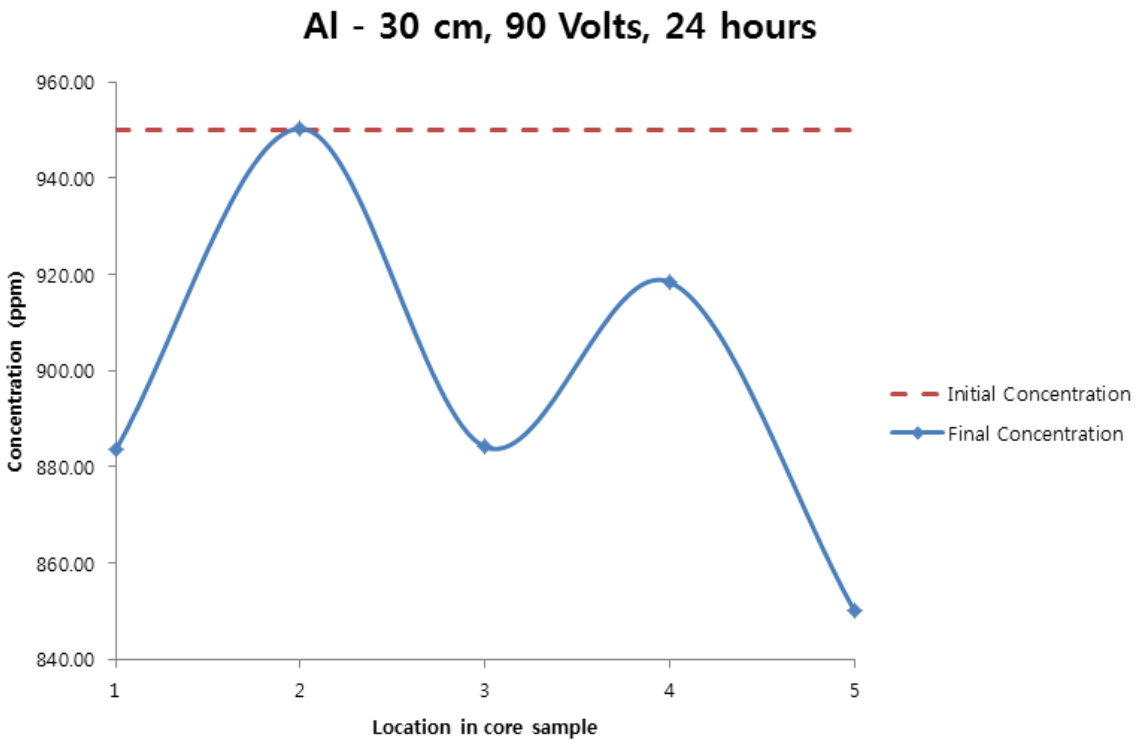

Figure 3-45: Concentration of Al upon EK treatment. – Length: 30 cm, 90 Vol., Treatment time: 24 hours.

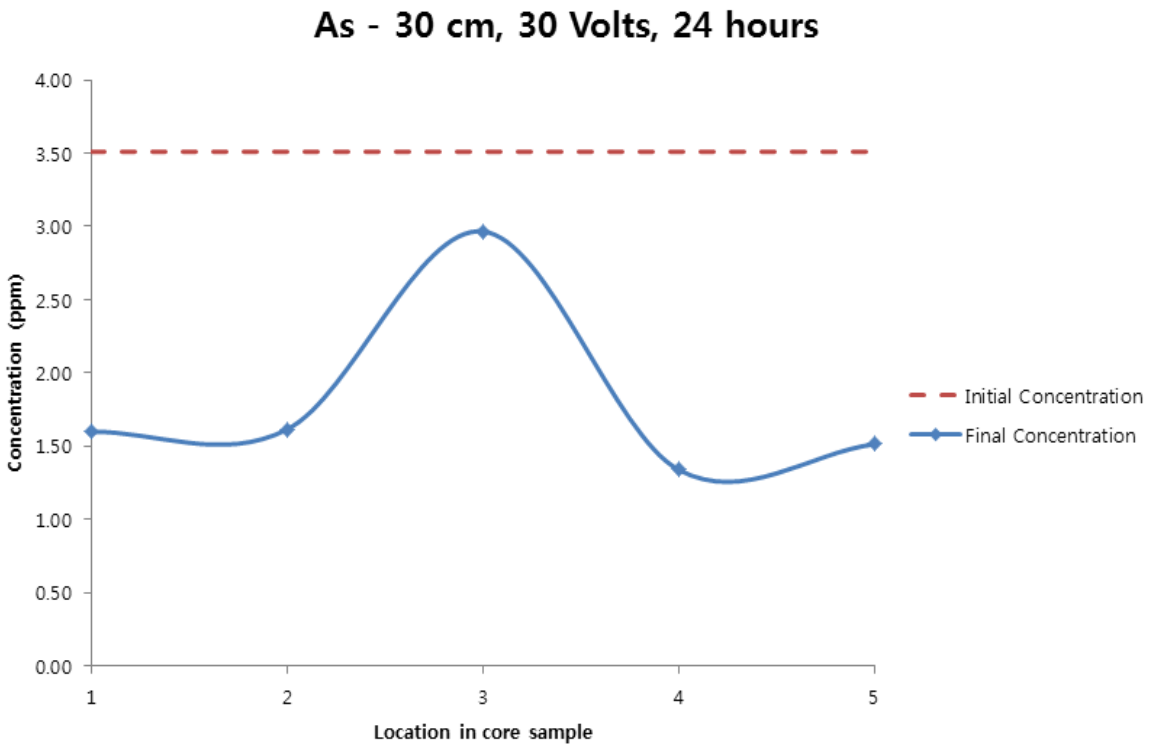

Figure 3-46: Concentration of As upon EK treatment. – Length: 30 cm, 30 Vol., Treatment time: 24 hours.

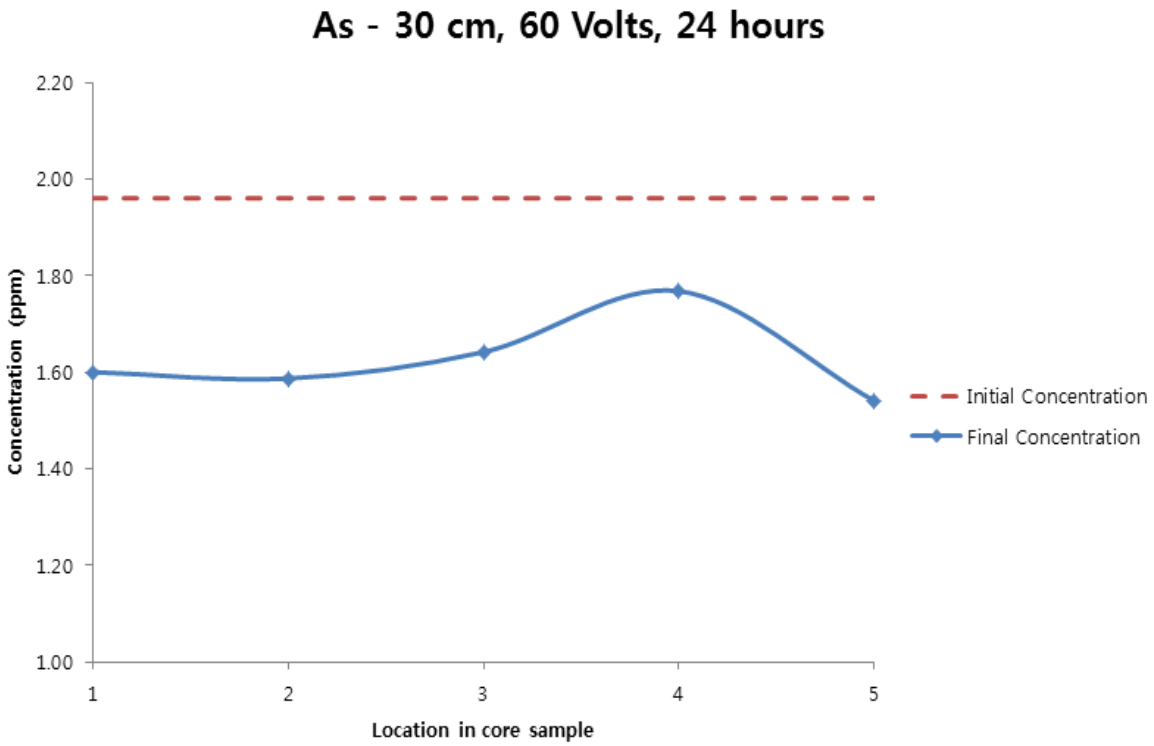

Figure 3-47: Concentration of As upon EK treatment. – Length: 30 cm, 60 Vol., Treatment time: 24 hours.

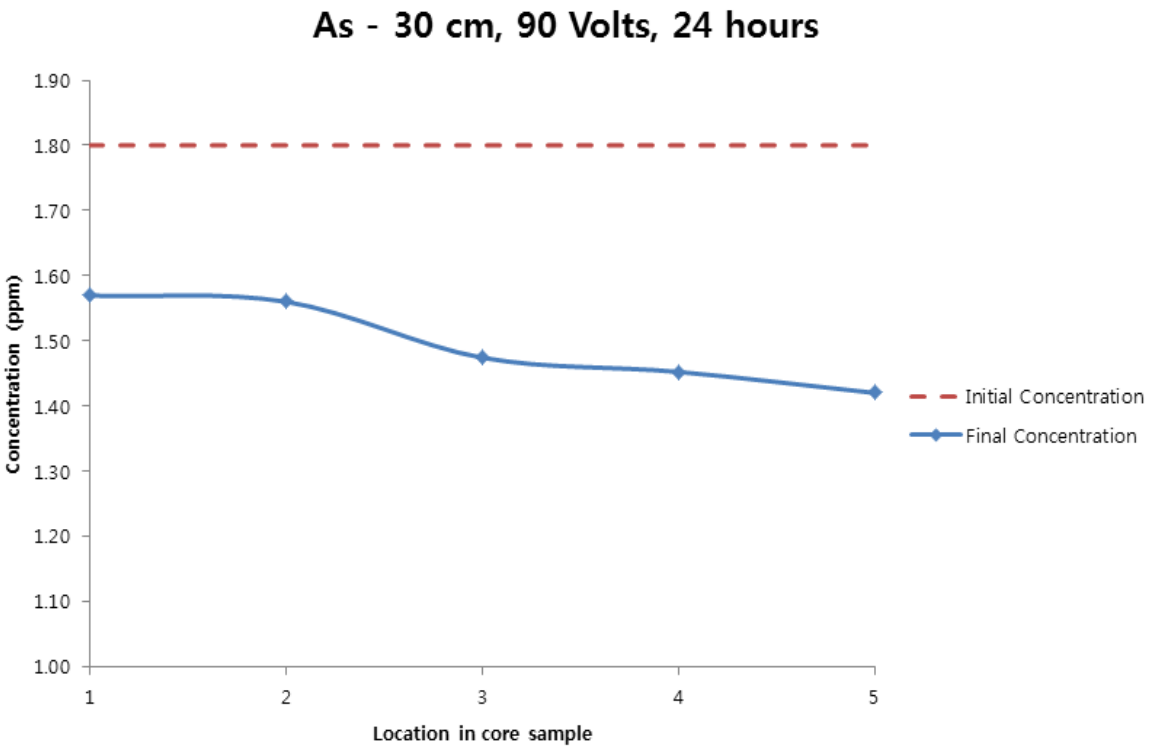

Figure 3-48: Concentration of As upon EK treatment. – Length: 30 cm, 90 Vol., Treatment time: 24 hours.

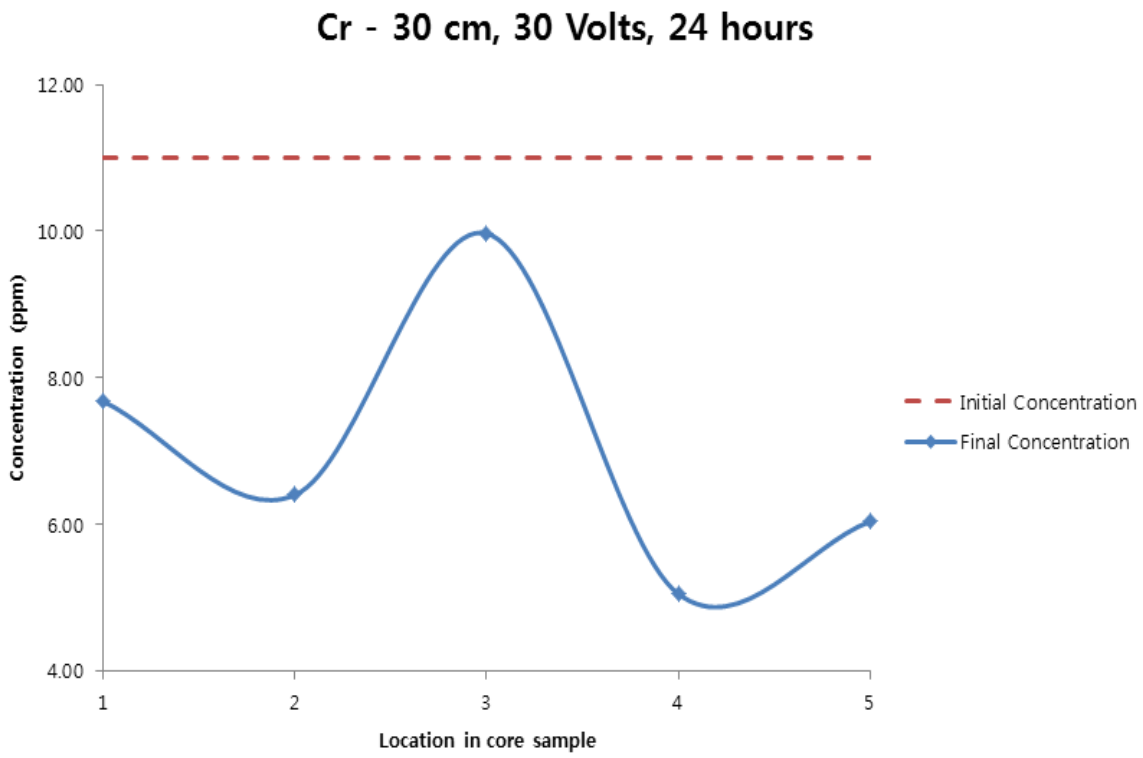

Figure 3-49: Concentration of Cr upon EK treatment. – Length: 30 cm, 30 Vol., Treatment time: 24 hours.

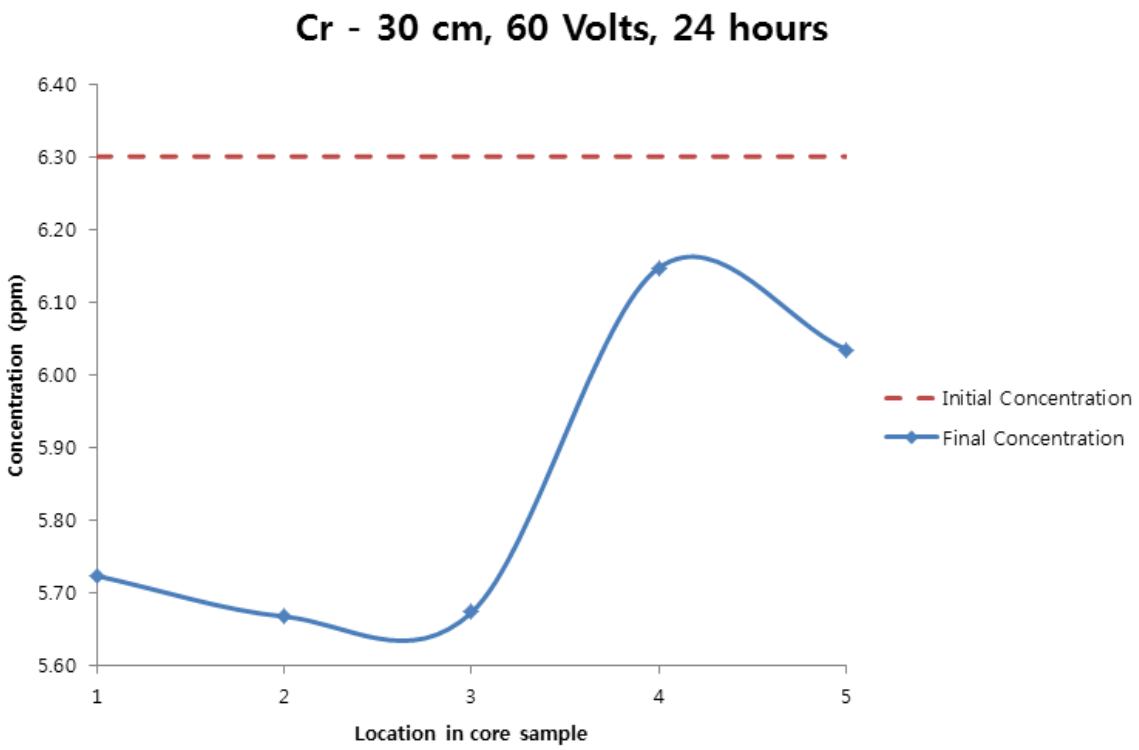

Figure 3-50: Concentration of Cr upon EK treatment. – Length: 30 cm, 60 Vol., Treatment time: 24 hours.

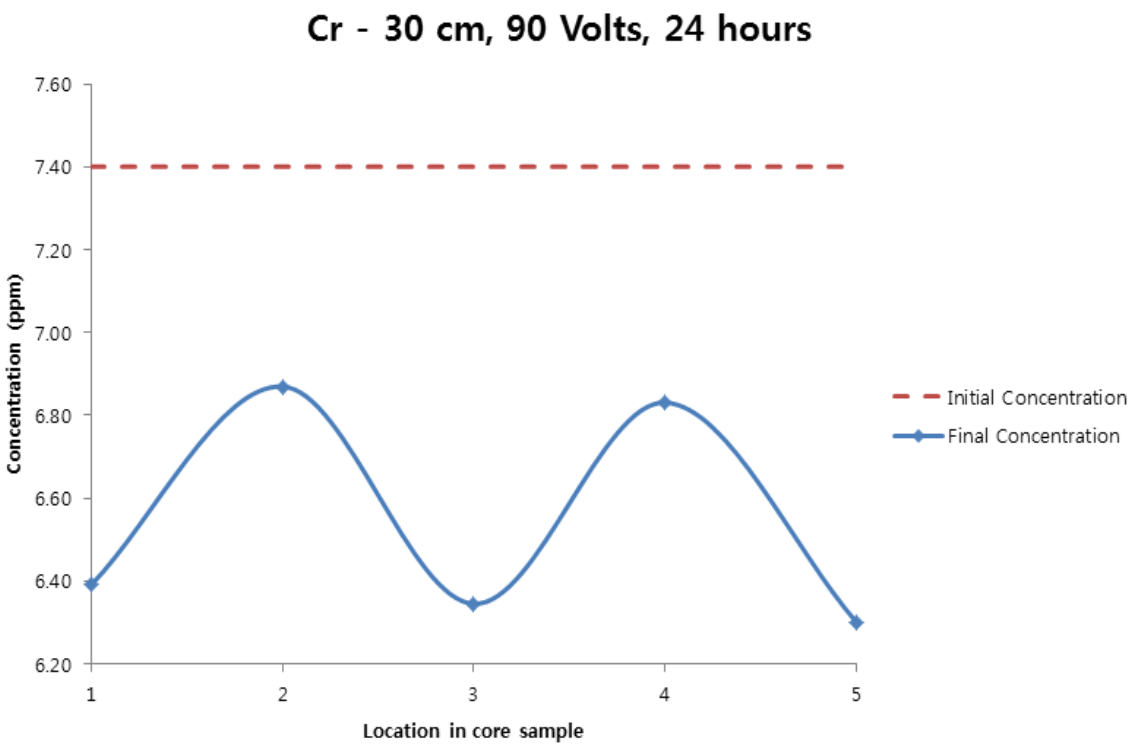

Figure 3-51: Concentration of Cr upon EK treatment. – Length: 30 cm, 90 Vol., Treatment time: 24 hours.

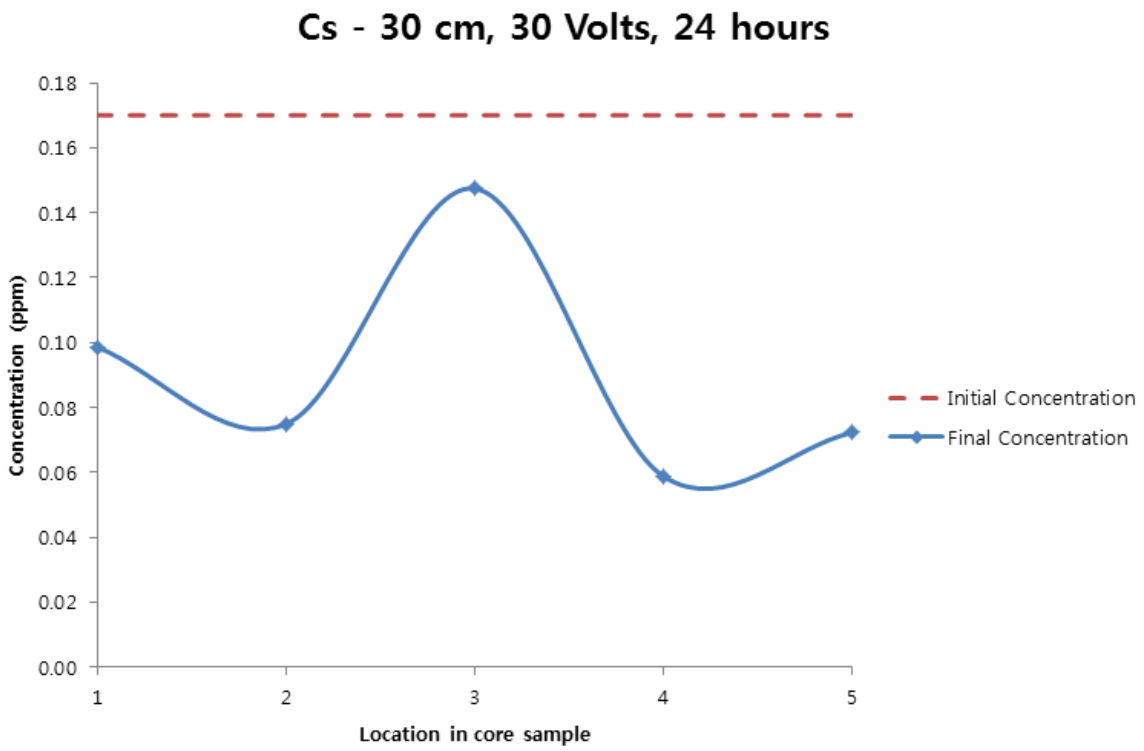

Figure 3-52: Concentration of Cs upon EK treatment.– Length: 30 cm, 30 Vol., Treatment time: 24 hours.

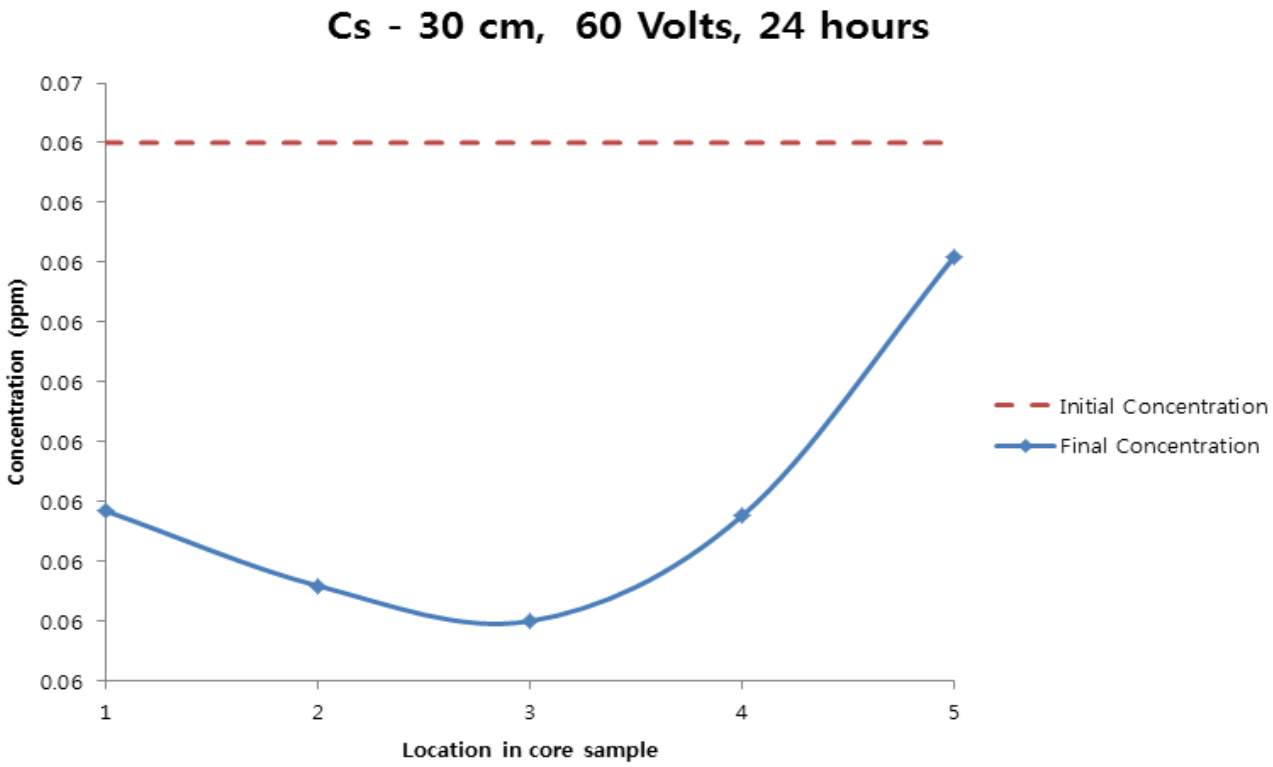

Figure 3-53: Concentration of Cs upon EK treatment.– Length: 30 cm, 60 Vol., Treatment time: 24 hours.

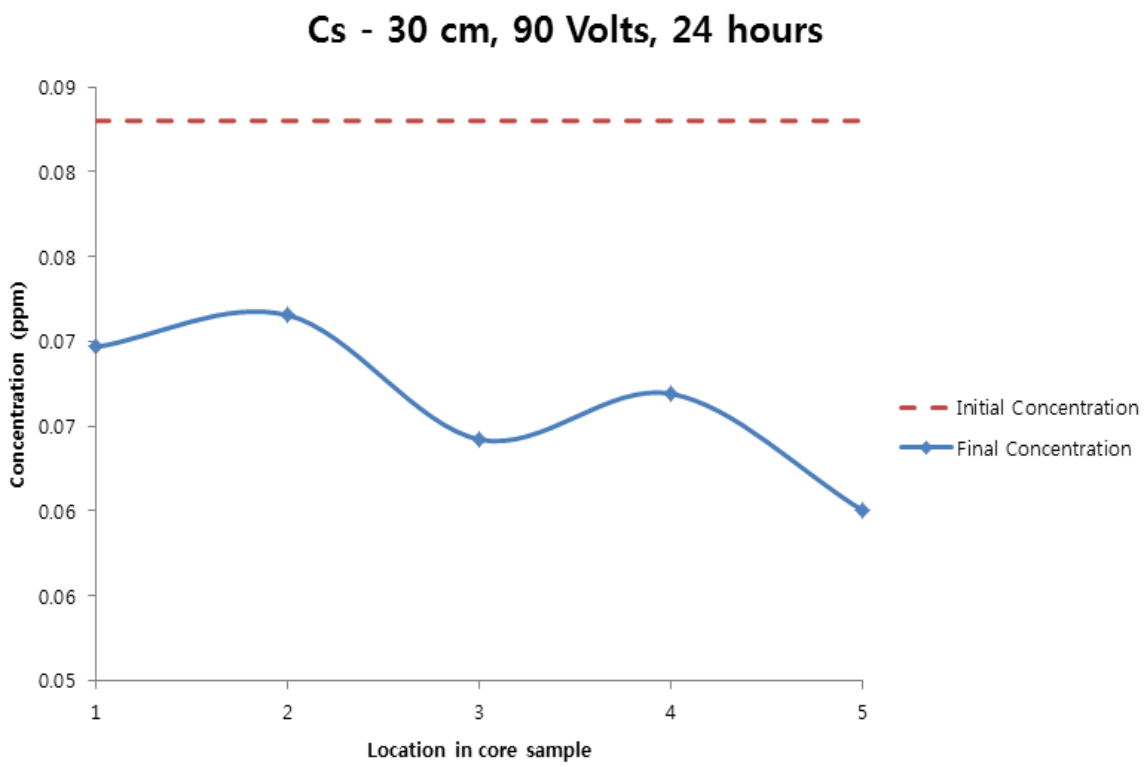

Figure 3-54: Concentration of Cs upon EK treatment.– Length: 30 cm, 90 Vol., Treatment time: 24 hours.

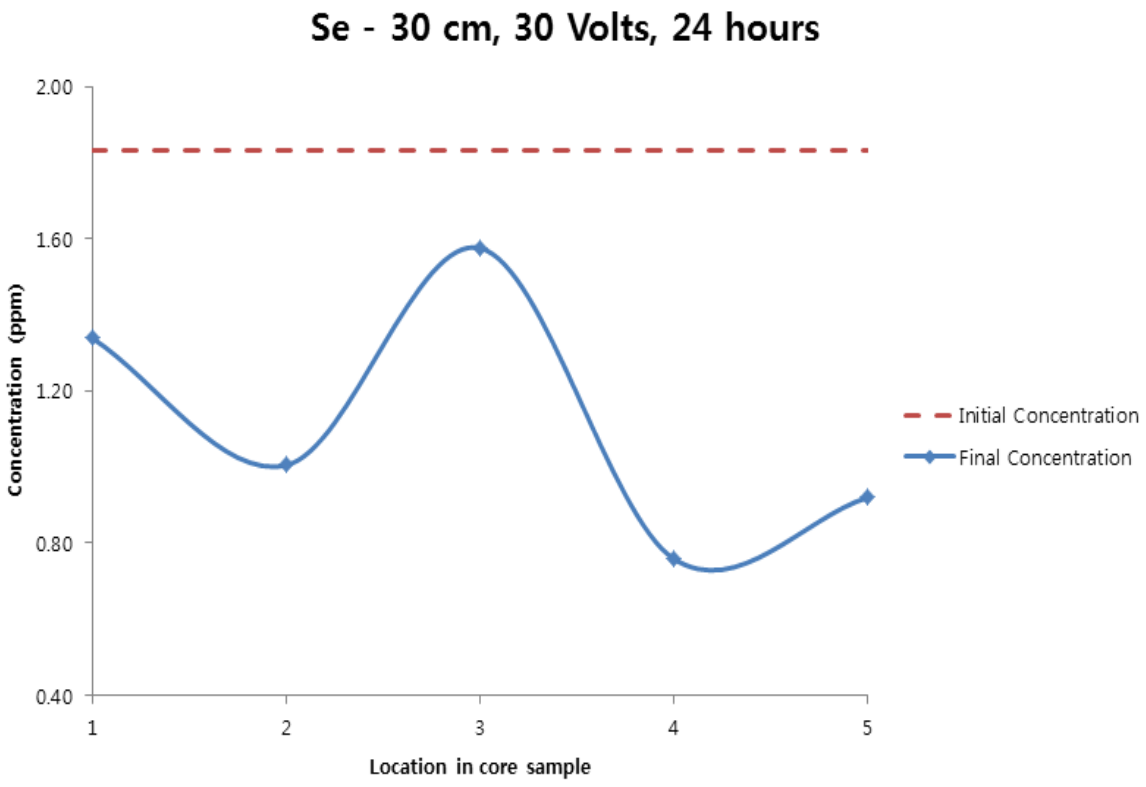

Figure 3-55: Concentration of Se upon EK treatment.– Length: 30 cm, 30 Vol., Treatment time: 24 hours.

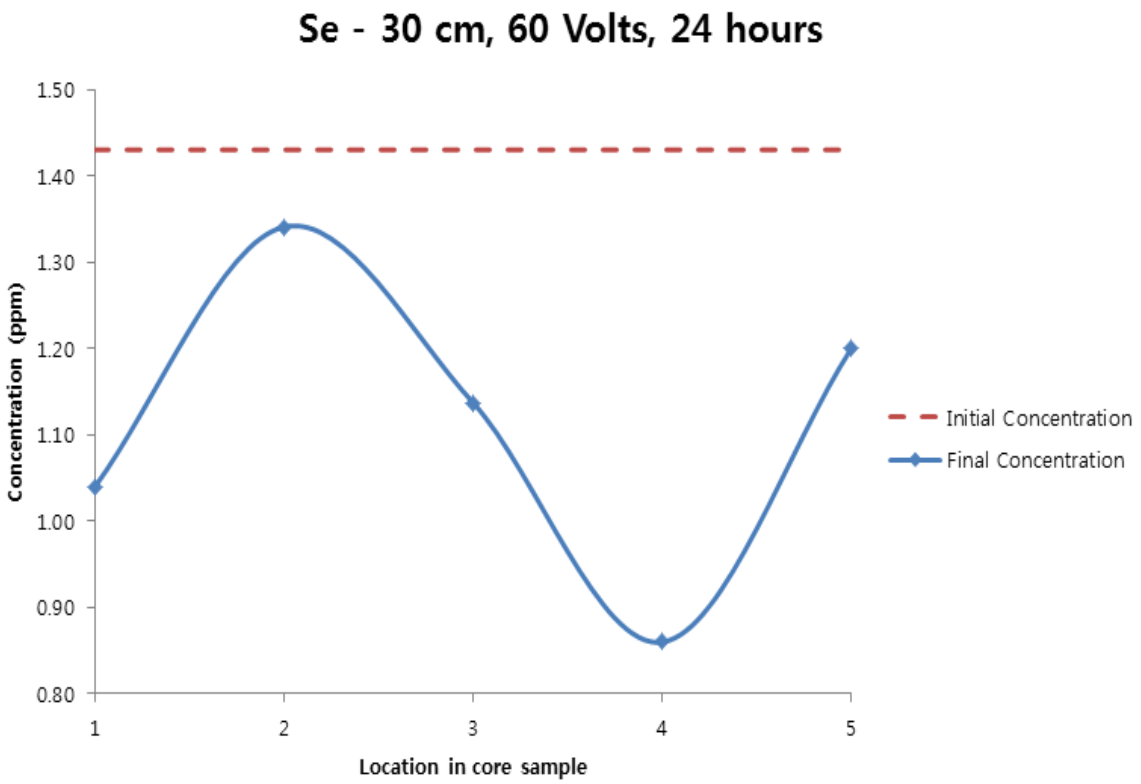

Figure 3-56: Concentration of Zn upon EK treatment.– Length: 30 cm, 60 Vol., Treatment time: 24 hours.

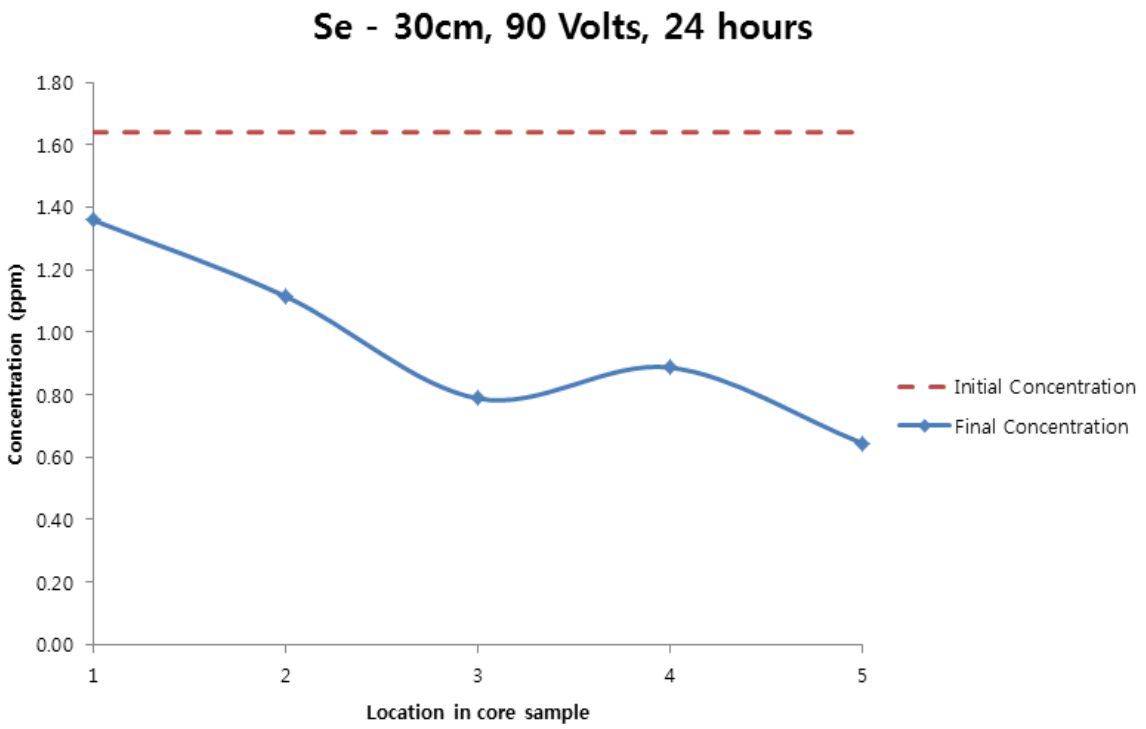

Figure 3-57: Concentration of Se upon EK treatment.– Length: 30 cm, 90 Vol., Treatment time: 24 hours.

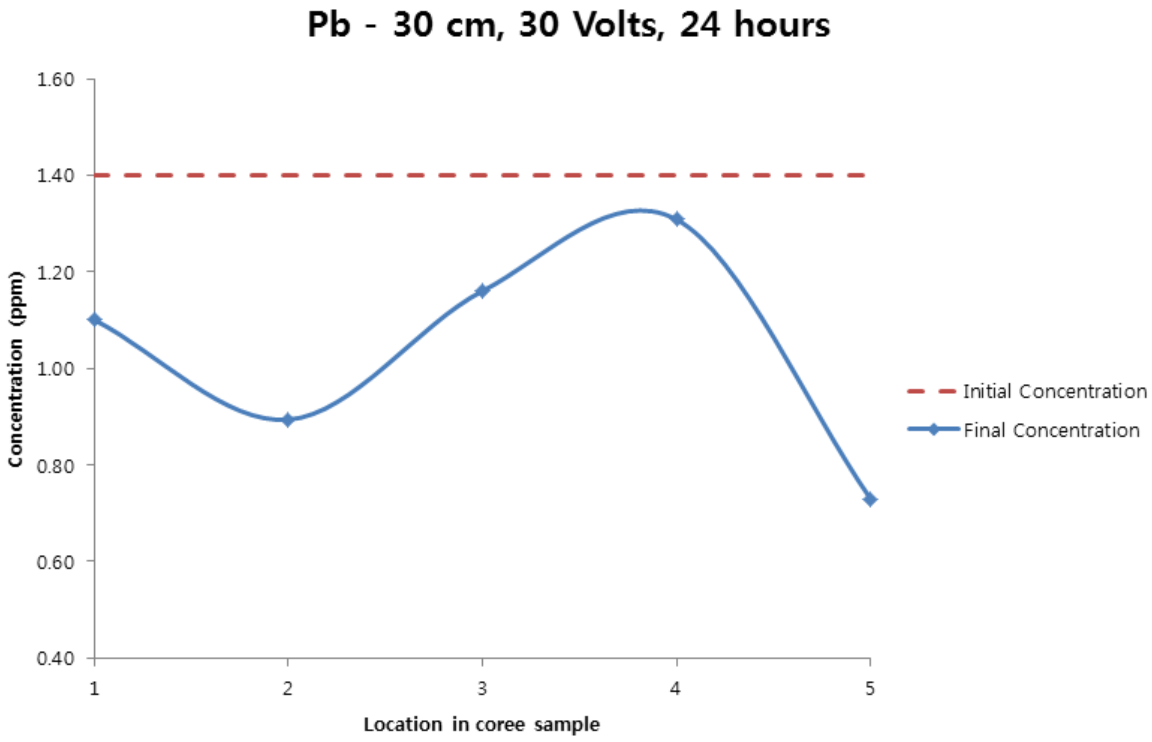

Figure 3-58: Concentration of Pb upon EK treatment – Length: 30 cm, 30 Vol., Treatment time: 24 hours.

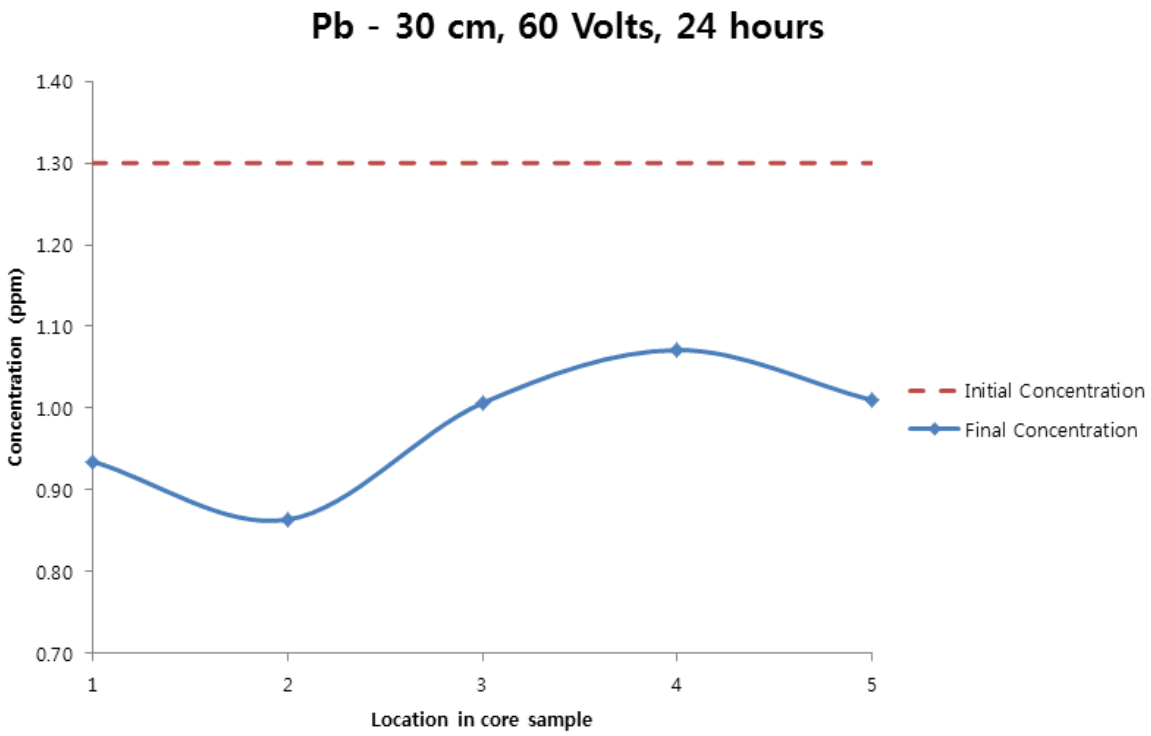

Figure 3-59: Concentration of Pb upon EK treatment.– Length: 30 cm, 60 Vol., Treatment time: 24 hours.

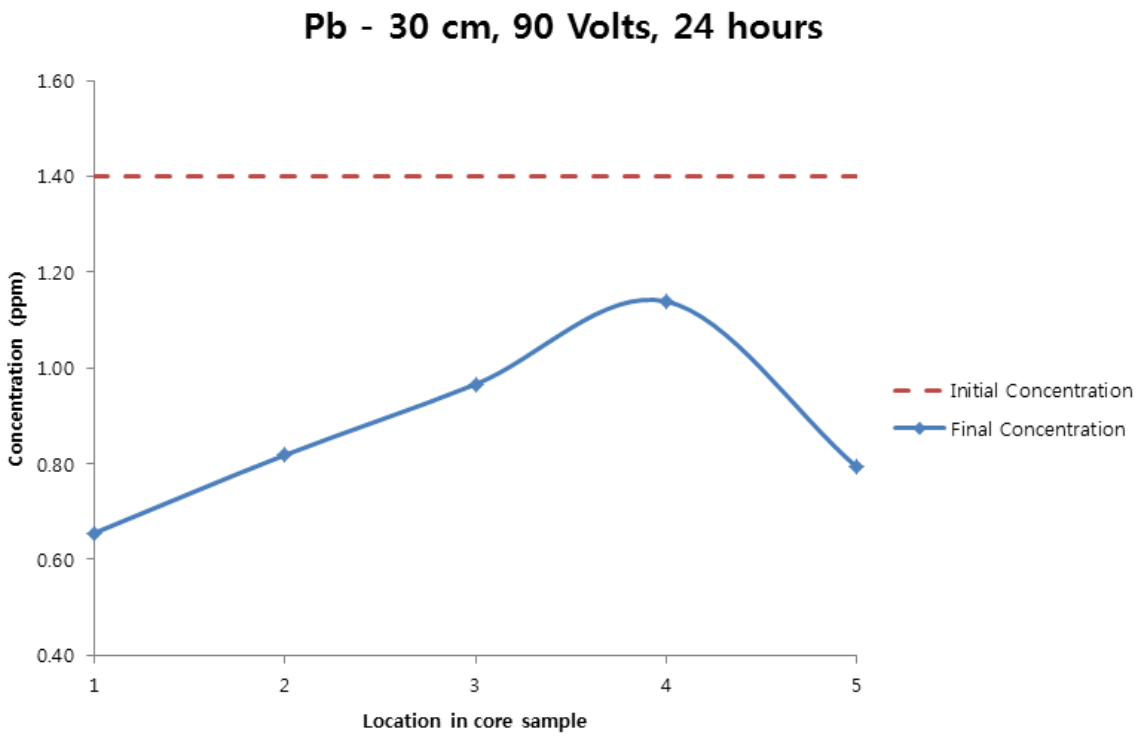

Figure 3-60: Concentration of Pb upon EK treatment.– Length: 30 cm, 90 Vol., Treatment time: 24 hours.

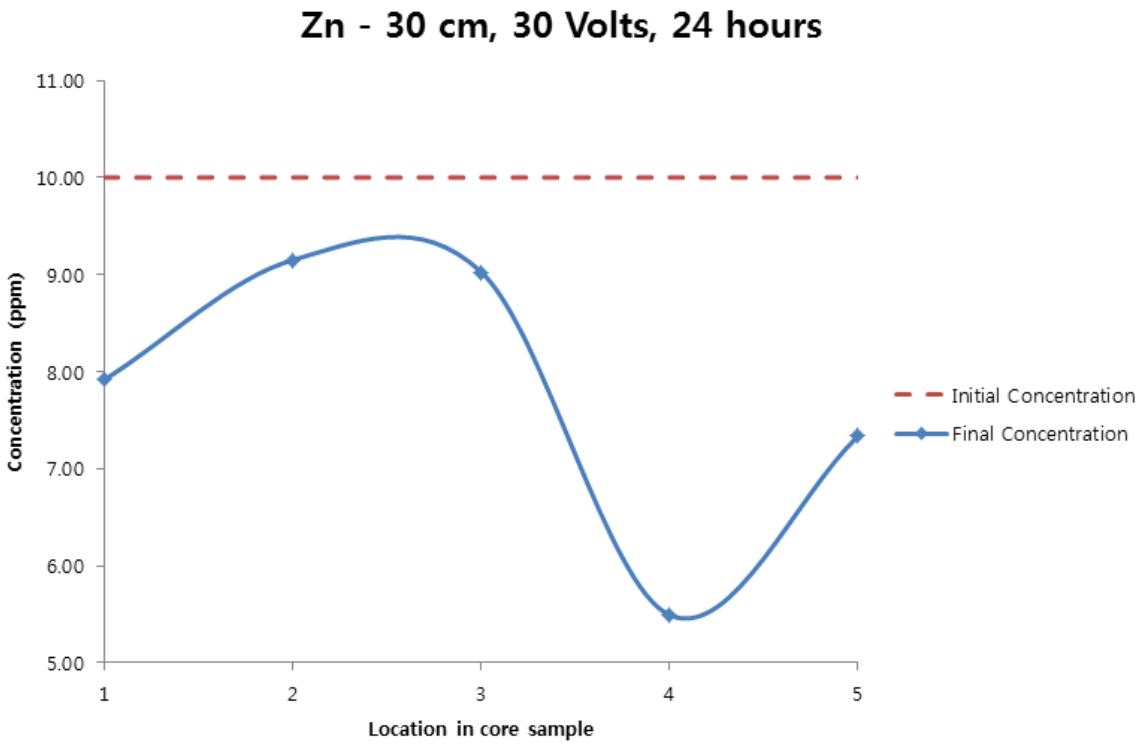

Figure 3-61: Concentration of Zn upon EK treatment.– Length: 30 cm, 30 Vol., Treatment time: 24 hours.

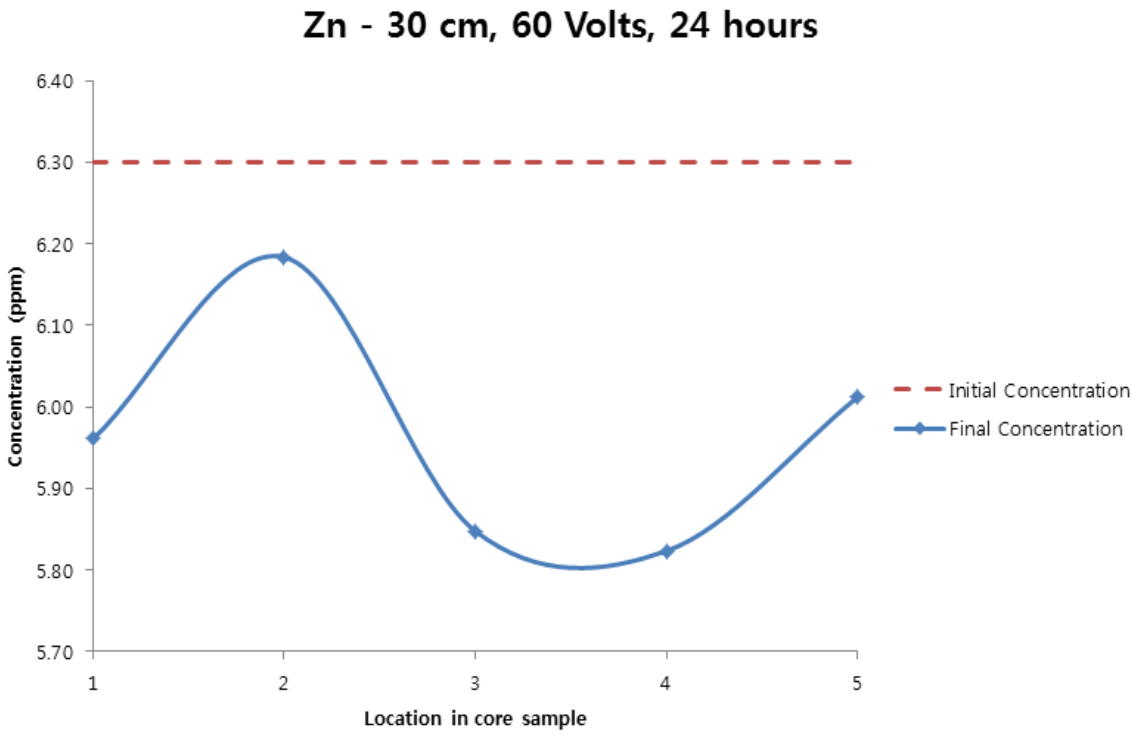

Figure 3-62: Concentration of Zn upon EK treatment.– Length: 30 cm, 60 Vol., Treatment time: 24 hours.

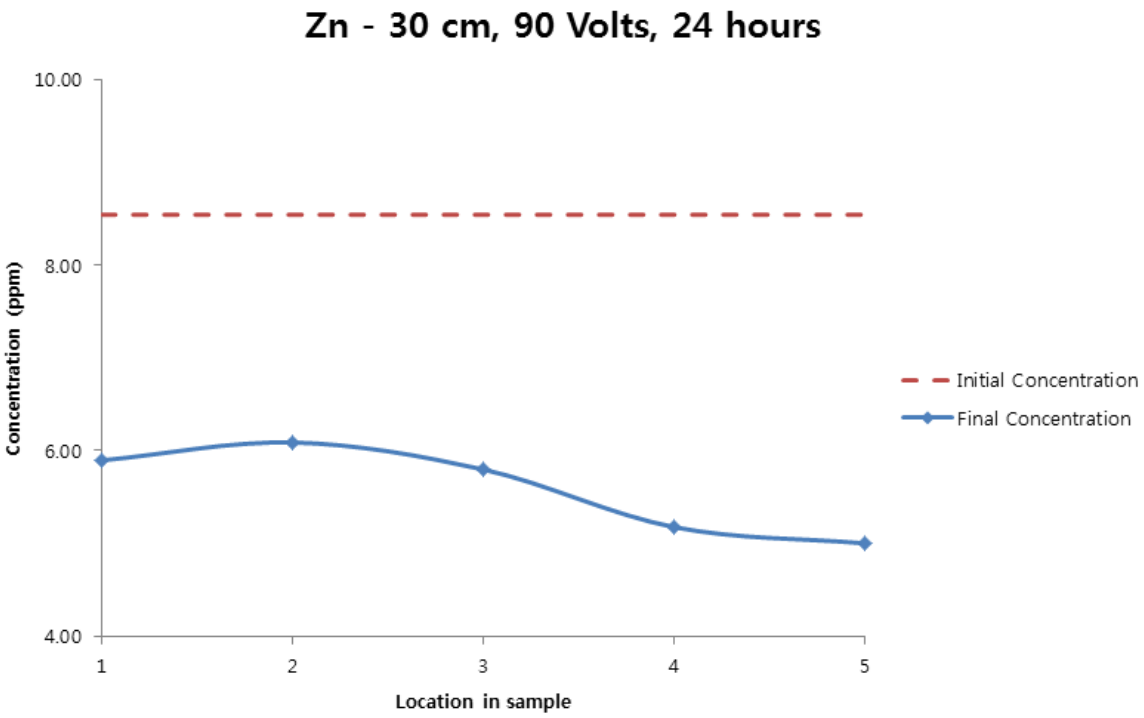

Figure 3-63: Concentration of Zn upon EK treatment.– Length: 30 cm, 90 Vol., Treatment time: 24 hours.

3.2 Comparison of Removal of Heavy Metals after 48 and 72 hours

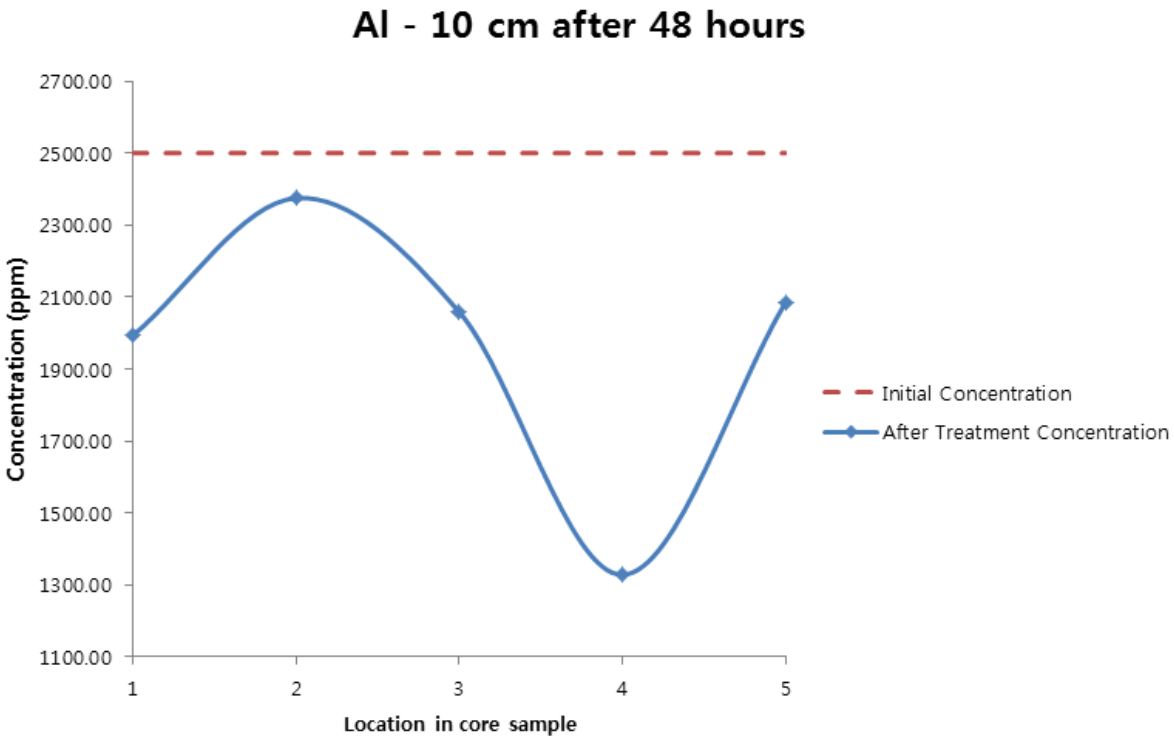

Figure 3-64: Concentration of Al upon EK Treatment after 48hours; length of core = 10 cm.

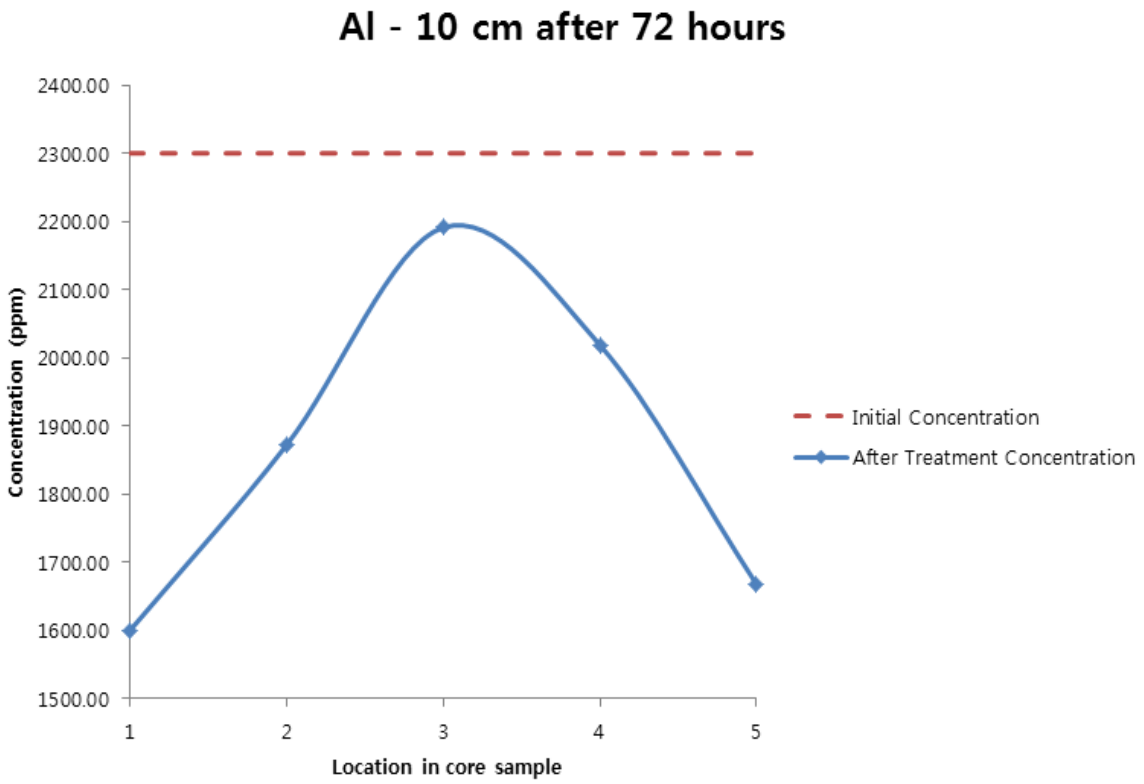

Figure 3-65: Concentration of Al upon EK Treatment after 72hours; length of core = 10 cm.

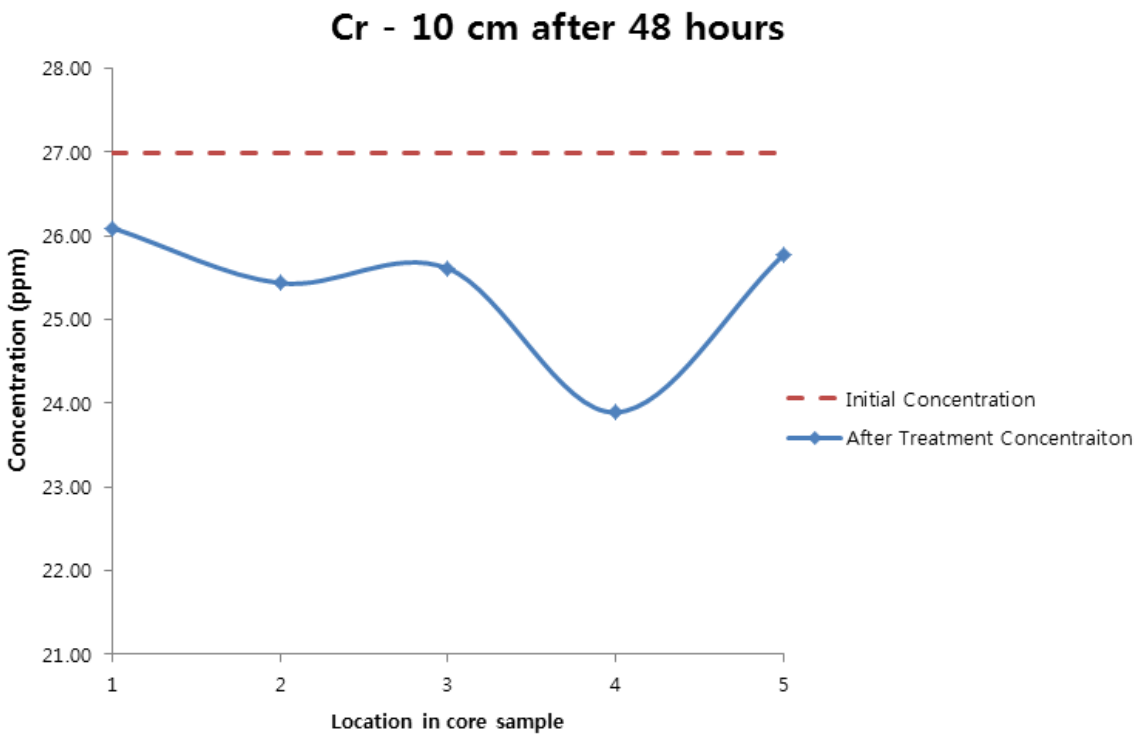

Figure 3-66: Concentration of Cr upon EK Treatment after 48hours; length of core = 10 cm.

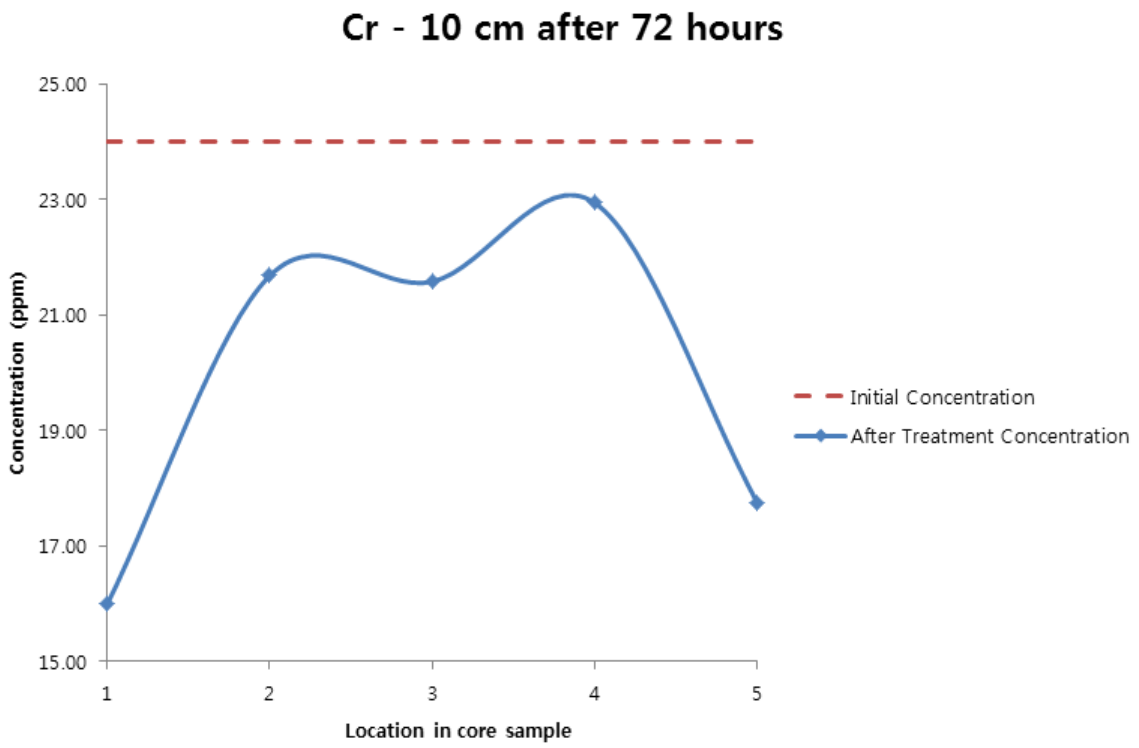

Figure 3-67: Concentration of Cr upon EK Treatment after 72hours; length of core = 10 cm.

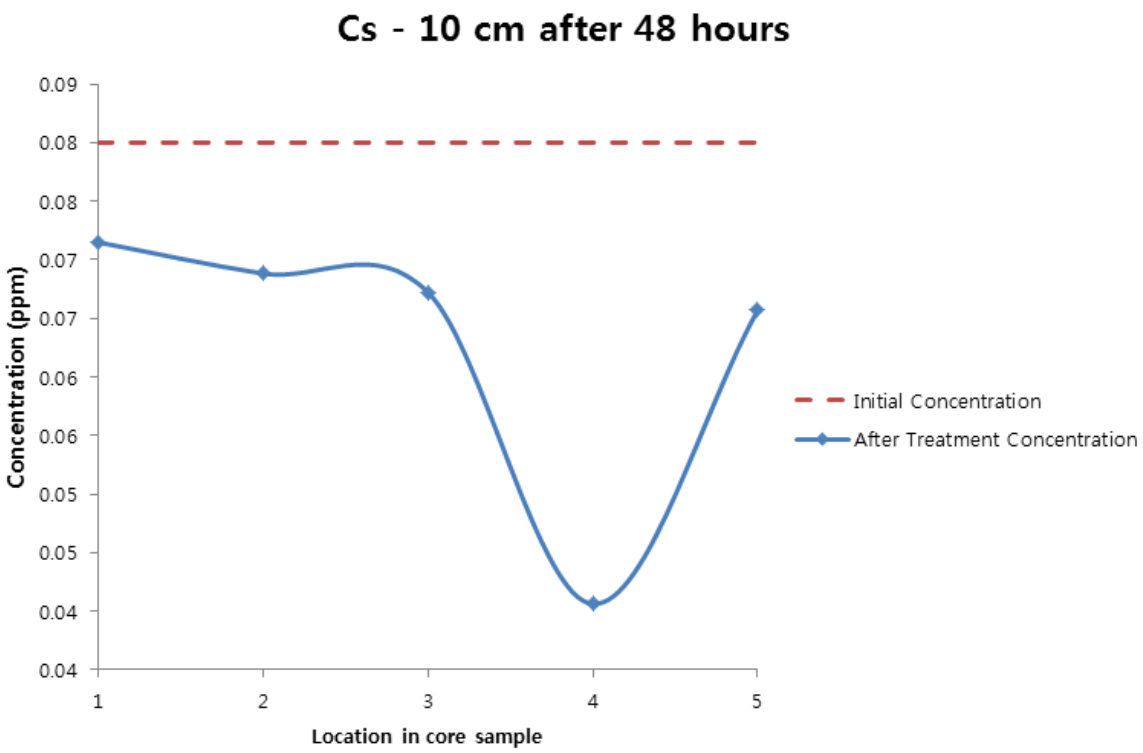

Figure 3-68: Concentration of Cs upon EK Treatment after 48hours; length of core = 10 cm.

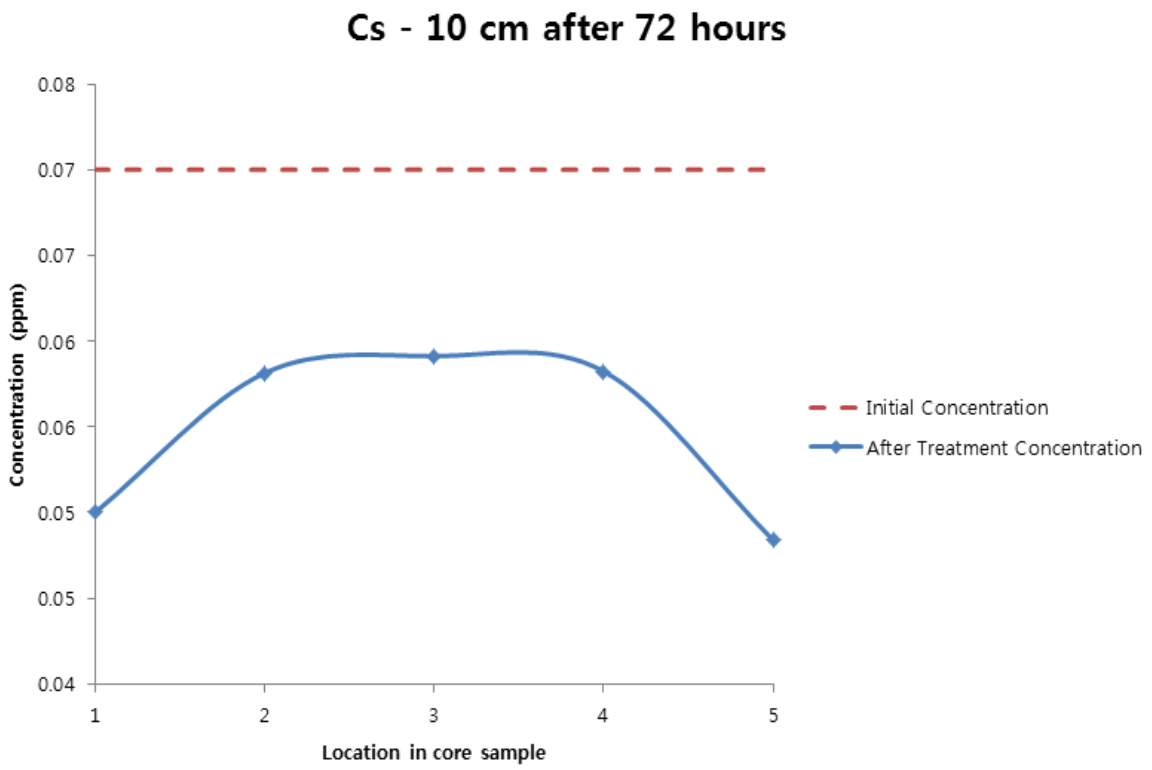

Figure 3-69: Concentration of Cs upon EK Treatment after 72 hours; length of core = 10 cm.

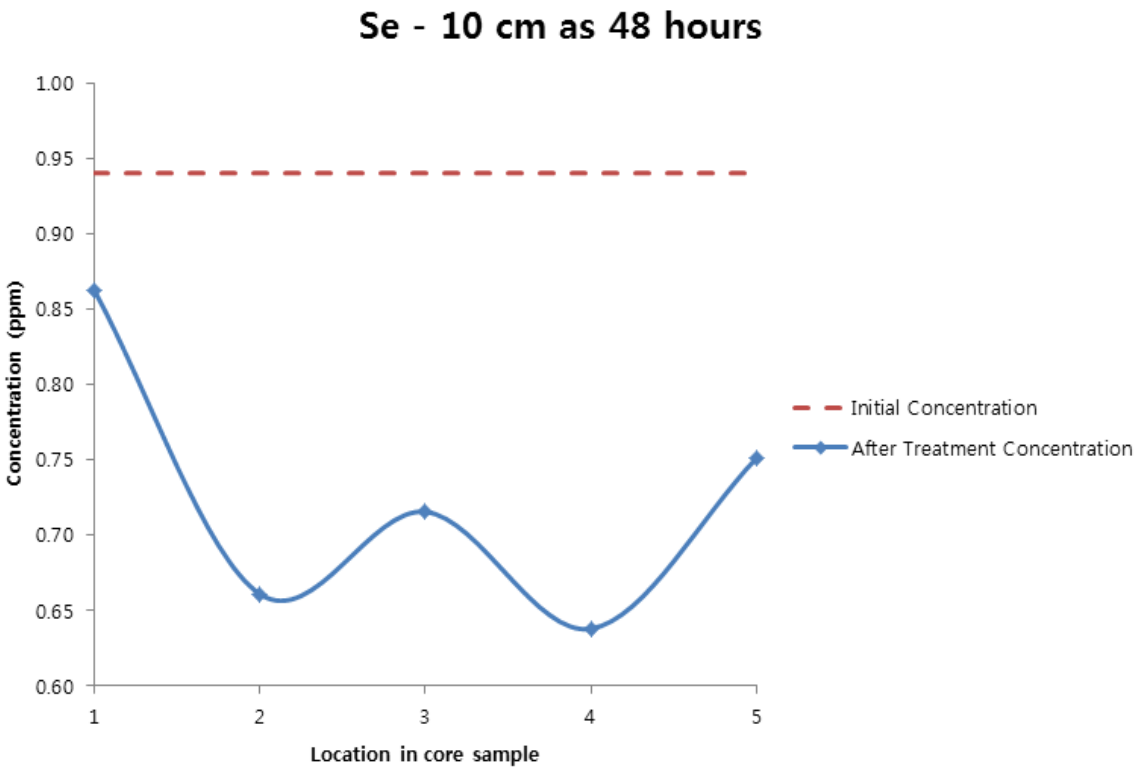

Figure 3-70:.Concentration of Se upon EK Treatment after 48 hours; length of core = 10 cm.

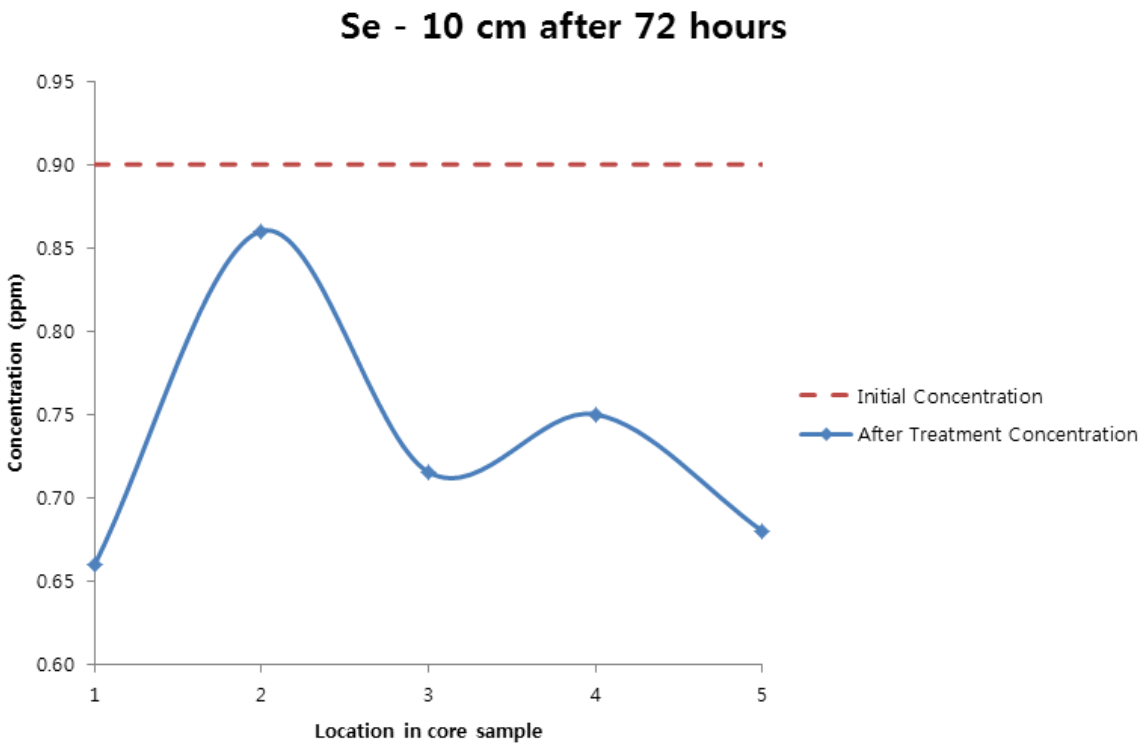

Figure 3-71: Concentration of Se upon EK Treatment after 72 hours; length of core = 10 cm.

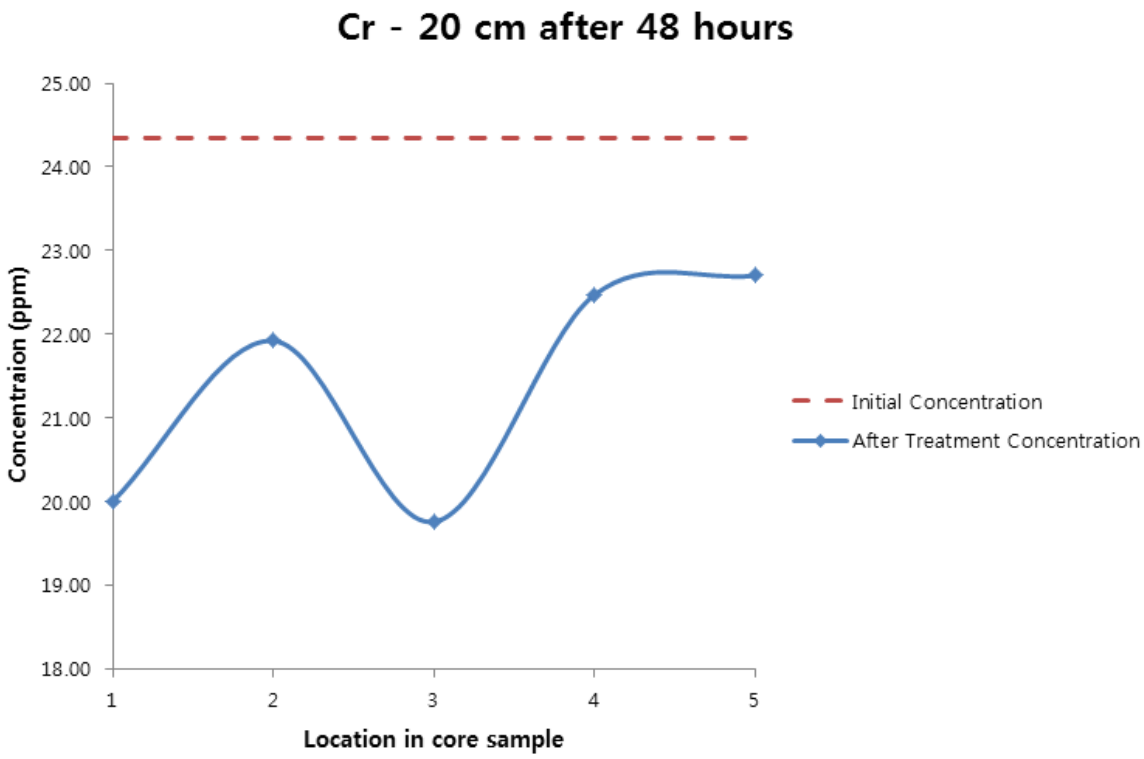

Figure 3-72: Concentration of Cr upon EK Treatment after 48 hours; length of core = 20 cm.

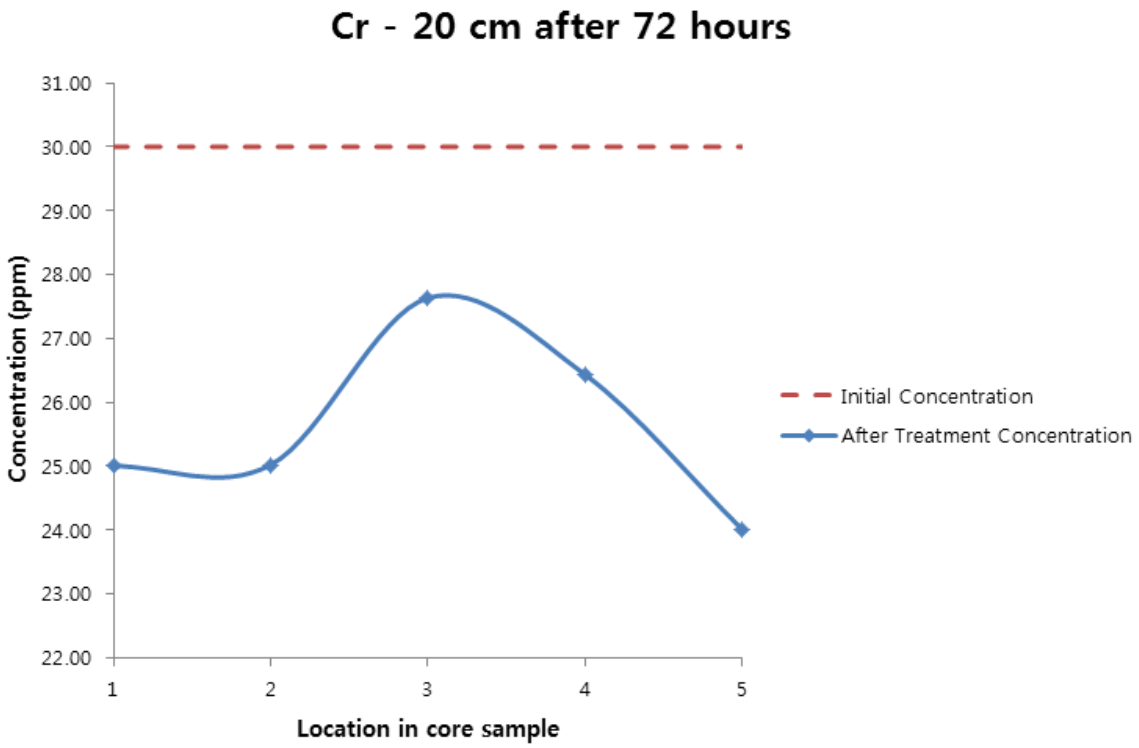

Figure 3-73: Concentration of Cr upon EK Treatment after 72 hours; length of core = 20 cm.

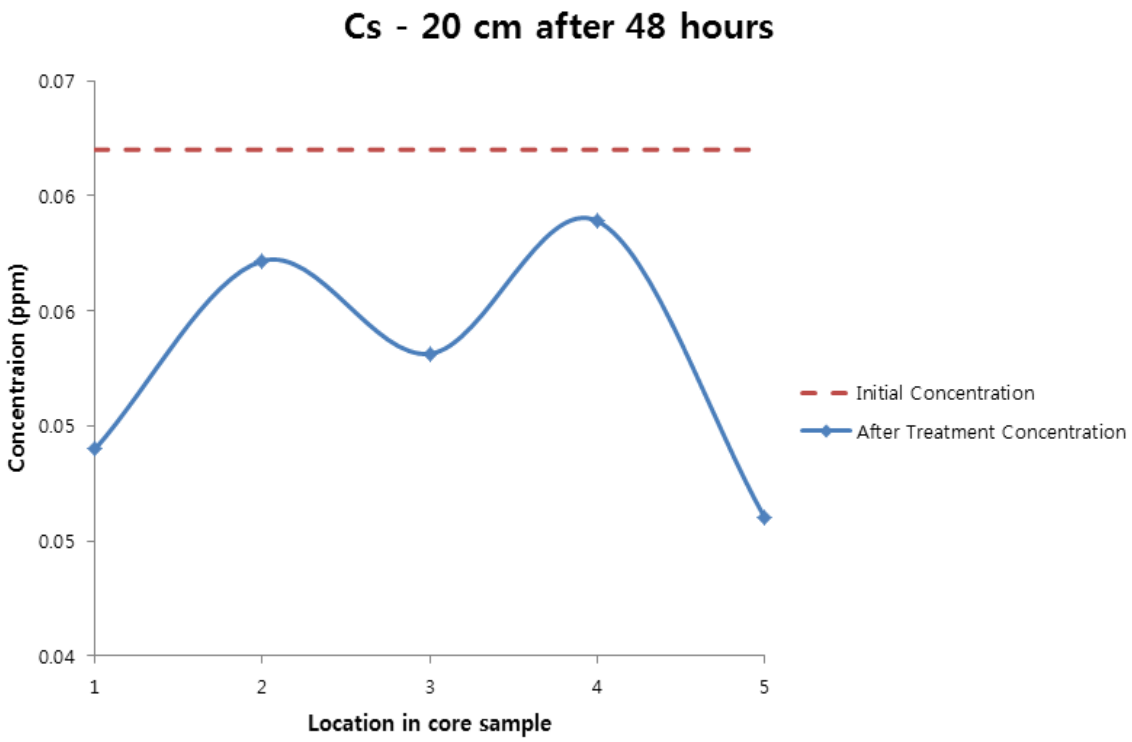

Figure 3-74: Concentration of Cs upon EK Treatment after 48 hours; length of core = 20 cm.

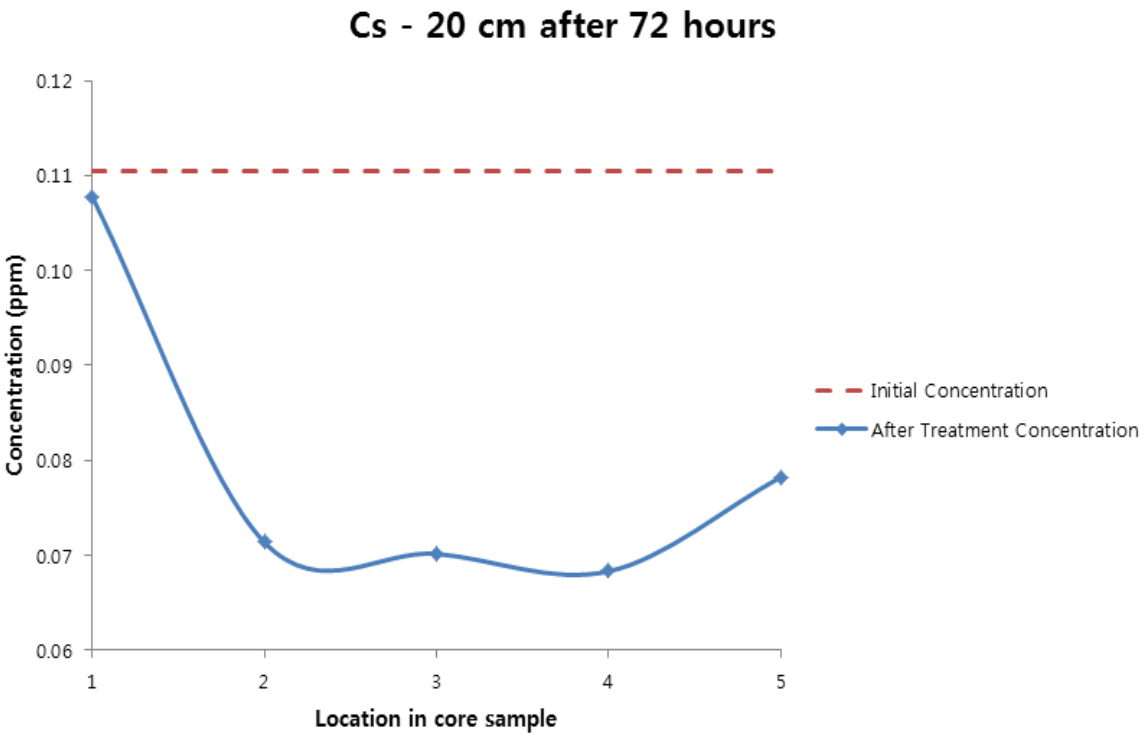

Figure 3-75: Concentration of Cs upon EK Treatment after 72 hours; length of core = 20 cm.

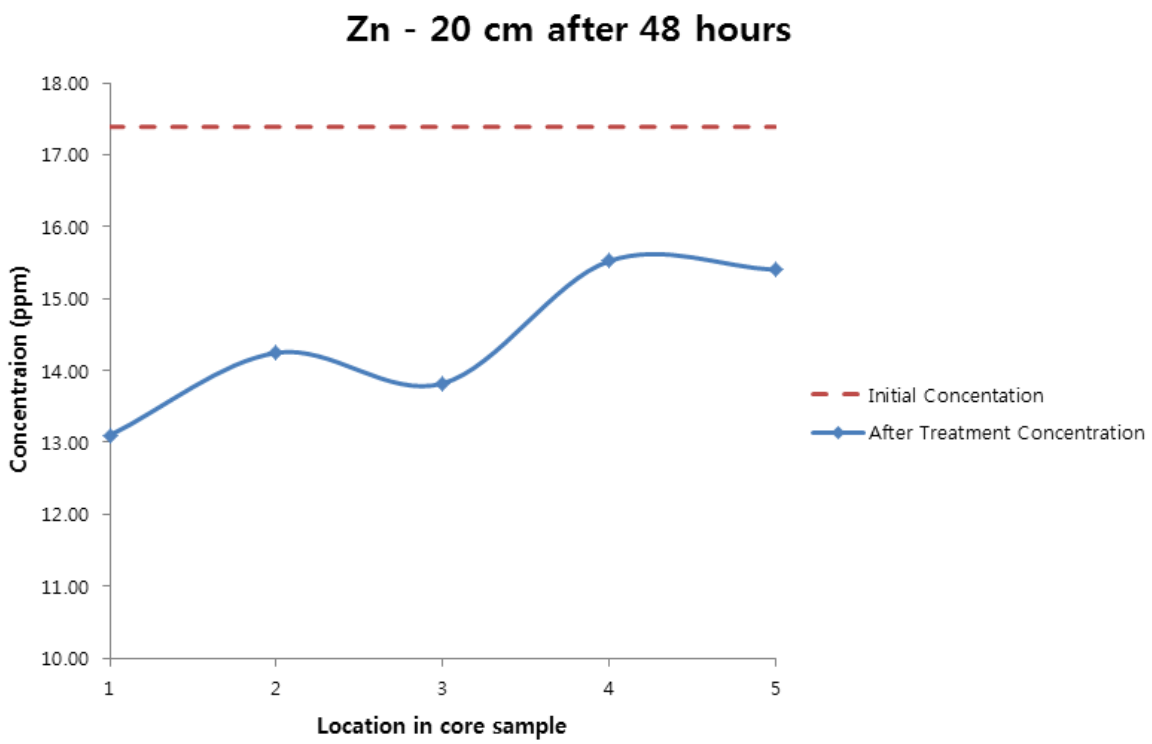

Figure 3-76: Concentration of Zn upon EK Treatment after 48 hours; length of core = 20 cm.

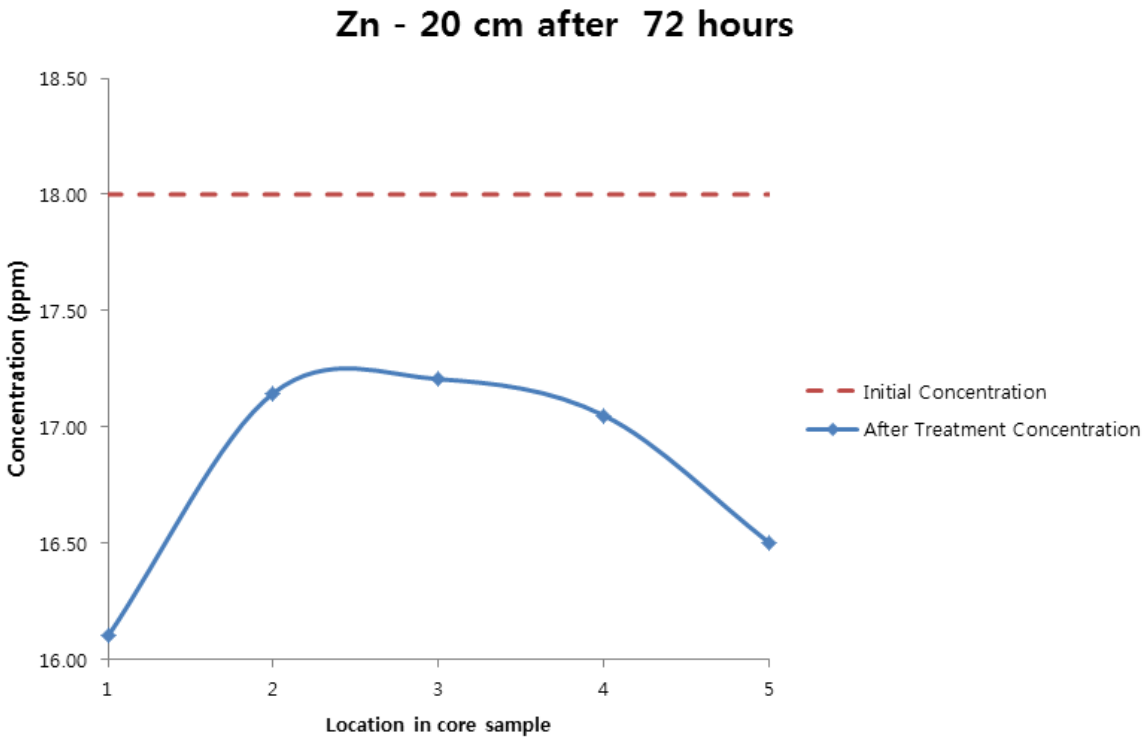

Figure 3-77: Concentration of Zn upon EK Treatment after 72 hours; length of core = 20 cm

3.3 Effect of Partial Chlorine Gas Removal

3.3.1 Partial Chlorine Gas Removal

In order to enhance the removal efficiency of heavy metals by management of the *in-situ* chlorine gas (Cl_2) production was successfully attempted. The tests showed a high removal efficiency of heavy metals at the anode end of cores after 24 hours of EK application. In the initial tests, high electrokinetic flow potential was achieved; however, high levels of chlorine gas were produced due to the high-salinity environment. Produced chlorine gas at the anode is toxic and acidic, causing corrosion of the equipment. The process was improved by controlling and maintaining a fraction of the chlorine gas (Cl_2) in place. An ideal fraction of chlorine gas maintained in the system to enhance the EK current was identified. In this study, two different fractions of chlorine gas (0, and 100 %) were used at various concentrations of heavy metals and voltage gradients. The sample diameter of cores was 3.81 cm (1.5 inch); pH and temperature were measured continuously.

H^+ was produced at the anode (3-1) and OH^- at the cathode (3-2).

$$H_2O - 2e^- \rightarrow \frac{1}{2} O_2 + 2 H^+ \qquad (3\text{-}1)$$

$$2H_2O + 2 e^- \rightarrow H_2 + 2 OH^- \qquad (3\text{-}2)$$

These two equations are fundamental electrode reactions occurring in the electrokinetic cell.

In this study, the chlorine gas (Cl_2) was produced at the anode, together with O_2 in the presence of saline water.

$$H_2O - 2e^- \rightarrow \frac{1}{2} O_2 + 2 H^+ \qquad (3\text{-}1)$$

$$2Cl^- - 2e^- \rightarrow Cl_2 \qquad (3\text{-}3)$$

The pH was continuously maintained at a value less than 10 at the cathode end, for increasing the efficiency and preventing the scaling in the cathode chamber. The value of pH at the anode was not controlled because saline water was flushed through the anode chamber by a peristaltic pump. The pH in the anode chamber was measured continuously and remained at less than about 2.5 (Figure 3-78). The chlorine gas (Cl_2) was treated using a filtration system before being released to air.

In a closed system, the Cl_2 gas was not allowed to escape with resulting increase in pressure, whereas in the open system the Cl_2 gas in allowed to escape to the atmosphere.

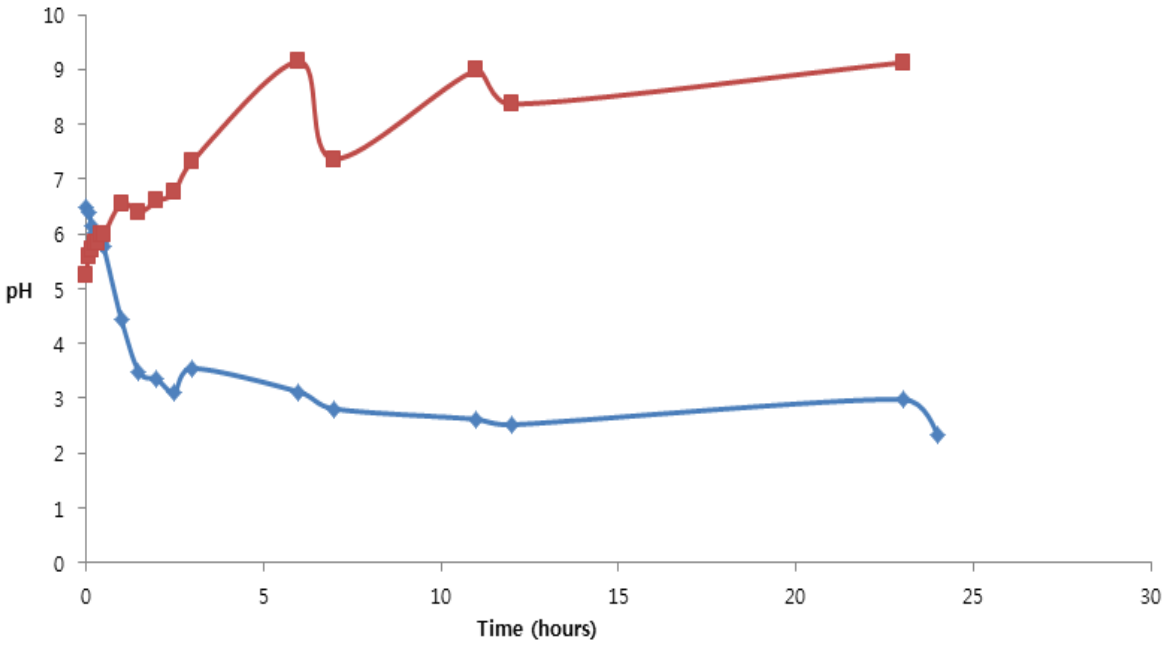

Figure 3-78: Change in pH at the anode and cathode with EDTA acid application. (Sample length = 10 cm; Voltage = 11 V; treatment time = 24 hours. Upper curve-- pH at the cathode. Lower curve -- pH at the anode.)

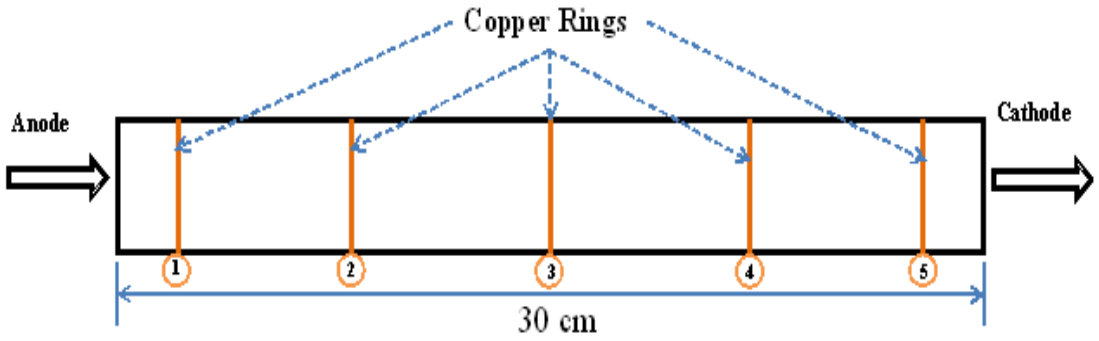

Figure 3-79: Five copper rings were mounted in mud samples.

Five copper rings were mounted inside each sample (Figure 3-79) and then examined for degree of corrosion.

Tests were performed with the following objectives in mind:

1. Reducing the cost of controlling pH by free Cl_2 gas and gas pressure generated at anode chamber.
2. Controlling pH by keeping a fraction of chlorine gas *in-situ*. Chlorine gas was transported from anode to cathode.
3. Improving the efficiency of removal of heavy metals from the contaminated muds

The samples were collected from two different contaminated areas in Abu Dhabi; (1) offshore muds adjacent to refinery--industrial area, and (2) offshore muds in port area.

Mud samples were sieved using a 1-mm sieve and then compressed in a cylinder 3.81 cm in diameter and 30-cm long for seven days. Applied pressure was 30 psi.

Two samples 30-cm in length were treated continuously with DC current for 24 hours: sample No.1, open system, and sample No.2, closed system. Two other samples were treated for 40 hours (sample No.3, open system, and sample No. 4, closed system) with two 8-hour interruptions (total treatment time = 24 hours).

The experimental results presented in Figures 3-80 through 99. Figures 3-82 through 3-91 show the results of 24-hour treatment, whereas Figures 3-94 through 3-99 show the results after EK treatment applied for 40 hours with two 8-hour interruptions (actual treatment time = 24hours). Water contents were reduced from 35% to 30% with temperature increase of 20 ºC to 45 ºC.

Figure 3-80 shows the results of application of different voltage gradients in two tests. Application of potential gradient of 3.5 V/cm in the open system resulted in an increased removal efficiency when compared to application of 3.5 V/cm. Figure 3 -82 demonstrates that the reduction in aluminum concentration was significantly greater with the open test. While applying almost 30% less voltage gradient, the electrokinetic remediation of aluminum proved to be up to 10 times more at the fourth tested location. Higher removal efficiency was obtained by taking advantage of the free Cl_2 gas generated at the anode and transported to the cathode in a closed system. Reduced power consumption with higher volumes of produced water was achieved in the closed system.

It is important to note that enough all the metals exhibited a similar w-shape pattern as can be seen in Figures 3-82 through 3-91, whereas the closed system test revealed higher removal efficiency at the fourth of five tested locations along the core length of 22.5 cm.

Figures 3-94 through 3-99 displayed results of a second set of tests to illustrate the effect of chlorine gas on removal efficiency. In both tests the application of EK was interrupted in a certain fashion to limit the production of chlorine. (interruption for a period of 8 hours after each 8 hours of EK application. These results compared to continuous EK application over 24 hours). It was clearly demonstrated that in the case of interruption the chlorine gas generation was restricted and, therefore, didn't go into solution to reduce the pH, and improve the efficiency of metal control capability as well as the potential of pressure displacement. In addition, the continuous system had a steady current induced over a longer period of time promoting more successful electrokinetic

application to allow for better transport of metals to take place.

The continuous application of D.C. in closed system gave better results than interrupted application of D.C. Final pH at the cathode was reduced with the aid of transported Cl_2 gas. Further studies are required to identify the optimum amount of chlorine gas to better control pH, further increase electroremediation performance, and reduce power consumption.

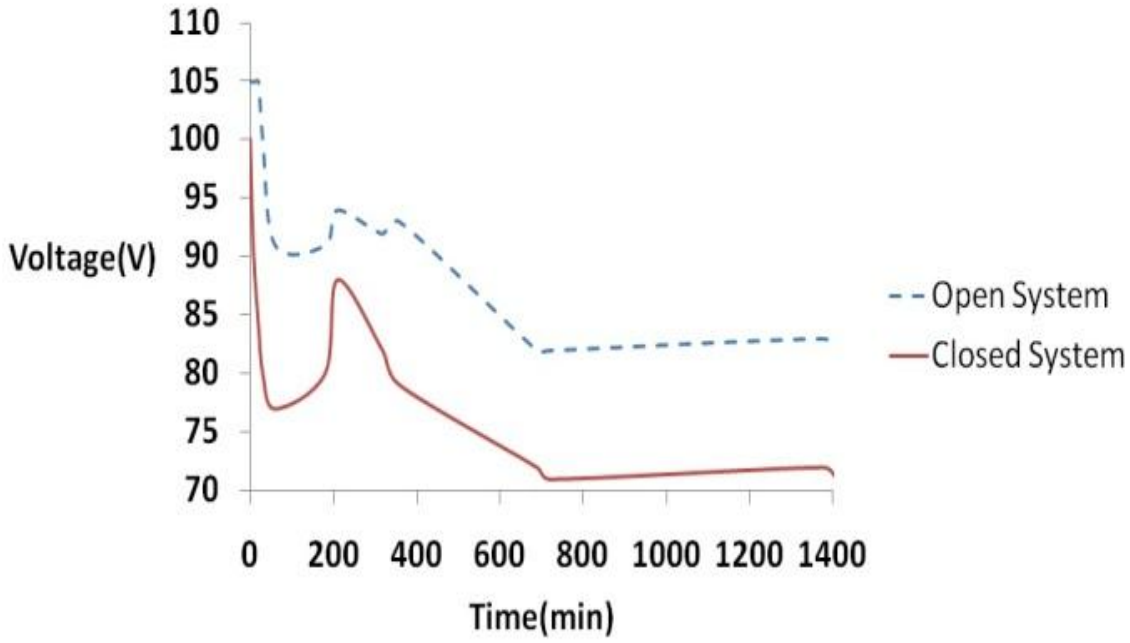

Figure 3-80: Variation of voltage with time for samples No.1 and No.2. Sample length = 30 cm; treatment time= 24 hours.

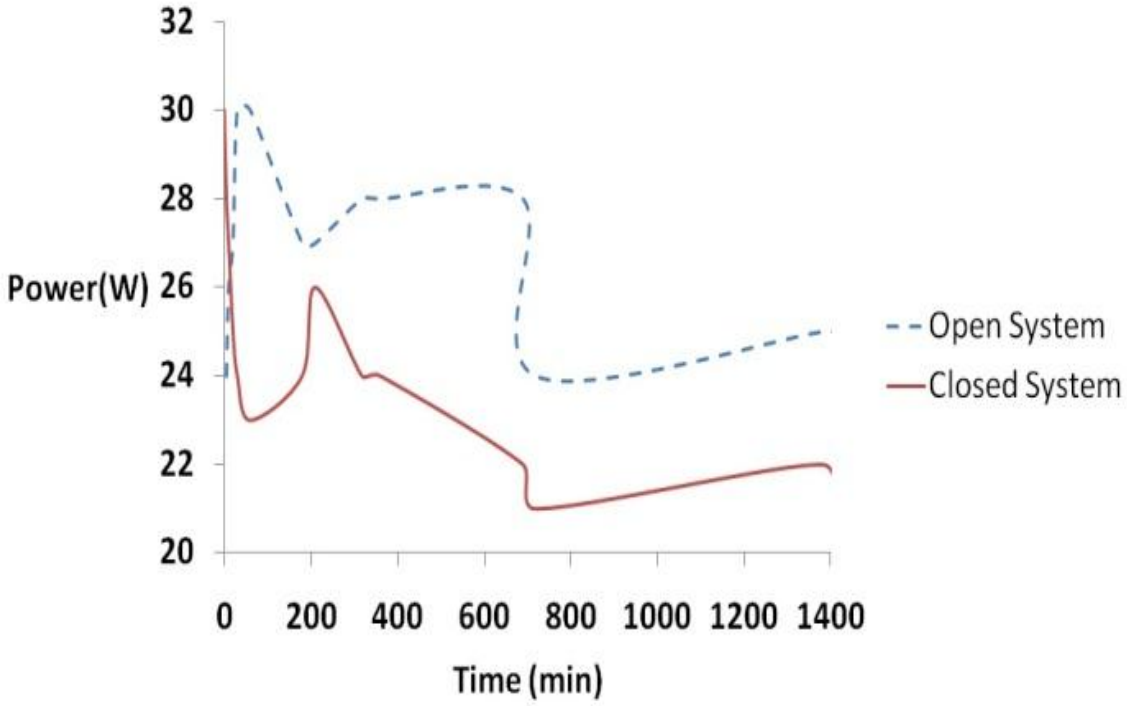

Figure 3-81: Variation of power with time for samples No.1 and No.2. Sample length = 30 cm; treatment time= 24 hours.

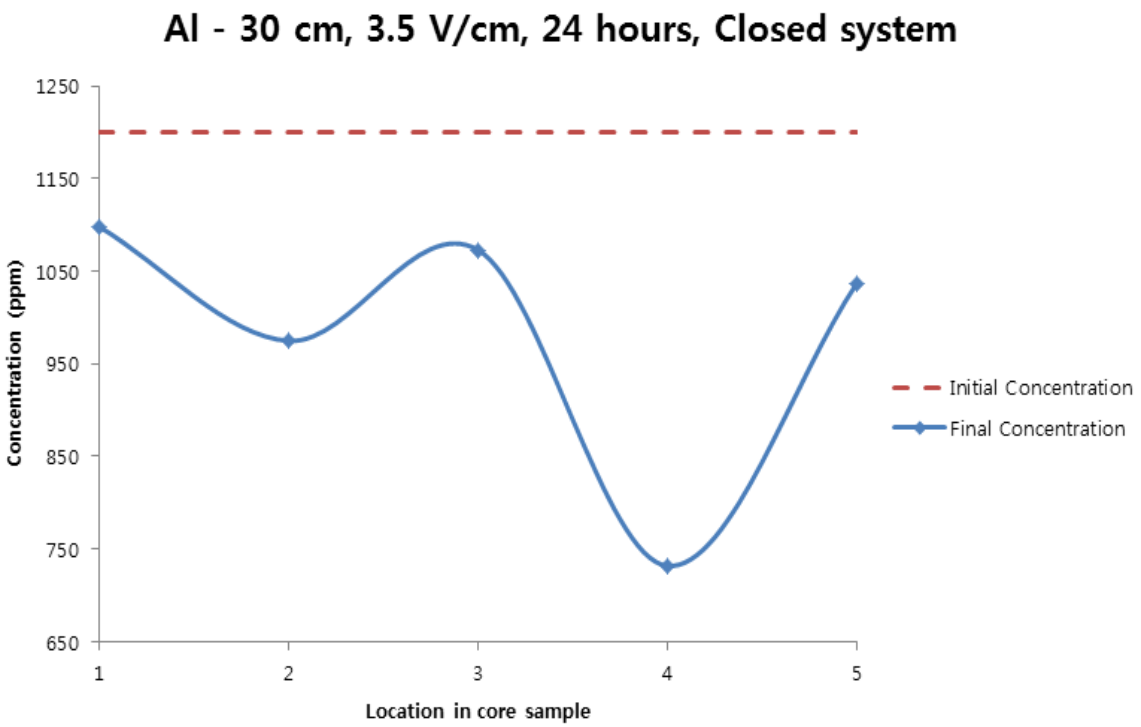

Figure 3-82: Concentration of Al upon EK treatment along the core length of 30 cm. Potential gradient = 3.5 V/cm, Treatment time = 24 hours.

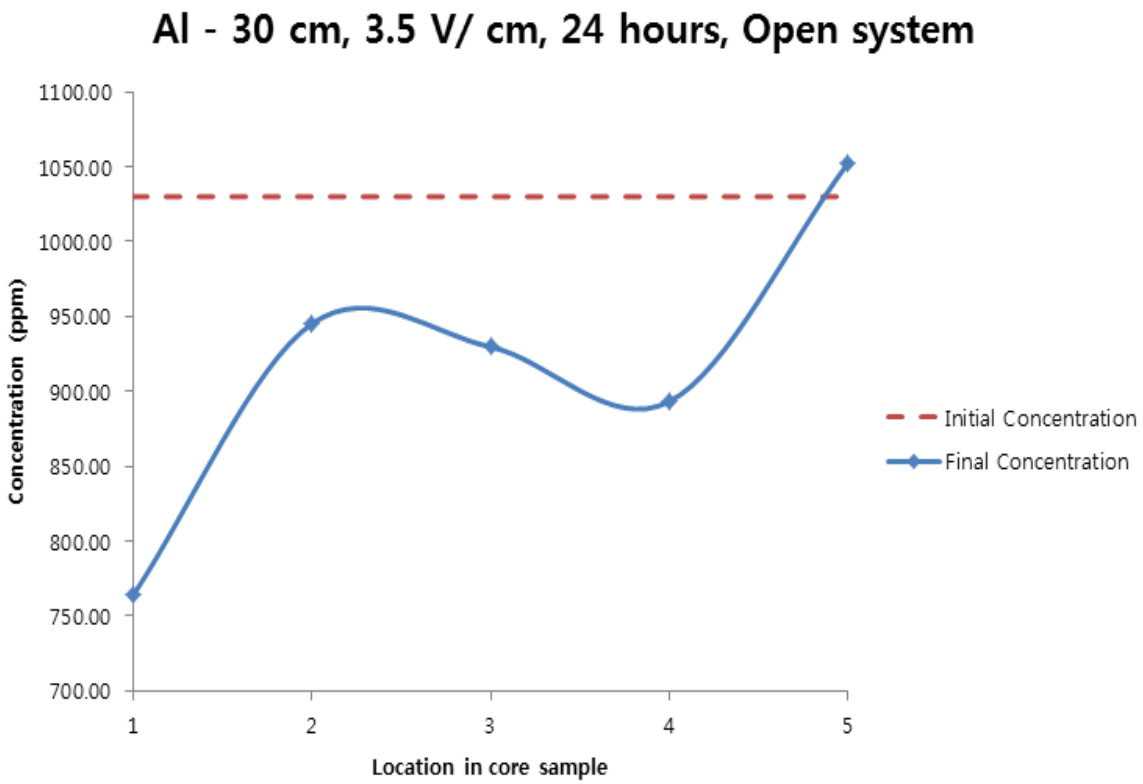

Figure 3-83: Concentration of Al upon EK treatment along the core length of 30 cm. Potential gradient = 3.5 V/cm, Treatment time = 24 hours.

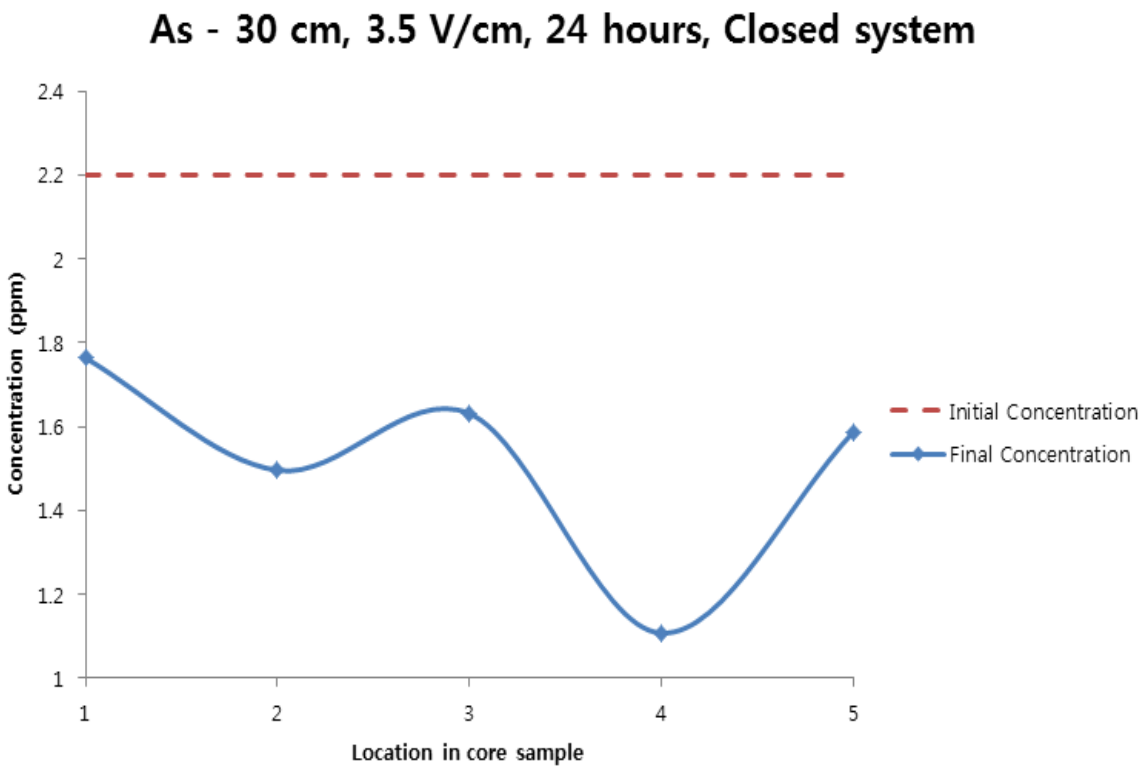

Figure 3-84: Concentration of As upon EK treatment along the core length of 30 cm. Potential gradient = 3.5 V/cm, Treatment time = 24 hours.

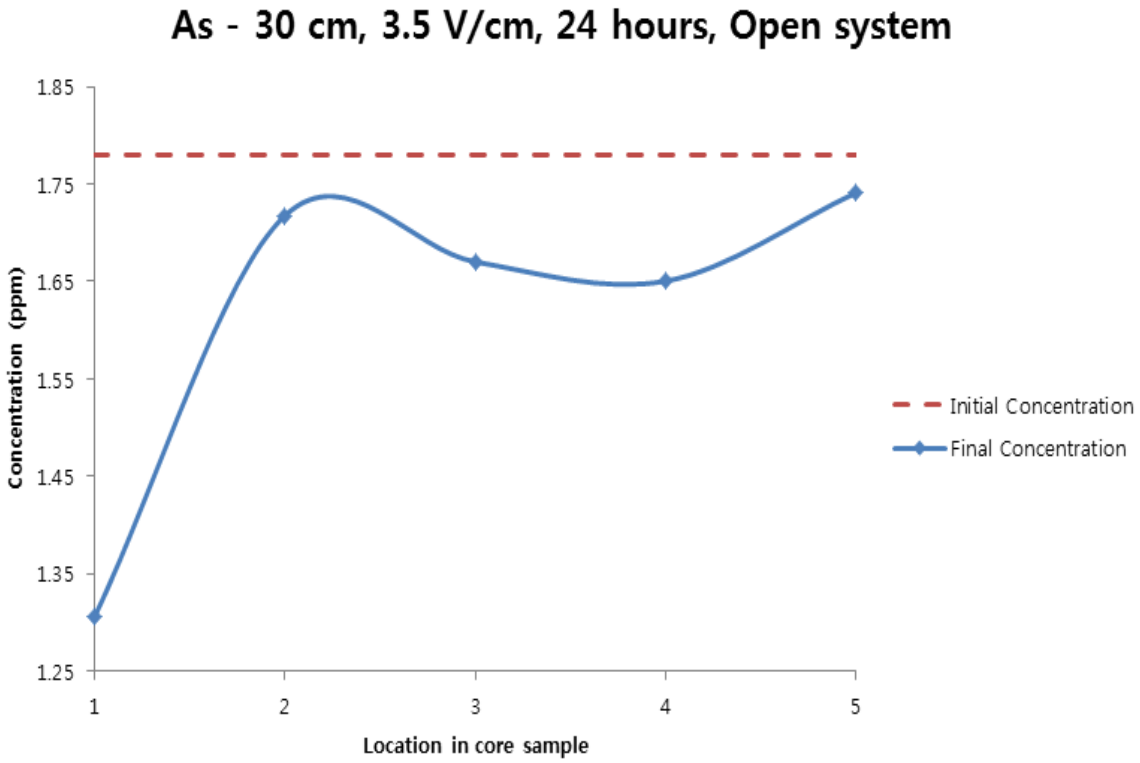

Figure 3-85: Concentration of As upon EK treatment along the core length of 30 cm. Potential gradient = 3.5 V/cm, Treatment time = 24 hours.

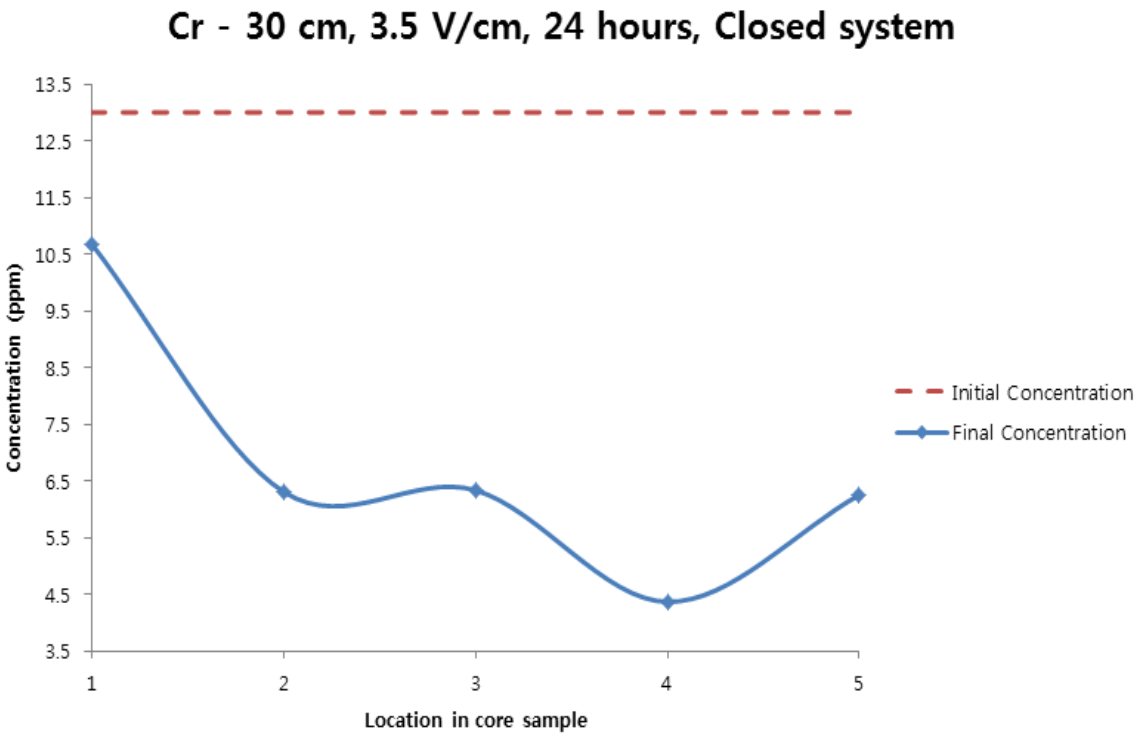

Figure 3-86: Concentration of Cr upon EK treatment along the core length of 30 cm. Potential gradient = 3.5 V/cm, Treatment time = 24 hours.

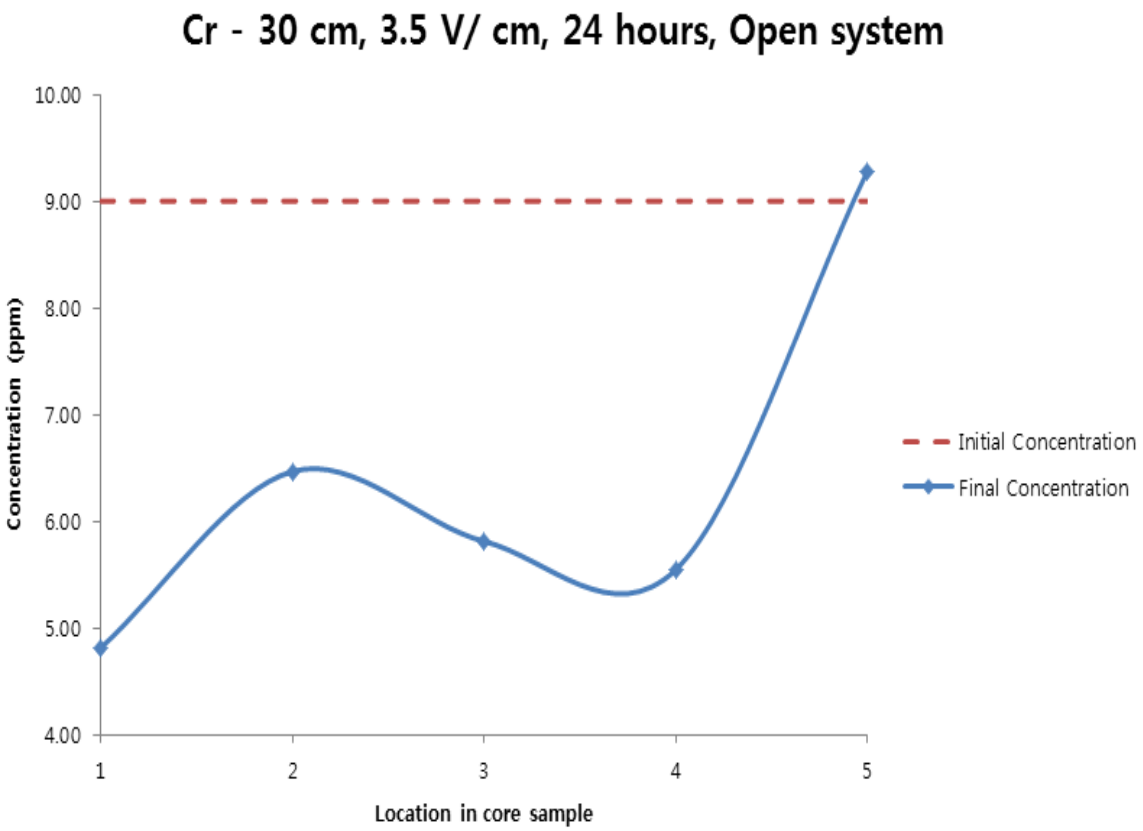

Figure 3-87: Concentration of Cr upon EK treatment along the core length of 30 cm. Potential gradient = 3.5 V/cm, Treatment time = 24 hours.

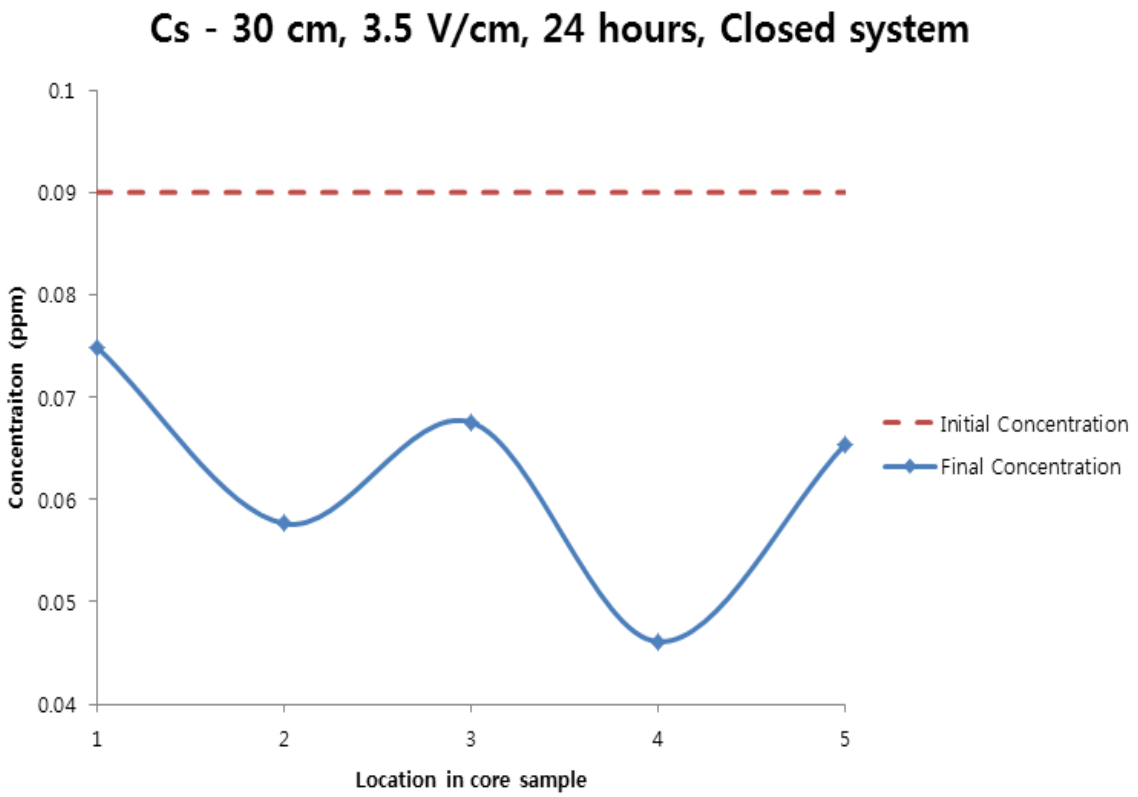

Figure 3-88: Concentration of Cs upon EK treatment along the core length of 30 cm. Potential gradient = 3.5 V/cm, Treatment time = 24 hours.

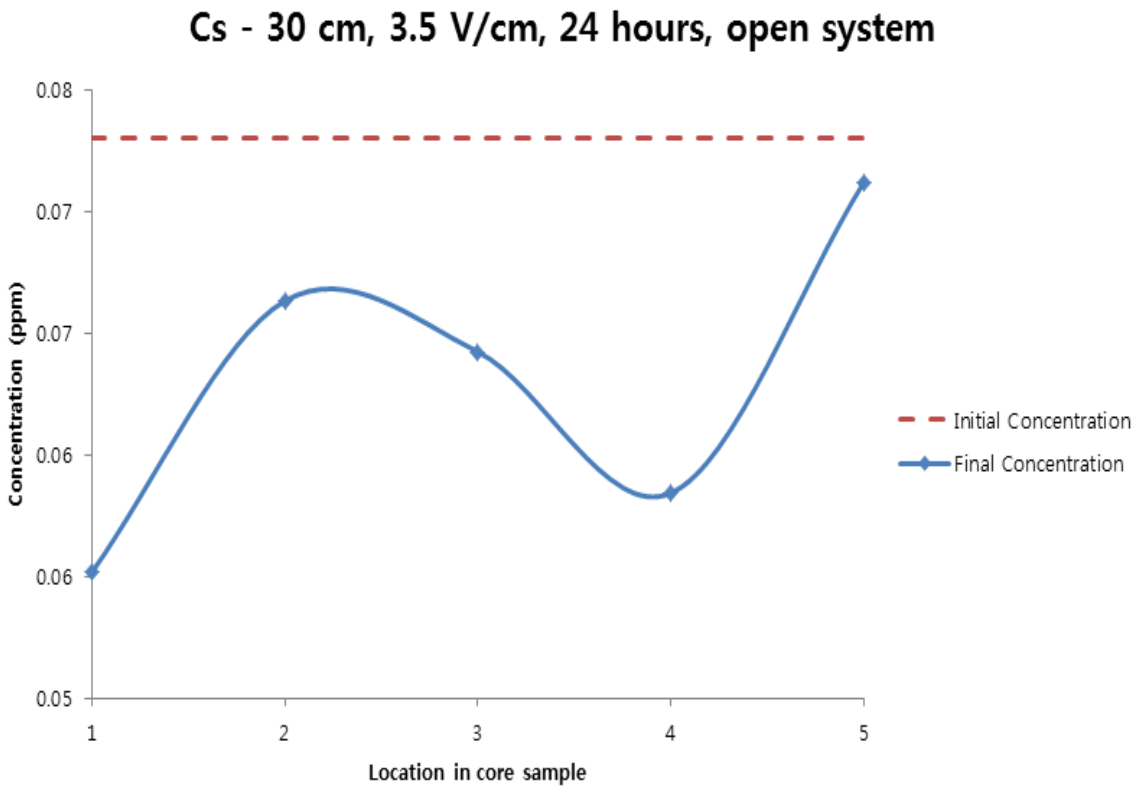

Figure 3-89: Concentration of Cs upon EK treatment along the core length of 30 cm. Potential gradient = 3.5 V/cm, Treatment time = 24 hours.

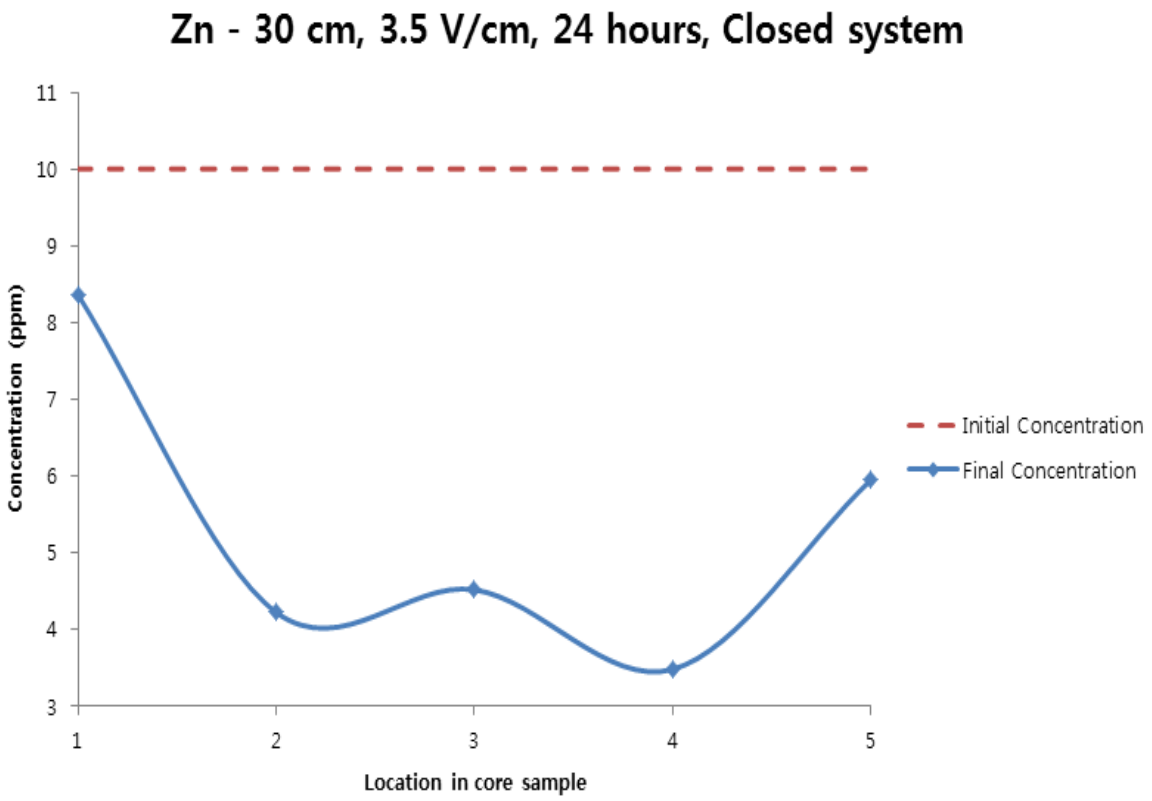

Figure 3-90: Concentration of Zn upon EK treatment along the core length of 30 cm. Potential gradient = 3.5 V/cm, Treatment time = 24 hours.

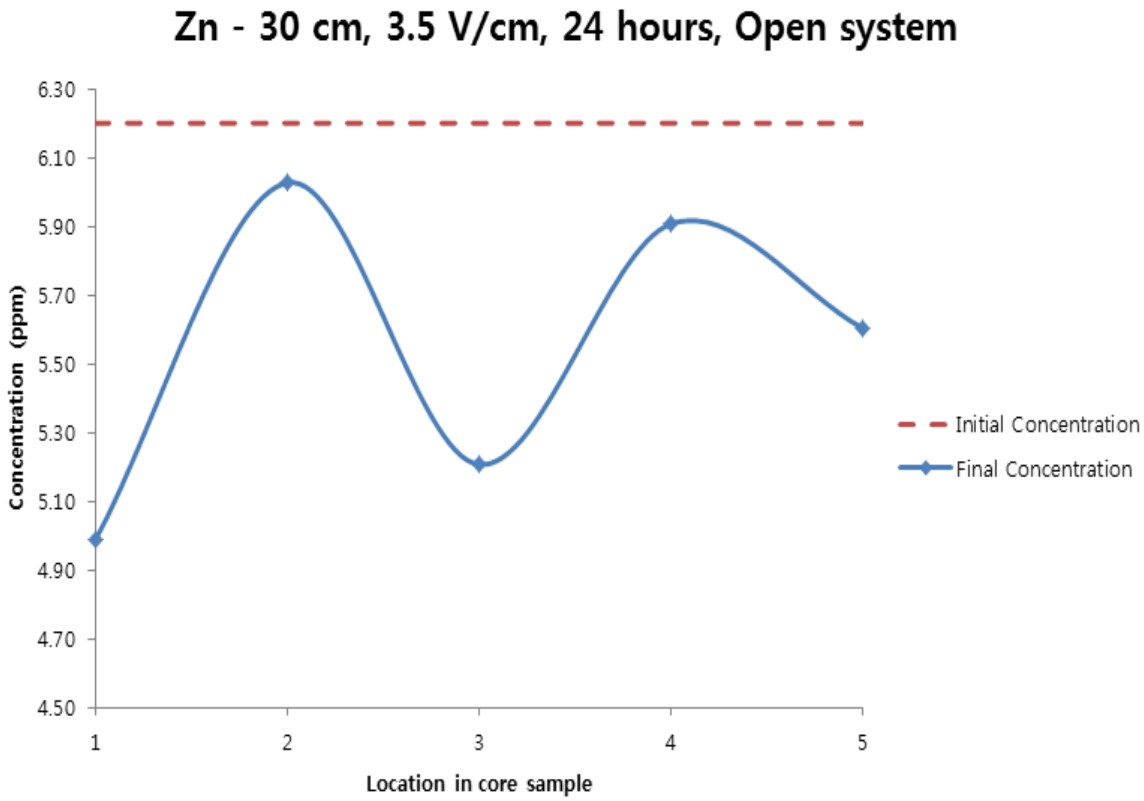

Figure 3-91: Concentration of Zn upon EK treatment along the core length of 30 cm. Potential gradient = 3.5 V/cm, Treatment time = 24 hours.

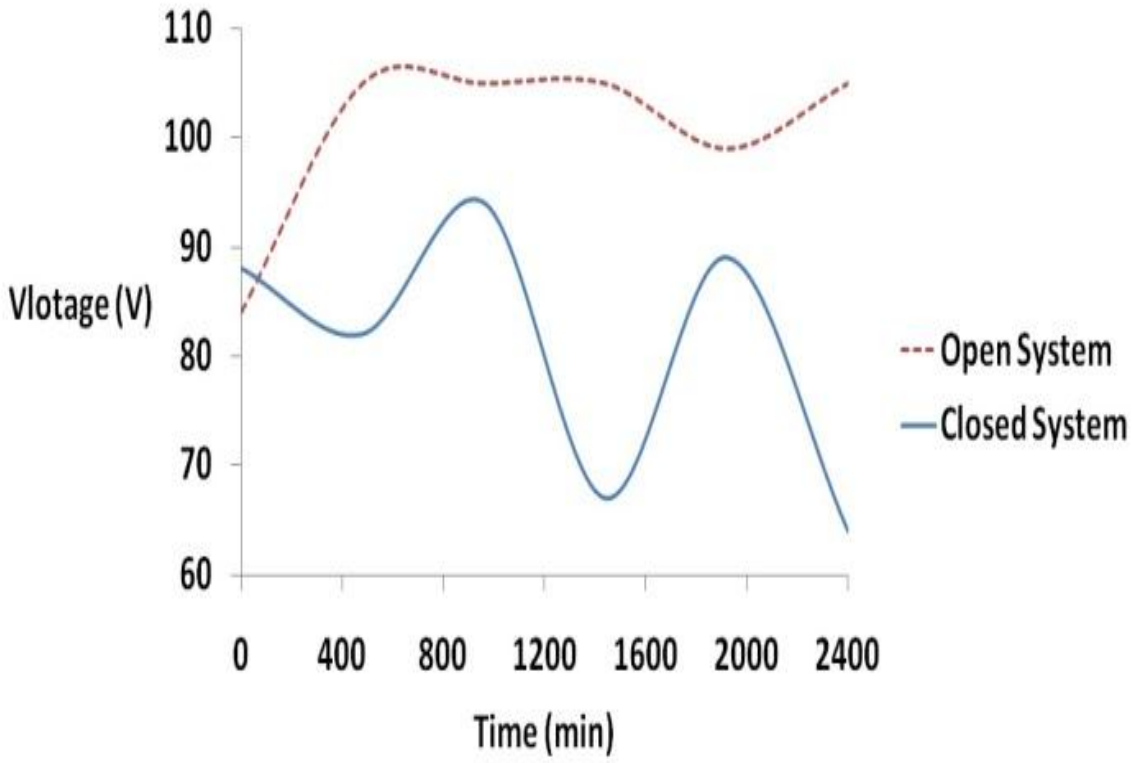

Figure 3-92: Variation of voltage with time for samples No.3 and No.4. Sample length = 30 cm; treatment time = 40 hours. (with two 8-hour interruptions.)

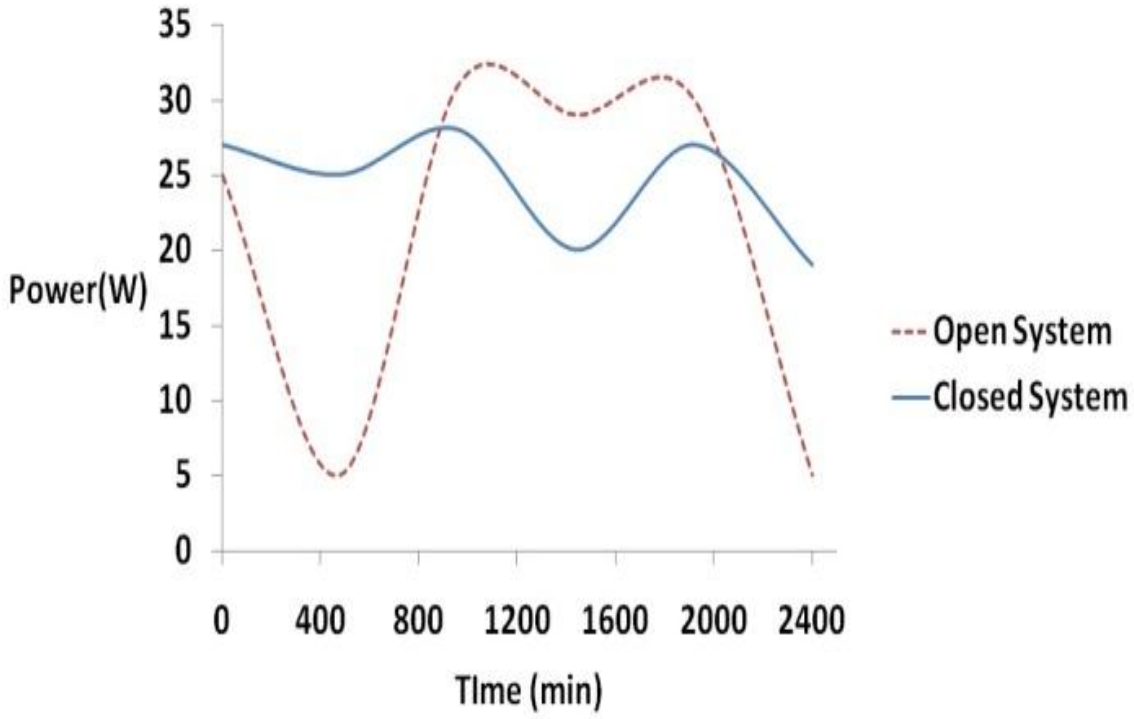

Figure 3-93: Variation of power with time for samples No.3 and No.4. Sample length = 30 cm; treatment time = 40 hours. (with two 8-hour interruptions.)

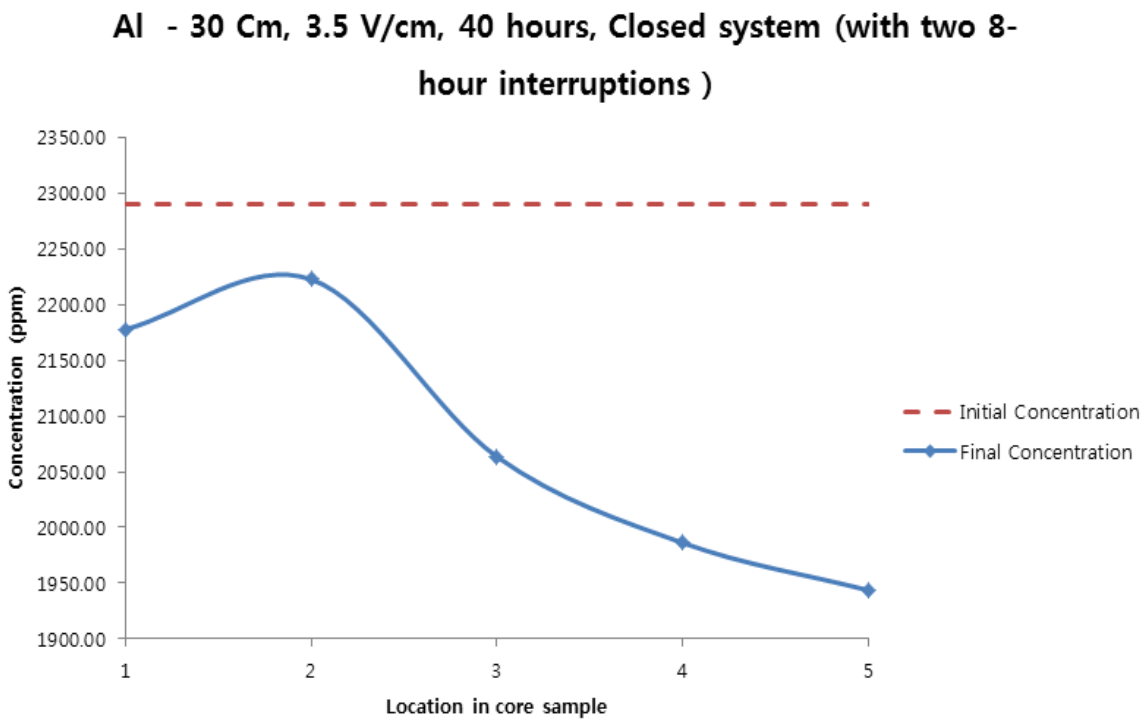

Figure 3-94: Concentration of Al upon EK treatment along the core length of 30 cm. Potential gradient = 3.5 V/cm, Treatment time = 40 hours. (with two 8-hour interruptions.)

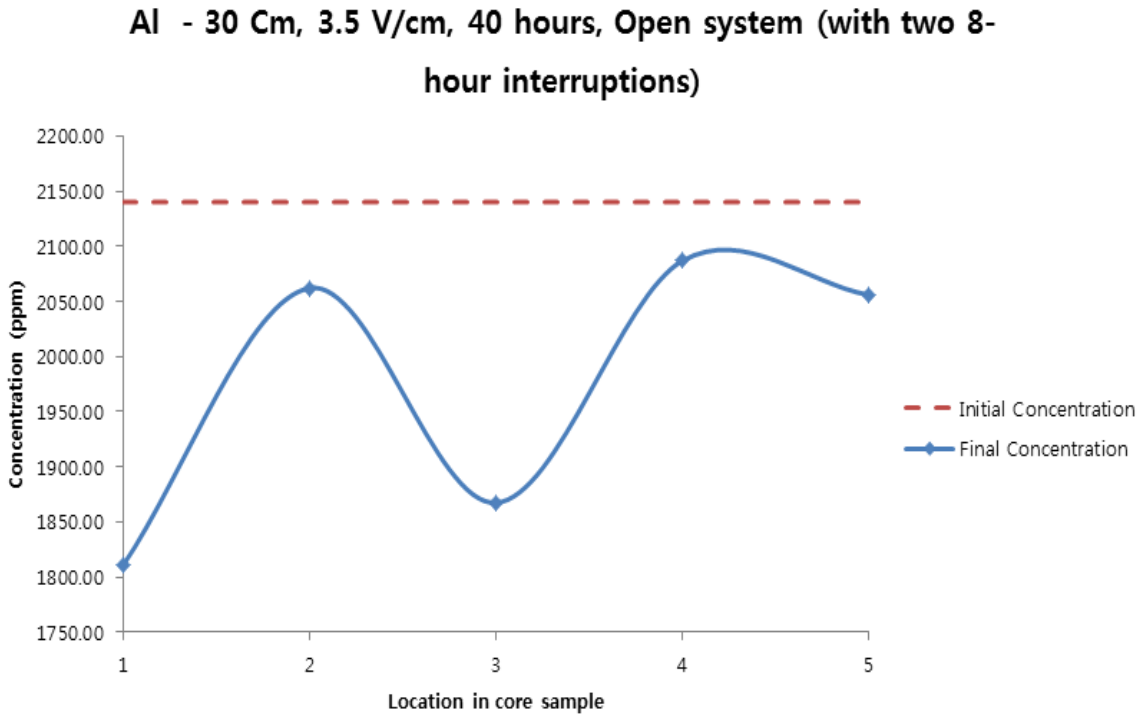

Figure 3-95: Concentration of Al upon EK treatment along the core length of 30 cm. Potential gradient = 3.5 V/cm, Treatment time = 40 hours. (with two 8-hour interruptions.)

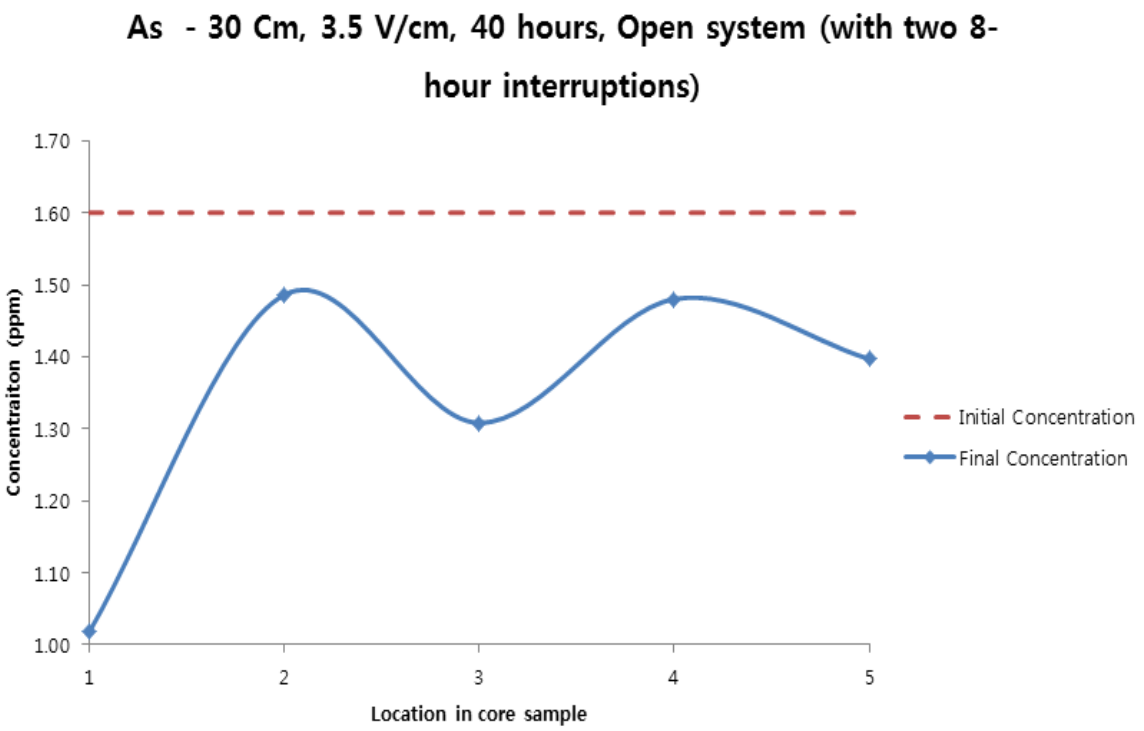

Figure 3-96: Concentration of As upon EK treatment along the core length of 30 cm. Potential gradient = 3.5 V/cm, Treatment time = 40 hours. (with two 8-hour interruptions.)

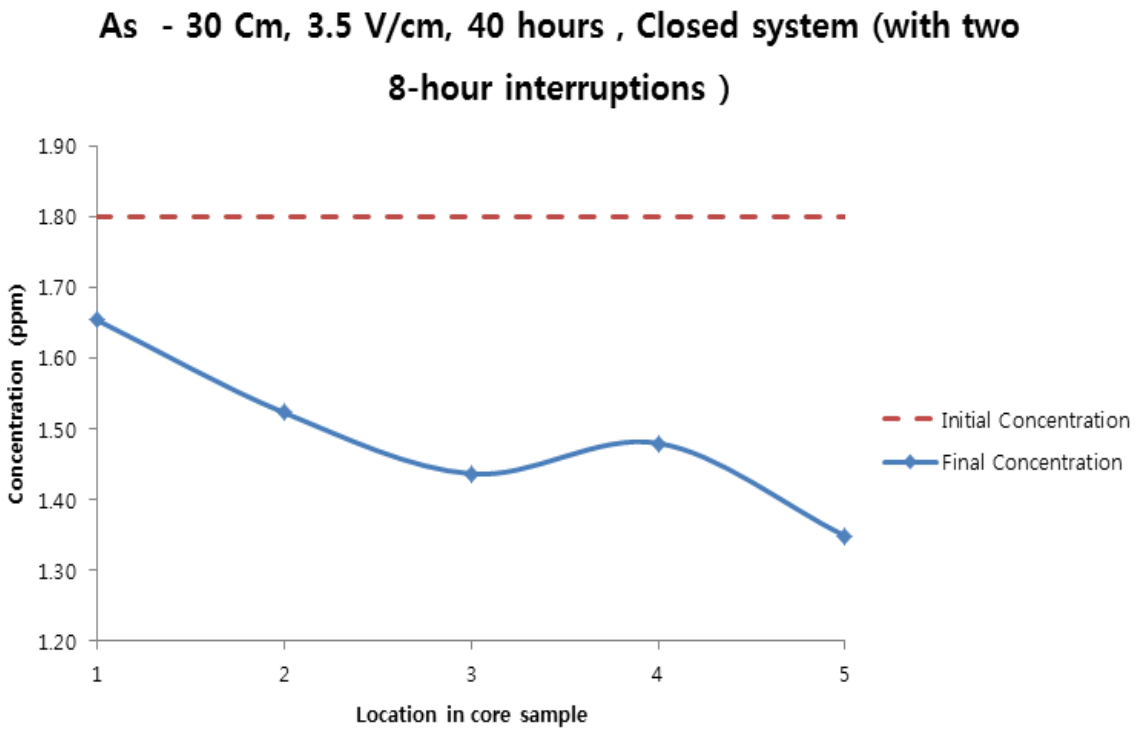

Figure 3-97: Concentration of As upon EK treatment along the core length of 30 cm. Potential gradient = 3.5 V/cm, Treatment time = 40 hours. (with two 8-hour interruptions

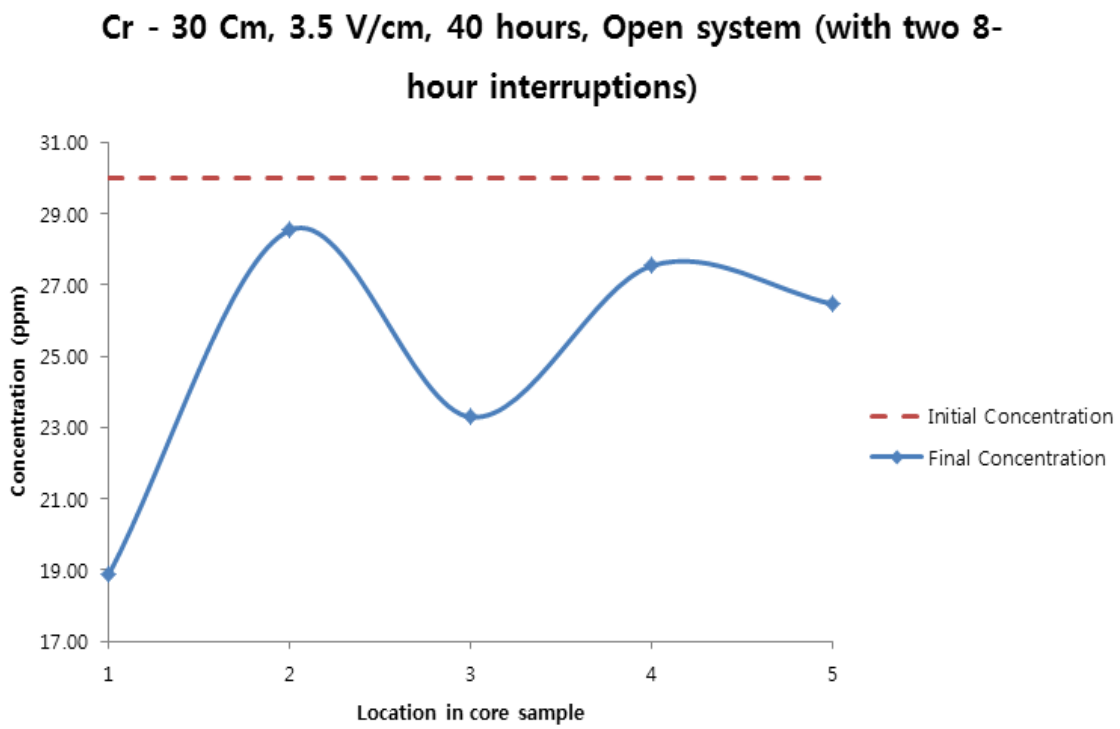

Figure 3-98: Concentration of As upon EK treatment along the core length of 30 cm. Potential gradient = 3.5 V/cm, Treatment time = 40 hours. (with two 8-hour interruptions.)

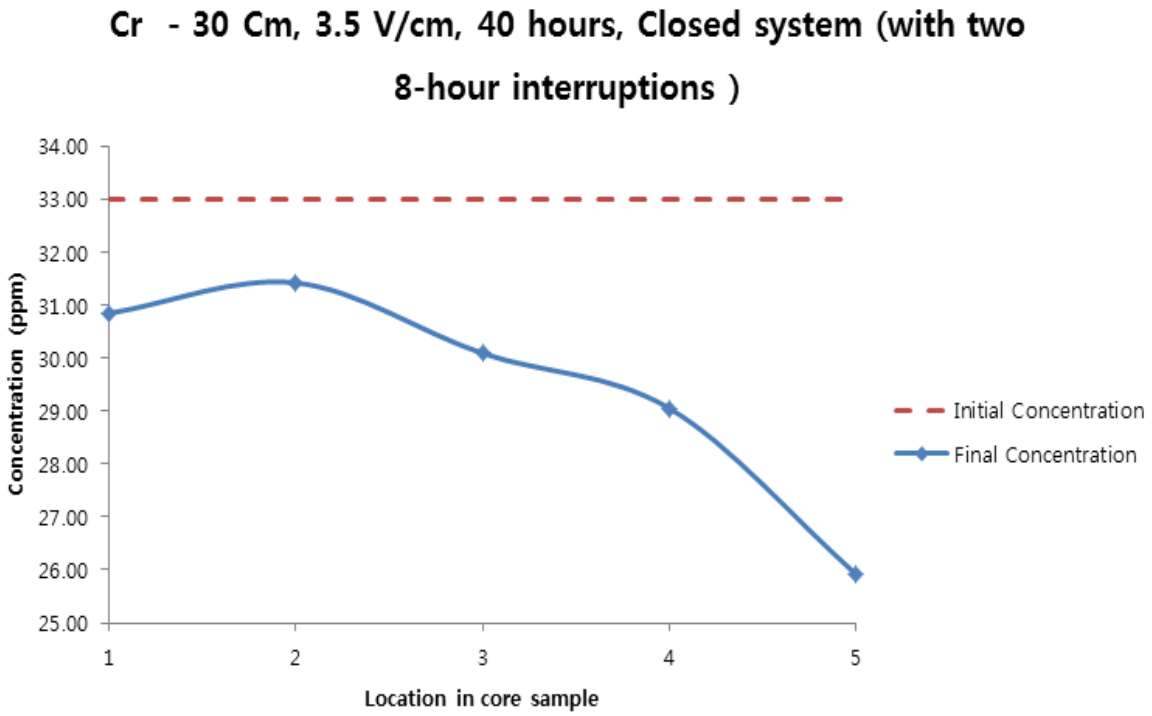

Figure 3-99: Concentration of As upon EK treatment along the core length of 30 cm. Potential gradient = 3.5 V/cm, Treatment time = 40 hours. (with two 8-hour interruptions.)

Chapter 4

Conclusions

In my study, I stressed gathering and classification of necessary data and the procedures of decision making aimed at identification and selection of the optimum operational parameters in up-scaling for electroremediation of heavy metals from offshore muds.

It is necessary to emphasize that the best remediation results are achieved *in situ* using a combination of various cleaning technologies. Only a few publications attempt to integrate the results of various disciplines (geology, geochemistry, chemistry, physics, etc.) into integrated study on industrial application of electrokinetics for decontamination of metals and hydrocarbons (Chilingar et al., 1997).

The main role in such a study must be given to the procedures of gathering and classifying the necessary data and procedures of decision making aimed at identification and selection of the best combination of remediation technologies (Chilingar et al., 1997). The most critical parameter is the voltage gradient applied to decontaminate heavy metals:

- Al, As, Cr and Cs all had the highest removal efficiency using 1 V/cm for a sample length of 10 cm and 3 V/cm for sample length of 30 cm.
- Se and Zn had the highest removal efficiency using 2 V/cm for a sample length of 20 cm, and 3 V/cm for sample length of 30 cm.
- Pb had the highest removal efficiency using 3 V/cm for a sample length of 10, 20

and 30 cm

Higher removal efficiency was achieved in longer tests even when using the non-optimum voltage gradient. The high salinity of Abu Dhabi's sea water is believed to contribute to the large flows achieved. These results indicate that sustainable *in-situ* electroremediation of heavy metals in high-salinity environments such as offshore muds is feasible.

In the case of tests involving Cl_2 gas, in a closed system with a potential gradient of 3.5 V/cm, removal efficiency was higher than in the open system with 3.5 V/cm electric potential. Higher removal efficiency was obtained by using the free Cl_2 gas generated at the anode and transported to the cathode in a closed system. Reduced power consumption with higher volumes of produced water was achieved in the closed system.

In this study, the continuous application of D.C. in closed system gave better results than interrupted application of D.C. Final pH at the cathode was reduced with the aid of transported Cl_2 gas.

The chlorine gas can have two impacts on the transport of metals in the system. One is to oxidize the metal ions to a higher oxidation state and the second is to form chloride complexes which will have higher mobility in the system.

In conclusion, it appears that presence of Cl_2 gas improves the efficiency of remediation.

The experiments conducted by the writer on field-collected offshore mud samples demonstrate that electroremediation is a very promising solution. At this stage, it is probably necessary to conduct a pilot test *in situ.*

References

Ace, A. G. 1955. An investigation of the influence of applied electrical potential gradients on flow of fluids in porous media. M.S. Thesis, *Department of Petroleum Engineering, The University of Southern California*, Los Angeles, CA.

Acar, Y. B., Gale, R. W., Hamed, J. and Putman. G. , 1990. Transportation Research Record, 1288, pp. 23-24. *Transportation Research Board*, National Research Council, Washington,D.C.

Adamson, L. G., Amba, S. A., Chilingar, G. V. and Beeson, C. M. ,1963a. Possible use of electric current for increasing volumetric rate of flow of oil and water during primary or secondary recovery. *Chimika Chronika,* 28(1):1-4.

Adamson, L. G., Chilingar, G. V. and Beeson, C. M., 1963b. Some data on electrokinetic phenomena and their possible application in petroleum production. *Chimika Chronika,* 28(10):121-127.

Adamson, L. G., Chilingar, G. V., Beeson, C. M. and Armstrong, R. A., 1966. Electrokinetic dcwatering, consolidation and stabilization of soils. *Engineering Geology,* 1:291-304.

Al-Sharhan, A.S. and El-Sammak, A.A., 2004, Grain size analysis and characterization of sedimentary environments of the United Arab Emirates coastal area, *J. of Coastal Research*, 20 (2): 464-477.

Ambah, S. A., Chilingar, G. V. and Beeson, C. M., 1964. Use of direct electrical current for increasing the flow rate of reservoir fluids during petroleum recovery. *J. of Canadian Petroleum Technology,* 3(1):8-14.

Ambah, S. A., Chilingar, G. V. and Beeson, C. M., 1965. Application of electrical current for increasing the flow rate of oil and water in a porous medium. *J. of Canadian Petroleum Technology,* 4(2): 81-85.

Ambah, S. A., Chilingar, G. V. and Beeson, C. M., 1965. Application of electrokinetic phenomena in civil and petroleum engineering. *Annals NewYork Acad. of Sci.,* 118(14):585-602

Atlas, R. M. 1977. Stimulated petroleum biodegradation. *Critical Reviews in Microbiology,* 5:371-386.

Atlas, R. M. 1981. Microbial degradation of petroleum hydrocarbons. *Microbiological Reviews,* 45:180-209.

Bell, C. W., and Titus, C. H., 1973, Electro-Thermal Process for Production of Offshore Oil through Onshore Wells, *US Patent* No. 3,724,543.

Bell, C. W., and Titus, C. H., 1974, Electro-Thermal Process for Promoting Oil Recovery, *US Patent* No, 3,782,465.

Bell, C. W., Titus, C. H., and Wittle, J. K., 1985,"In Situ Method for Yielding a Gas from a Subsurface Formation of Hydrocarbon Material, *US Patent* No. 4,473,114.

Bell, G, T., 1957, Electrolytically Promoting the Flow of Oil from a Well, *US Patent* No. 2,799,641.

Bcar, J. 1973. *Dynamics of Fluids in Porous Media,* 764 pp. Elsevier, Amsterdam.

Bhandari, A., Dennis, C. D. and Novak, J., 1994. Soil washing and biotreatment of petroleum-contaminated soils. *J. of Environmental Engineering,* 120(5):1151-1169.

Blacker, S. and Goodman, D., 1994. Risk-based decision making ease study: Application at a Superfund cleanup. *Environmental Science and Technology* 28(11):471-477.

Briant, J. 1961. Theses: Les phenomenes electrocinetiques en milieu hydrocarbure et l'epaissuer de la double couche. La revue de l'institut Francais du petrole et annals des combustibles liquids. XVI, 6; 1 – 48; (7-8): 49 – 75.

Burnett, W. E., and Loo, W. W., 1994. In-situ bioremediation of gasoline in soil and groundwater: A case history. Paper presented at the Superfund XV Conference, Washington, D. C.

Casagrande, I. L. 1937. Full-scsle experiment to incresse besring capacity of piles by electrochemical treatment. *Bautechnique* 1(1): 14-16.

Casagrande, I. L. 1941. The drainsge of fine soils. *Strasse* 8(19/20): 324.

Casagrande, I. L.. 1941. On the problem of drsinage of fine soils. *Stuttgart* 36: 556.

Casagrande, I. L. 1947. The spplication of electroosmosis to practi- cal problems in foundstions and earthworks. *Building Res. Tech. Paper No. 30. Dept. Sci. Indust. Res*. London, England.

Casagrande, I. L. 1948. Electroosmosis. *Proc. Second Int. Conf. Soil Mechanics.* 1: 218-223.

Casagrande, I.L., *Bautechnique*, 1949, 1(3): 1- 29.

Casagrande, I.L., *Harvard Soil Mechanics*, 1959, Ser. No.45

Casagrande,I.L., Soderman, L. G., and Loughney, R.W.,1960, "Increase of Bearing Capacity of Friction Piles by Electroosmosis," *ASCE Convention*, Boston, Mass.

Chilingar, G. V. 1952. Possible utilization of electrophoretic phenomenon for separation of fine sediments into grades. *Journal of Sedimentary Petrology* 22(1): 29-32.

Chilingar, G. V., Adamson, L. G., Armstrong, R. A. and Beeson, C. M., 1964. Soils stabilized through electroosmosis. *Southwest Builder and Contractor* 145(24): 100-102.

Chilingar, G. V., Adamson, L. G. and Rieke, H. H., 1966. Notes on application of electrokinetic phenomena in soil stabilization. In *Proceedings of the International Clay Conference, Jerusalem,* Vol. *1,* pp. 81 -89.

Chilingar, G. V., Adamson, L. G., Rieke, H. H. and Gray, R. R. 1968b. Electrochemical treatment of shrinking soils. *Engineering Geology* 2(3): 197-203.

Chilingar, G. V., Amba, S. A. and Beeson, C. M., 1965. Application of electrokinetic phenomena in civil engineering and petroleum engineering. *Annals of the New York Academy of Science* 118(14): 585-602.

Chilingar, G. V., Beeson, C. M. and Amba, S. A., 1968a. Uso de corriente electrica directa para aumentar la proportion del fluxo de fluidos en 10s yacimientos: Effecto del tipo de arcilla sobre la produccion de flujo. *Ingenieria Petrolera* 5(3): 22-32.

Chilingar, G. V., Chang, K. S., Davis, J. E., Farhanghi, H. J., Adamson, L. G. and Sawabini, S., 1968c. Possible use of direct electrical current for augmenting reservoir energy during petroleum production. *Compass of Sigma Gamma Epsilon* 45(4): 272-285.

Chilingar, G. V., El-Nassir, A. and Stevens, R. G., 1970. Effect of direct electrical current on permeability of sandstone cores. *J. of Petrol. Tech.* 22(7): 830-836.

Chilingar, G. V., Loo, W.W., Khilyuk, L.F. and Katz, S. A., 1997. Electrobioremediation of soils contaminated with hydrocarbons and metals: progress report. *Energy Sources*, 19:129-146.

Chilingar, G. V., Buryakovsky, L.A., Eremenko, N.A., and Gorfunkel, M.V., 2005. *Geology and Geochemistry of Oil and Gas*, Elsevier, 370 pp.

Cozzarelli, I. M., Herman, J. S. and Baedecker, M. J., 1995. Fate of microbial metabolites of hydrocarbons in a coastal plain aquifer: The role of electron acceptors. *Environmental Science and Technology* 29: 458-469.

El Gawad, E. A., Lotfy, M.M. and Sadooni, F.N., 2008, Sedimentology and hydrocarbon potentiality of arid Sabkha, UAE., *J. of Applied Sciences Research*, 4 (9): 1124-1130.

Fairless, B. 1990. Applying total quality principles to Superfund planning, Part 11: DQOS in Superfund-A dioxin case study. In: *Proc. American Society of Quality Control 17thAnnual Meeting, Enew Division Session L, Tucson, Arizona,* 17-21.

Haroun, M. H. 2009. *Feasibility of in-situ Decontamination of Heavy Metals by Electroremediation of Offshore Muds*. Doctoral Dissertation in Environmental Engineering, University of Southern California, 313 pp.

Harton, J. H., Hamid, S., Abi-Chedid, E. and G. V. Chilingar. 1967. Effect of electrochemical treatment on selected physical properties of clayey silt. *Engineering Geology* 2(3): 191-196.

Hicks, R. E. and Tondorf. S., 1994. Electrorestoration of metal contaminated soils. *Environmental Science and Technology* 28(12): 2203-2210.

Hinchee, R. E., Downey, D. C., Dupont, R. R., Aggarwal, P. K. and Miller, R., 1991.Enhancing biodegradation of petroleum hydrocarbons through soil venting. *J. Hazardous Materials* 27: 315-325.

Hopper, D. R., 1989. Cleaning up contaminated sites. *Chemical Engineering,* August: 94-110. Huesemann, M. H., 1994. Guidelines for landtreating petroleum hydrocarbon contaminated soils. *J. Soil Contamination,* 3:299-318.

Huesemann, M. H. 1995. Predictive model for estimation of extent of petroleum hydrocarbon biodegradation in contaminated soils. *Environmental Science and Technology,* 29(1): 7-18.

Katz, S. A., Khilyuk, L. F. and Chilingar, G. V., 1996. Sensitivity analysis and multivariant modeling for formation pressure and temperature fields in inhomogeneous media. *J. Petroleum Science and Engineering* 1695-108.

Kendall, C. G., Alsharhan, A.S. and Whittle, G.L., 1995. Holocene carbonate/evaporites of Abu Dhabi, United Arab Emirates-Field trip guidebook, *International Conference* on "Quaternary Deserts and Climatic Change,"published by the United Arab Emirates University.

Kruyt,H.R., 1952. Colloid Science, 1: 389. *Elsevier Pub. Co.,* New York, N.Y.

Lancelot, F., Londiche, H. and De Marsily, G., 1990. Experimental results on the influence of electric fields on the migration of oil, ionic species and water in porous media. *J. Petroleum Science and Engineering*, 4: 67-74.

Langnes, G.I., Robertson, J.O., and Chilingar, G.V., 1972. *Secondary Recovery and Carbonate Reservoirs*, Elsevier, 304 pp.

Leahy, J. G., and R. R. Colwell. 1990. Microbial degradation of hydrocarbons in the environment. *Microbiology Review,* (54): 305-315.

Lee, M. D., Thomas, J. M., Borden, R. S., Bedient, P. B., Ward, C. H. and Wilson, T. J., 1988. Biorestoration of aquifers contaminated with organic compounds. *CRC Critical Reuiews in Environmental Control,* 18: 29-89.

Loo, W. W. 1991. Heat enhanced bioremediation of chlorinated solvents and toluene in soil. *Pmc. of HMCRI R & D Conf., Anaheim, Calif.,* pp. 133-136.

Loo, W.W. 1993. Biotreatment of chlorinated solvents in soil and groundwater utilizing glucose as the co-substrate. Paper presented at the *Hazmacon Conf*., San Jose, Calif.

Loo, W. W. 1994. Electrokinetic enhanced passive in situ bioremediation of soil and groundwater containing gasoline, diesel and kerosene. Paper presented at the *Hazmacon Conf*., San Jose, Calif.

Loo, W. W., Wang, I. S. and Fan, K. T., 1994. Electrokinetic enhanced bioventing of gasoline in clayey soil: A case history. Paper presented at the *Superfund XV Conference*, Washington, D. C.

Mahaffey, W. R., Compeau, G., Nelson, M. and Kinsella, J., 1991. Developing strategies for PAH and TCE bioremediation. *Wafer and Environmental Technology:* 3233-86.

McCarty, P. L. 1991. Engineering concepts for in situ bioremediation. *J. Hazardous Materials* 28: l-10.

Mitchell,J. K., 1993, Fundamentals of Soil Behaviour, *John Wiley and Sons, Inc*., New York.

Morgan, P. and Watkinson, R. J., 1989. Hydrocarbon degradation in soils and methods for biotreatment. *Critical Reuiews in Biotechnology* 8:305-333.

Nash, J. H. and Traver, R. P., 1988. Field application of pilot soil-washing system. *EPA Document* EPA/68-03-3450. Office of Research and Development, US. Environmental Protection Agency, Cincinnati, Ohio.

Nunno, T. J., Hyman, J. A. and Pheiffer, T. H., 1988. Assessment of international technologies for Superfund applications. *EPA Document* EPA/540/2-88/003, 37 pp. Office of Solid Waste and Emergency Response. U.S. Environmental Protection Agency, Washington, D.C.

Overbeek, J. T. and Lijiklema, J, 1969, Electric Potential in Colloidal Systems, *Electrophoresis,* M. Bier, Ed., Academic Press, New York, 25-35.

Pamukcu, S. and Wittle, J.K. 1993. Electronically enhanced *in-situ* soil decontamination.

Pamukcu, S. and Wittle, J.K. 1993. Electrokinetic treatment of contaminated soils, sludges and lagoons. *DOE Contract No. 02112406.*

Pamukcu, S. and Wittle, J.K. 1994. Electrokinetic removal of coal tar constituents from contaminated soils. *EPRI TR-103320, Project 2879-21.*

Pamukcu, S., Weeks, A. and Wittle, J.K. 1997. Electrochemical extraction and stabilization of selected inorganic species in porous media. *J. hazardous materials,* 55, 305 – 318.

Pamukcu, S., Weeks, A. and Wittle, J.K. 2004. Enhanced reduction of Cr(VI) by direct electrical current in a contaminated clay. *Environmental Science Technology,* 38, 1236 – 1241.

Pamukcu, S., L. Hannum, J.K. Wittle, 2008. Delivery and Activation of Nano-iron by DC Electric Field, *J. Environ. Sci. Health, Part A*,43 (8): 934-944.

Pheiffer, T. H. 1990. EPA's assessment of European contaminated soil treatment techniques. *Environmental Progress* 49582-587.

Pheiffer, T. H. 1990. EPA's assessment of European contaminated soil treatment techniques.*Environmental Progress* 49582-587.

Pollard, S. J. T., Hmdey, S. E. and Fedorak, P. M., 1994. Bioremediation of petroleum and creosote-contaminated soils: A review of constraints. *Waste Management and Research* 12:173-194.

Probstein, R. F., Renaud, P. S. and Shapiro, A. P., 1991. Electroosmosis techniques for removing hazardous materials from soil. *US. Patent* 5074986.

Raymond, R. L., Hudson, J. O. and Jamison, V. W., 1976. Oil degradation in soil. *Applied Environmental Microbiology* 31: 522-535.

Renaud, P. S., and Probstein, R. F., 1987. Electroosmotic control of hazardous waste. *PhysicoChemical Hydrodynamics* 9(1/2): 345.

Rudenberg,P.A. 1945. Grounding principle and practice. *Elect.Engr.* 64 (1):1-15
Shapiro, A. P., and Probstein, R. F., 1993. Removal of contaminants from saturated clay by electroosmosis. *Environmental Science Technology* 27(2): 283-291.

Shapiro, A. P., Renaud, P. S. and Probstein, R. F., 1989. Preliminary studies on the removal of chemical species from saturated porous media by electroosmosis. *PhysicoChemical Hydrodynamics* 11(5/6):785.

Shin,S., Haroun, M., Ghosh,B., Pillay, A., Al Badawi,M., Chilingar, G.V., Pamukcu, S., and Wittle, J.K., 2010 Electroremediation of Heavy Metals from Offshore Muds upon Partial Chlorine Gas Removal. *The 9th Symposium on Electrokinetic Remediation* (EREM 2010) June 27-30, Kaohsiung, Taiwan

Sims, R. S. 1990. Soil remediation techniques at uncontrolled hazardous waste sites: A critical review. *J. the Air Waste Management Association* 40: 704-732.

Smoluchowski, von M. 1921. Handbuch der Electrizitat und des Magnetismus, 11. Translated by P. E. Bocque. In. *Engineering Research Bulletin* 33:47-158.

Stinson, M. K., H. S. Skovronek, and W. D. Ellis. 1992. EPA Site demonstration of the BioTrol soil washing process. *J. the Air and Waste Management Association* 42:96-103.

Street,N.,1961. Electrokinetic effects in laboratory permeability measurement: Produces monthly,25, 1:12-14

Titus, C.H., Wittle, J.K. and Bell, C.W., 1985, Apparatus for Passing Electrical Current Through an Underground Formation, *US Patent* No.4,495,990.

Ungcrcr, *P.,* Burrus, J., Doligez, B., Chenet, P. Y. and Bessis, F., 1990. Basin evaluation by integrated two-dimensional modeling of heat transfer, fluid flow, hydrocarbon generation, and migration. *Petroleum Geology Bulletin* 74(3):309-335.

Visschcr, K., Brinkman, J. and Soczo, E. R., 1990. Biotechnology in hazardous waste management in the Netherlands. In *Biotechnology and Biodegradation: Advances in Applied Biotechnology,* 4: 389-403. Gulf Publ. Co., TX.

Winterkorn, H. F. 1947. Fundamental similarities between electroosmotic and thermooamotic phenomena*. Proc. Highway Res*. Bd. 27: 443- 455.

Winterkorn, H. F. 1948. Physicochemical properties of soils. *Proc. Second Into Con£. Soil Mechanics*. 1: 23-29.

Winterkorn, H. F. 1952. Surface-chemical properties of clay miaersls and soils from theoretical snd ..xperimental developments in electroomosis. *ASTM Symposium on Exchange Phenomena in Soils. Spec. Tech. Pub.* No. 142. : 44-52.

Winterkorn, H. F. 1955. Water movement through porous hydrophilic systems under capillary, electrical, and thermal potential. *ASTM Symposium on Permeability of Soils. Spec. Tech. Pub*. No. 163.: 27-35.

Wittle, J. K., and Bell, C. W., 2005a, Electrochemical Process for Effecting Redox-Enhanced Oil Recovery, *US Patent* No. 6,877,556 Bl.

Wittle, J. K., and Bell, C. W., 2005b, Method for Enhancing Oil Production Using Electricity, *US Patent Application* No. 2005/0199387 AI.

WillIe, J. K., and Hill, D. G., 2006a, Use of Direct Current Electrical Stimulation for Heavy Oil Production*, Society of Petroleum Engineers Applied Technology Workshop* - Technologies for Thermal Heavy Oil and Bitumen Recovery and Production, Calgary, March 14 - 15.

WillIe, J. K., and Hill, D. G., 2006b, Direct Current Electrical Stimulation - A New Approach to Enhancing Heavy Oil Production, *First World Heavy Oil Conference, Beijing*, November 12 - 15.

Wittle, J. K., and Hill, D. G., 2006b, Direct Current Electrical Enhanced Oil Recovery in Heavy-Oil Reservoirs to Improve Recovery, Reduce Water Cut, and Reduce H2S Production while Increasing API Gravity, *SPE*. 114012-MS.

Wittle, J.K.; Hill, D.G. and Chilingar, G.V., 2008, Direct current electrical enhanced oil recovery in heavy-oil reservoirs to improve recovery, reduce water cut, and reduce H_2S production while increasing API gravity, *SPE* 114012.

Wittle, J. K., Hill, D. G., and Chilingar, G. V., 2008a. Direct current stimulation for heavy oil production. Paper 2008-374. *Second World Heavy Oil Congress*, Edmonton, March 10–12.

Wittle, J. K., Hill, D. G. and Chilingar, G. V., 2011. Direct Electric Current Oil Recovery (EEOR)—A New Approach to Enhancing Oil Production, *Energy Sources, Part A: Recovery, Utilization, and Environmental Effects*, 33: 9, 805 — 822

Wilson, J. T., 1985. Biotransformation of soil. *Applied Environmental Microbiology,* 1: 242-243.

Appendix

New Technology (Electrokinetics) to Greatly Improve Acidizing of Carbonate Reservoir Rocks (Possibly to Double Recoverable Reserves)

As the writer was conducting experiments at the electrokinetics laboratories of Petroleum Institute of Abu Dhabi, headed by Dr. Mohammad Haroun, he came up with an idea how to improve acidizing operation in Petroleum Industry. The writer was working with Dr. Haroun in Abu Dhabi for a period of 6 months.

The new technology proposed by the writer, Dr. M. Haroun, and G.V. Chilingar is a real breakthrough, which will result in doubling recovery from tight carbonate reservoirs (60 % of World oil reserves reside in carbonates).

This novel technology(electrokinetics) is proposed to improve acidizing operations, i.e., increase the penetration distance. Aqueous solutions of hydrochloric acid (usually 15%) are pumped into the carbonate formations to enlarge the pores and pre-existing fractures. However, the penetration distance of acid is very short. By applying D.C. current, one can drive the acid for long distances into the formation being acidized.

Introduction

Stimulation of carbonate reservoirs is achieved chiefly by acidizing treatments (Hendrickson, 1972, p. 336). Acids may be injected into pores and pre-existing fractures or at hydraulic fracturing rates depending upon the results desired. The acid dissolves the carbonates (limestones/dolomites), enlarging the pores and increasing the width of pre-existing fractures. This gives rise to an increase in permeability. The principal acid used is hydrochloric (HCl), which is pumped through tubing.

In the case of acidizing through pre-existing fractures, with increasing width of fractures, (1) the specific surface area decreases, (2) the spending time increases, and (3) the penetration distance increases.

The main problem in acidizing is the fact that the radial distance the acid will penetrate until being spent is short, especially in tight carbonates.

As shown in Eq. (A-1), in order to increase r_a, either t or q_i should be increased. As the experimental data obtained by the writers indicate, the injection rate q_i, can be increased considerably by application of D.C. current (electrokinetic effect) (see Chilingar et al., 1968,1970, for example).

On assuming a homogeneous formation, the volume of acid injected is equal to the pore volume invaded $[q_i\, t = \pi\, \phi\, h\, (r_a^2 - r_w^2)]$, the radial distance the acid will penetrate until being spent, r_a (ft), is equal to;

$$r_a = \sqrt{\frac{q_i\, t}{\pi\, \phi\, h} + r_w^2} \qquad \text{(A-1)}$$

where, q_i = acid injection rate (bbl/min); t = spending time (sec); ϕ = fractional porosity; h = formation thickness (ft); and r_w = wellbore radius (ft).

In the case of uniform penetration of acid, the reaction rate declines uniformly with decreasing acid concentration. The weight of carbonate dissolved per increment of distance penetrated declines uniformly until the acid is completely spent. With stronger acid, the spending time decreases.

In the case of matrix acidizing, with enlargement of pores, (1) the specific surface area decreases, (2) the velocity decreases, (3) spending time increases, and (4) the penetration distance increases.

Electrokinetics

When the imposed electrical potential gradient (E) is in the same direction as the pressure drop, the flow rate increases:

$$q_t = \frac{A\,k\,\Delta p}{\mu\,L} + \frac{A\,k_e E}{\mu\,L} \qquad \text{(A-2)}$$

where: q_t = total volumetric rate of flow (electrokinetic plus hydrodynamic) ; k = hydrodynamic permeability; A = cross-sectional area; L = length of porous media; Δp = pressure drop; μ = viscosity; $k_e = \left(\frac{D\,\xi}{4\,\pi\,F}\right)$ = the electrokinetic permeability; F = formation resistivity factor (Archie's); D = dielectric constant ; and ξ = zeta potential.

If Eq.A-2 is presented in a dimensionless form by normalizing the flow rates and, thus, eliminating the viscosity, area and length terms:

$$\frac{q_t}{q_i} = 1 + \frac{k_e\,E}{k\,\Delta p} \qquad \text{(A-3)}$$

and

$$\frac{(q_t - q_i)}{q_i} = 1 + \frac{k_e\,E}{k\,\Delta p} \qquad \text{(A-4)}$$

where q_i = initial hydrodynamic stabilized flow rate.

Equation A-3 shows that an increase in the flow rate in dependent upon the zeta potential, dielectric constant, brine concentration, Darcy permeability, and pressure drop. This equation also suggests that as the hydrodynamic permeability decreases, the percent increase in flow rate due to electrokinetics will become more significant. It should be remembered, however, that viscosity does change with increase in temperature, which increases on application of an electrical potential. In tight formations, k_e may exceed k considerably.

Deployment System for Enhanced Acidizing

As shown in Fig.A-1 , using electrokinetics it is necessary deploy an anode in the well adjacent to the formation being acidized, and cathode either at the surface or in the adjoining well. The electrokinetic flow will occur from the anode to the formation to be acidized, enabling the acid to move faster and deeper into the formation. The two electrodes (anode and cathode) must be connected by cables to the Direct Current power supply located on the surface. The acid must be injected with corrosion inhibitors into the formation; however, the aluminum anode in bolehole may also serve as sacrificial anode (Fig. A-1):

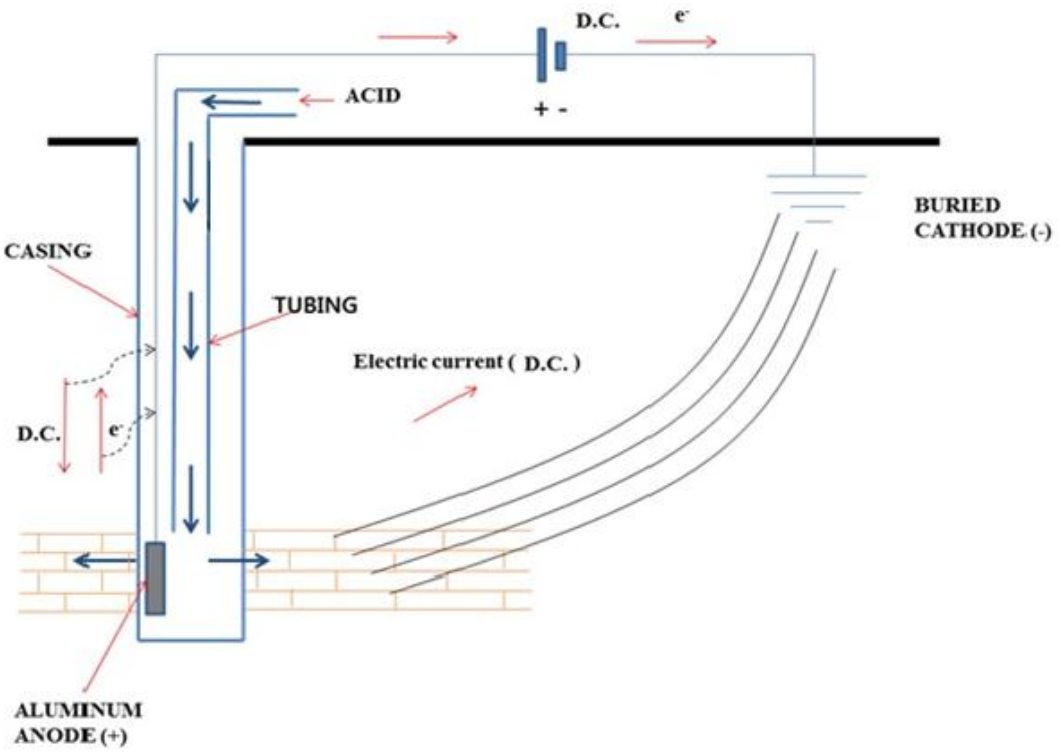

Figure A-1: Electrodes arrangement for acidizing operation

Conclusions

The proposed technology (electrokinetics) to improve acidizing operations is indeed a breakthrough. By applying D.C current, the volumetric rate of flow increases, which, is turn, increases the penetration distance of the acid before it is being spent. Without application of D.C current, the penetration distance is usually very short, especially in tight rocks.

Appendix References

Chilingar, G.V., Chang Kim Sang, Davis, J.E., Farhanghi, H.J., Adamson, L.G., and Sawabini, S.,1968. Possible use of direct electrical current for augmenting reservoir energy during petroleum production. *Compasss*, 45(4): 272-285

Chilingar, G.V., El-Nassir, A. and Stevens, R.G., 1970. Effect of direct electrical current on permeability of sandstone cores. *J. Petrol. Technol*., (22): 830 – 836.

Chilingar, G.V., Mannon R.W., and Rieke, H.H. *Oil and Gas Production form Carbonate Rocks*, Elsevier, New York, 408 pp.

Chilingrian, G.V., Mazzullo, S.V. and Rieke, H.H., 1972. *Carbonate Reservoir Characterization. A Geologic-Engineering Analysis*, Part I, Elsevier, Amsterdam, 639 pp.

Herdrickson, A.R., 1972. *Stimulation of Carbonate Reservoirs (Chapter 7)*, pp. 309-339.

Haroun, M.R., Chilingar, G.V., Pamukcu, S., Wittle, J.K., Belhaj, H.A., Al Bloushi, M.N., 2009. Optimizing Electroosmotic Flow Potential for Electrically Enhanced Oil Recovery (EEOR^{TM}) in Carbonate Rock formations of Abu Dhabi Based on Rock Properties and Composition. *IPTC*13812, December, 2009.

Wittle, J.K., Hill, D.G., and Chilingar, G.V., 2008, Direct Current Electrical Enhanced Oil Recovery in Heavy-oil Reservoirs to Improve Recovery, Reduce Water Cut, and Reduce H2S Production While Increasing API Gracity, SPE-114012, *Society of Petroleum Engineers*.